CHALMERS UNIVERSITY OF TECHNOLOGY **CHARMEC**

Mechanics and Maritime Sciences **Chalmers Railway Mechanics**

Tore Vernersson 2021-10-27

Anders Ekberg 93 pages

Roger Lundén

Report for

Ryo Yamazaki

Transportstyrelsen

Swedish tests of LL brake blocks under winter conditions - winter 2020–2021

Summary

The Swedish Transport Agency arranged testing of LL brake blocks in the northern part of Sweden. The tests were performed from January through to April 2021, using a train built-up by one locomotive and five (mostly) unloaded (empty) test wagons (2 × Bgu block configuration). The locomotive was unbraked during the tests. Two sets of five wagons were used, where one wagon set was equipped with organic composite blocks and one set was equipped with sinter blocks. Both wagon sets had a detailed sensor instrumentation on three of the wagons during the entire test campaign, except for one day mid-April with no instrumentation when testing of braking distances at reference conditions were performed.

During the test campaign, four stop braking tests per day were performed from 100 km/h. Three different locomotive driver instructions were employed that prescribed the brake applications to be performed in-between the stop braking tests and one aim was to investigate braking performance for these instructions. The first instruction is denoted “normal” brake conditioning and the brakes are then applied for 13 s every 10 minutes with main brake pipe pressure lowered by 0.6 bar. The “enhanced” brake conditioning is that the brakes are applied for 10 s every 15 minutes with main brake pipe pressure lowered by 1.0 bar. The third one is denoted “provocative” brake conditioning which means that no brake applications are performed for some prolonged periods between stop braking tests.

The present report contains three parts. In Part 1 the focus is on braking distances of the test train. Part 2 focuses on measured forces in hanger links and brake triangles. In Part 3, bedding-in state of brake blocks, block temperatures and build-up of ice on blocks are analysed in relation to braking performance during testing. In this context bedding-in of the brake blocks refers to the part of the block contact surface that actually is in contact with the wheel as compared to the nominal (maximum) contact surface. The grading of build-up of ice and snow is based on videos regularly recorded along one side of the train set. Analysis of the bedding-in state of the brake blocks were based on photos of the brake block contacting surfaces as documented before and after the test campaign.

Chalmers tekniska högskola AB Mechanics and Maritime Sciences Phone: 031-772 8501

412 96 GÖTEBORG Hörsalsvägen 7 Email: tore.vernersson@chalmers.se

Org nr 556479-5598

A total of 127 stop braking cycles were performed by the instrumented test train, 78 stops with organic composite LL-blocks and 49 with sinter LL-blocks. For organic composite brake blocks and braking with loaded wagons (15 tonnes axle load), very strong braking action was found, which resulted in locking-up of wheel axles and formation of wheel tread damage in the form of wheel flats. Because of this, tests with loaded wagons were only performed on the first day of testing and all remaining tests were performed with unloaded wagons. The wheel flats were machined by an angle grinder so that acceptable levels of wheel-rail contact forces were achieved, although it can be presumed that some test wagons had somewhat increased vibration levels for the remainder of the test campaign.

For organic composite blocks and unloaded wagons with an axle load of 6.5 tonnes it is found for perfectly bedded-in blocks that the stopping distances when using the normal brake instructions are the shortest, followed by the ones for the enhanced instructions, and the longest are found to result when employing the provocative driver instructions. No extremely long stopping distances (longest stopping distance is 910 m) are resulting, which can be compared to a nominal braking distance (based on information in UIC leaflet 544-1) for the train being 850 m. Ice and snow were present on the blocks during testing to a high degree for all three driver instructions, often in such amounts that the actual blocks could not be seen.

For sinter blocks and unloaded wagons with an axle load of 6.5 tonnes it is found for *not perfectly* bedded-in blocks that they behave rather well when employing normal brake instructions; in fact the performance is somewhat better than for "enhanced driver instructions". This finding is the same as for the organic composite blocks. Braking employing the provocative instructions causes occurrences of substantially prolonged braking distances, with longest stopping distance 1100 m that can be compared to the nominal braking distance 850 m. For one such stop, two wagons more or less lost their braking abilities as an effect of massive amounts of ice and snow, that had accumulated between blocks and wheels, fell off at the test. The stopping distance for the train under these conditions was 1550 m, which constitute more than a doubling of the braking distance as compared to the shortest stopping distances registered. The sinter blocks are not very well bedded-in at the tests; the degree of bedding-in is between about 60% and 100% for the test wagons. One effect of a low degree of bedding-in is that it seems to help keeping the brake blocks frictionally active, a conclusion drawn from the fact that they are less prone to high reductions in friction and the related low block temperatures at tests.

One reason for the weaker braking for the sinter brake blocks as compared to the organic composite blocks is that the time until the friction force reaches a significant level, after the brake is applied, is almost the double.

A study of the metrological winter conditions during the four latest winters is also provided in the present report. It shows that the winter season 2020–2021 is rather a normal winter.

Contents

1. BACKGROUND AND AIM

Reported safety incidents and general problems with winter braking performance for novel types of freight wagon brake blocks (read "not cast iron brake blocks") in Sweden (but also Norway and Finland) have drawn the attention of the Swedish Transport Agency (Transportstyrelsen). For this reason, the agency has arranged winter testing of LL type brake blocks in the northern part of Sweden during four consecutive years. LL type brake blocks have been developed to be a retrofit solution for wagons with cast iron brake blocks, with the main aim to reduce noise emission from freight wagons.

Tests during the winter 2017–2018 were performed using wagons with a mix of cast iron and LL-type brake blocks, meaning that a comparison of braking distances resulting from the different types of brake blocks was not possible. The winter test performed 2018–2019, again employing wagons with mixed blocks types, were unfortunately delayed until April 2019, just after the winter had ended. A few days of testing were nonetheless performed as a precursor for the larger test campaign performed during the winter 2019–2020 for which the results were analysed and documented in a report[1]. During this test campaign, a stop braking test was performed approximately every 15 minutes during each day. However, the winter 2019–2020 was extremely mild also for the region of testing in the northern part of Sweden, with -8 °C being lowest temperature while testing organic composite blocks. For this reason, no clear conclusions could be drawn on braking performance. Additionally, one needs to interpret the results from the 2019–2020 test campaign based on the frequent and intense utilization of the braking system. The influence of locomotive driver instructions could not really be analysed, since the short time between stops did not allow for additional brake applications (according to driver instructions).

From January through to April 2021, similar to the two previous winters, a dedicated test train built-up by one locomotive and two sets of five test wagons, was employed for winter testing. Train length was 132 m with locomotive being 15.5 m and five wagons each with length 23.3 m. The wagons were of type Habbins and had 2 × Bgu[2] brake block configuration. For the first wagon set, organic composite blocks of type IcerRail / Becorit IB116* were mounted while the second set had sinter blocks of type CoFren C952-1. The locomotive (Green Cargo locomotive of RD type) was unbraked during the brake tests when it was hauling one of the wagon sets. The set-up was basically the same as during the winter 2019–2020, but now two sets of wagons were used, each with one brake block type.

One focus of the 2020–2021 tests was on investigating the influence of locomotive driver instructions. The campaign was performed in line with the test specification issued by the Swedish Transport Agency[3]. One main difference is that only two of the six test sites between

[1] T. Vernersson, A Ekberg and R. Lundén, Swedish tests of block brake performance in winter conditions – Winter 2019-2020. Chalmers Railway Mechancs, Chalmers University of Technology, 2020

[2] Two brake blocks on each side of the wheel.

[3] M. Aho, Test Specification: Driver instructions for winter testing 2020-2021, Version 1.5 (in Swedish), *Transportstyrelsen*, 2021

Boden and Haparanda now are used for stop braking tests. This allows for the locomotive driver to perform additional brake applications between test sites[4].

Part 1 of the present report focusses on braking distances for the two types of brake blocks. The trains are here composed of the (unbraked) locomotive and one of the braked wagon sets featuring organic or sinter brake blocks. Measured data processed include train speed and pneumatic pressure of the main brake pipe (connection between locomotive and trailing wagon) and of the brake cylinders.

Part 2 of the report focusses on analysis of force sensor data from the data acquisition system. Forces in hanger links and brake triangles are studied. The measuring system employed during the test campaign is detailed in a separate report[5]. The analyses are based on data provided on Excel data sheets by on-train test engineers and on the data files that were generated during the tests[6].

Part 3 of the report treats measured brake block temperatures, the degree of build-up of ice on brake blocks and the bedding-in states of the brake blocks. Additionally, metrological data[7] from weather stations (VViS, supplied by the Swedish Transport Administration, Trafikverket) are studied.

All data were imported into Matlab[8] to allow for straightforward processing, structuring and visualization of results.

Three types of locomotive winter driver instructions were employed. Two of the types represent proper driver behaviour that is in line with the usage guidelines for LL brake blocks provided in UIC leaflet 541-4[9] with short (10 to 15 s) brake applications being performed every 10 to 15 min. The third type represents driving without proper brake conditioning, meaning that the driver proceeds with no brake applications for longer duration prior to a stop braking test. For the sinter blocks, also a case of frequent stop braking with no additional intermediate brake applications was studied. This case is denoted driver instruction 4, see footnote 10. This latter case basically mimics the brake testing performed during the 2019–2020 test campaign and is not a realistic winter driving technique for railway freight traffic. A short description of these four different ways of performing the tests are given in the following. Note that the locomotive is unbraked for all the tests and that a speed of 100 km/h

[4] For the 2019–2020 tests this was not the case since brake tests to stop were performed at all the six test sites, leaving insufficient time between stops for further brake applications.

[5] I. Brottare, Brake performance tests of brake blocks in winter conditions, *AFRY Test Center*, Report No 6213414:01, 2021-05-03

[6] Nominal braking information in xlsx-format and time history data files in DeWeSoft-format supplied by AFRY Test Center, uploaded to common SharePoint drive.

[7] Personal communication, V. Moberg (Trafikverket) and T. Vernersson, 2021-06-21.

[8] Matlab, version R2019b, *The MathWorks, Inc.*, Natick, Massachusetts, USA, 2019

[9] UIC CODE 541-4, Composite brake blocks – General conditions for certification and use, 5th edition, *UIC*, November 2018.

[10] It is actually denoted version 1.5 in the background information, but 4 is chosen here for easier implementation in computer codes.

is aimed for. Also note that for driver instructions 1 – 3, only two (of the available six) tentative stop braking sites on the test track between Boden and Haparanda were used for stop braking tests. For driver instruction 4 all six sites were used (as was the case during the 2019–2020 tests).

Driver instruction 1 “normal brake conditioning”: Every 10 minutes the brakes are applied by lowering the pressure in the main brake pipe by 0.6 bar. The brakes are applied for 13 s (from the time the brake lever is first engaged).

Driver instruction 2 “enhanced brake conditioning”: Every 15 minutes the brakes are applied by lowering the pressure in the main brake pipe by 1.0 bar. The brakes are applied for 10 s (from the time the brake lever is first engaged).

Driver instruction 3 “provocative brake conditioning”: When travelling from Boden to Haparanda employ “driver instruction 2” up to midway of the test track (this includes the first site for stopping test). Make no further brake applications at all after this except for the stop braking test at the second utilized test site. Repeat the arrangement in the opposite direction, starting out with driver instruction 2.

Driver instruction 4 “frequent stop braking”: Every 15 minutes a braking test is performed to stop. No additional brake applications.

The general aim of the Swedish winter tests is to objectively investigate winter performance of LL brake blocks. In particular an objective is to identify specific weather conditions (if any) during which the braking performance may be deteriorated. The work presented in this report is targeting these aims.

2. TEST TRAIN, TEST SITES AND DATA ACQUISITION SYSTEM

The test train, see Figure 1 was provided by Green Cargo. The ten wagons of type Habbins-15, see Figure 2, have Y25 bogies and are equipped with one brake cylinder per wagon. The brake block configuration of the wagon is 2 × Bgu. The wheel diameters of the wagons range from 898 mm to 923 mm. The tare weight of a wagon for the unloaded (empty) state is about 26 metric tonnes and about 60 tonnes for the employed loaded state[11]. The wagons were subjected to maintenance prior to testing at which the brake rigging system was lubricated. The plan was to measure the efficiency of the brake systems of all wagons at the Borlänge workshop, but after performing measurements of half a bogie on one of the wagons, a force sensor failed, rendering further measurements impossible. Based on the performed measurements the efficiency was 90 % for braking corresponding to an unloaded wagon and 93 % for a loaded wagon. However, the instrumentation of the wagons allows for a direct assessment of brake efficiency. Block normal forces are calculated (from measured brake triangle forces and hanger link forces) and the theoretical block forces are calculated using measured brake cylinder pressures, see Appendix E. By this method, it is found that the

[11] The chosen loaded state is, according to the theoretical brake calculation for this wagon type, the lowest load for which the wagon is braking at its maximum brake cylinder pressure. Upon further increase of the load there is no further increase of the brake cylinder pressure. Maximum axle load 22.5 tonnes or 90 tonnes wagon weight.

average calculated efficiency is 88% for both the instrumented wagon set equipped with organic blocks and the set with sinter blocks[12]. The result of the latter method is more representative for all wagons owing to the larger set of measured data and it is consequently assumed that the efficiency is 88 % during the test campaign.

No artificial de-icing of the wagons was performed during the test campaign.

The test train is powered by an RD type locomotive, equipped with the ERTMS signalling system. The mass of the locomotive[13] is 78 tonnes and its dynamic mass is 89 tonnes. The locomotive had no operating brakes[14] during the test runs.

Figure 1 Test train consisting of locomotive and five freight wagons an early morning in Boden, February 2021.

[12] The calculated average efficiency 0.88 is the same as the average measured for the five Habbins wagons used during the 2019-2020 test campaign, see S. Heinz and C Schmidt, Determining the efficiency of five freight car wagons of Habbiins type, Document 59869-TVP21-192841-PR01, *DB Systemtechnik*, Minden, 2020-02-17.

[13] Järnvägsföretagets säkerhetsbestämmelser, del A, *Green Cargo*, Document Number C82-08 A, second edition.

[14] A pneumatic valve was operated to immobilize the locomotive brakes. The locomotive has no ED braking.

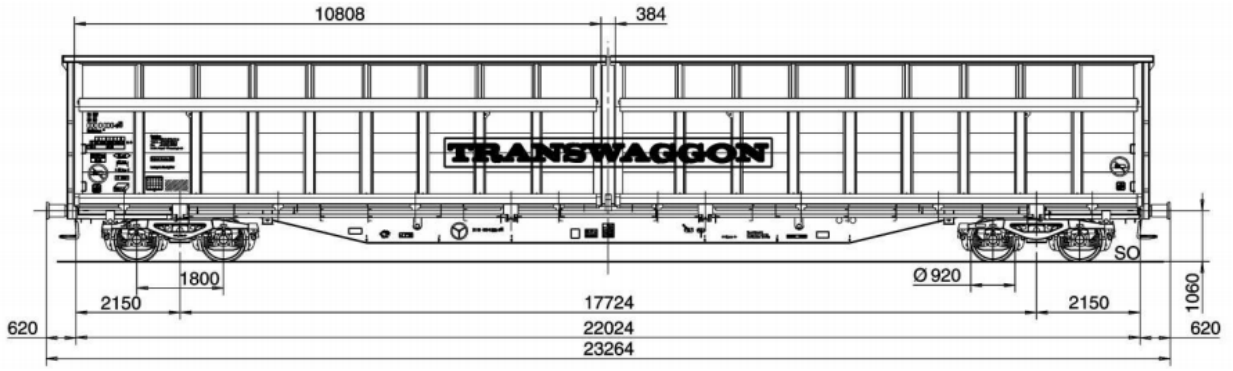

Figure 2 Test wagon of type Habbiins-15, extract from *https://transwaggon.com/images/pdf/wagons-specs/HB_15.pdf*.

The reported tests were performed on the line between Boden and Haparanda, except for the additional reference tests with sinter blocks, which were performed in mid-April 2021 on the line between Ställdalen and Hällefors. An overview of the test sites is given in Figure 3. Also marked on the map are weather stations from which metrological data were extracted. Note that only two of the test sites, namely sites 2 and 4, were used for stop braking tests under Driver instructions 1 – 3. For Driver instruction 4 all six sites were used.

An overview of the data acquisition system employed during the testing period is given in Figure 4. To measure forces, strain gauges were mounted on brake block hanger links, on brake triangles of wagons 2 and 3 and on the first bogie of wagon 4. Some details on the instrumentation are provided in Figure 6.

Brake block temperatures were measured only in the brake blocks on one side of wagon 3, see Figure 5. Thermocouples were drilled into the brake blocks to a point about 10 mm from the wheel tread contact surface, axially in the middle of the blocks and about 30 mm from block external ends. Thermocouple leads were drilled in from the back side of the blocks (that is in contact with the holder) to protect them from the harsh surroundings with plenty of ice and snow. Additionally, the thermocouple wires were protected by pieces of extruded polystyrene insulation. This set-up was very successful with only one failing thermocouple during the entire test campaign. This can be compared to an immediate 100 % failure rate during the 2019–2020 test campaign when an obviously too simple set-up was used.

In the locomotive a laptop was plugged in to the data bus that connected the separate measurement systems located on the wagons (not detailed here). Not shown in the overview are 1) the GPS sensor which supplied speed signal and GPS coordinates, and 2) the video camera that was mounted outside of the locomotive and provided a view of trailing wagons. Sensor data were sampled using the DEWESoft software[15] at a rate of 100 Hz.

[15] DEWESoft X3 SP10, DEWESoft d.o.o, Gabrsko 11a, 1420 Trbovlje, Republic of Slovenia, see www.dewesoft.com

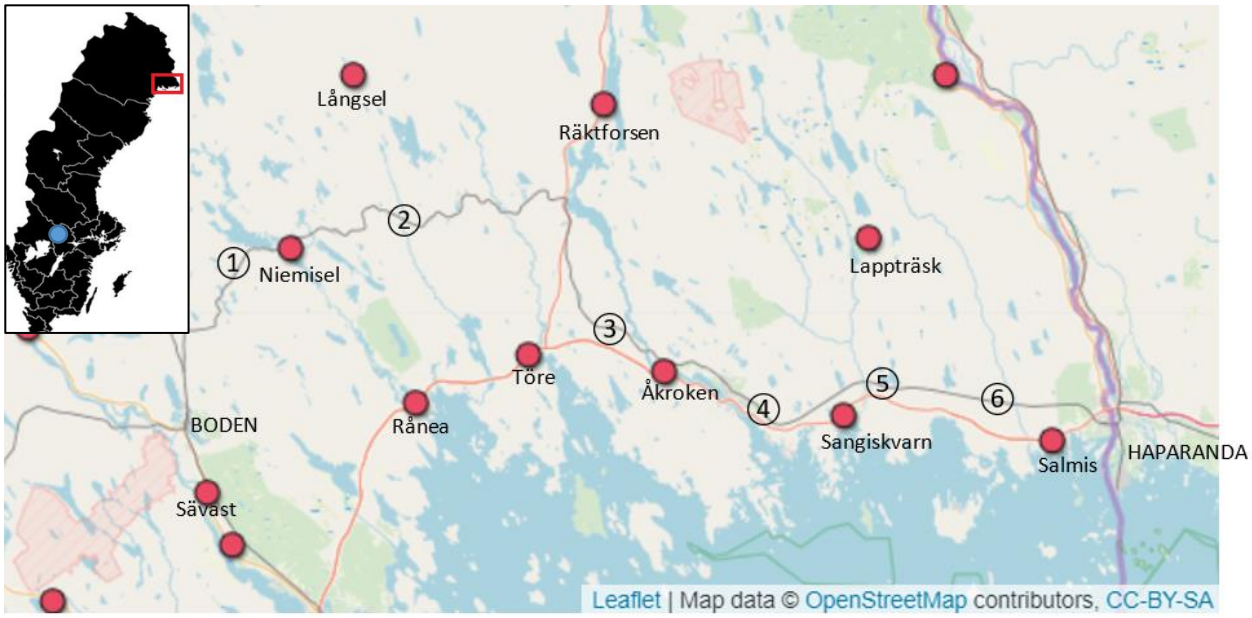

Figure 3 Map of test track between Boden and Haparanda with test sites indicated by encircled site numbers ① - ⑥. Red markers show locations of relevant weather stations (positioned along roads). Inset indicates the test region via the red square and the location of the additional test site between Ställdalen and Hällefors via the blue circle.

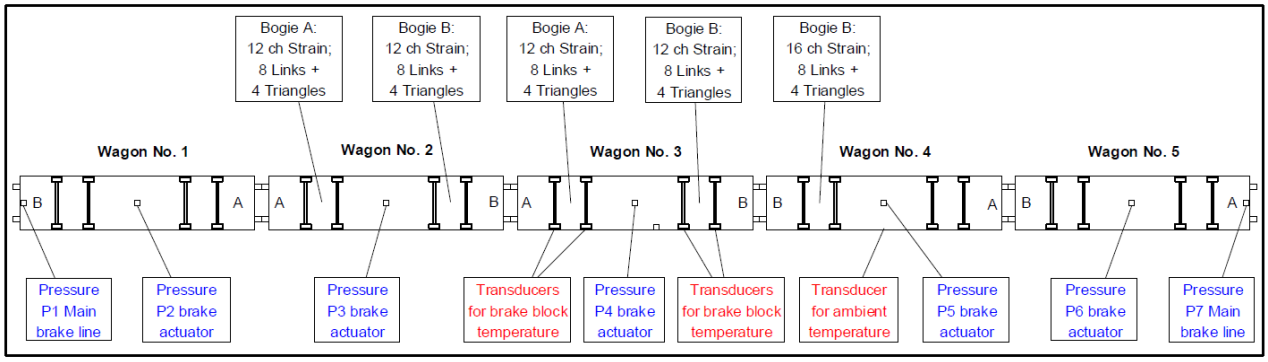

Figure 4 Overview of train and DAQ systems, adapted from AFRY-report (reference given in footnote 5 on page 6), indicating positions of sensors for main pipe pneumatic pressures, brake cylinder pneumatic pressures, forces and temperatures. For instrumented bogies on wagons 2 and 3, forces in all hanger links are measured together with the total force on each brake triangle. Only one bogie is instrumented in wagon 4, where forces in all hanger links are measured together with the brake triangle forces, both for left and right sides.

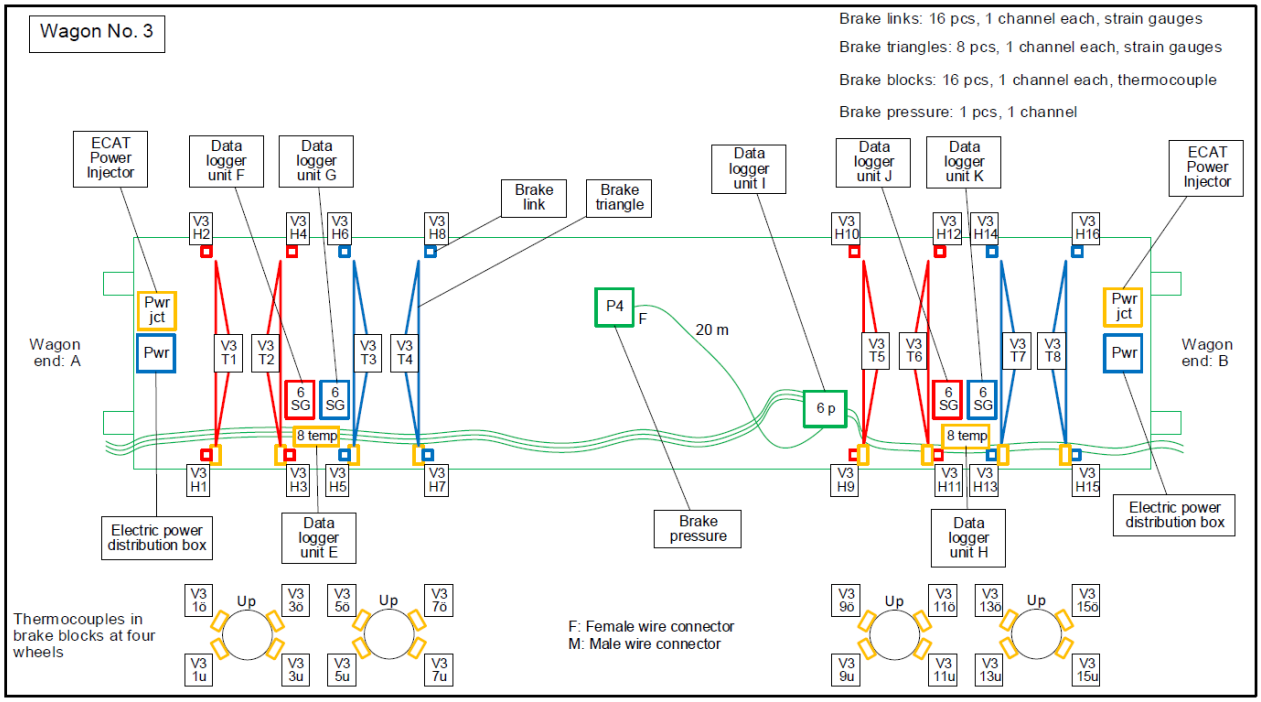

Figure 5 Overview of transducers and data logger on wagon no 3. Temperatures are measured in all brake blocks on one side of the wagon.

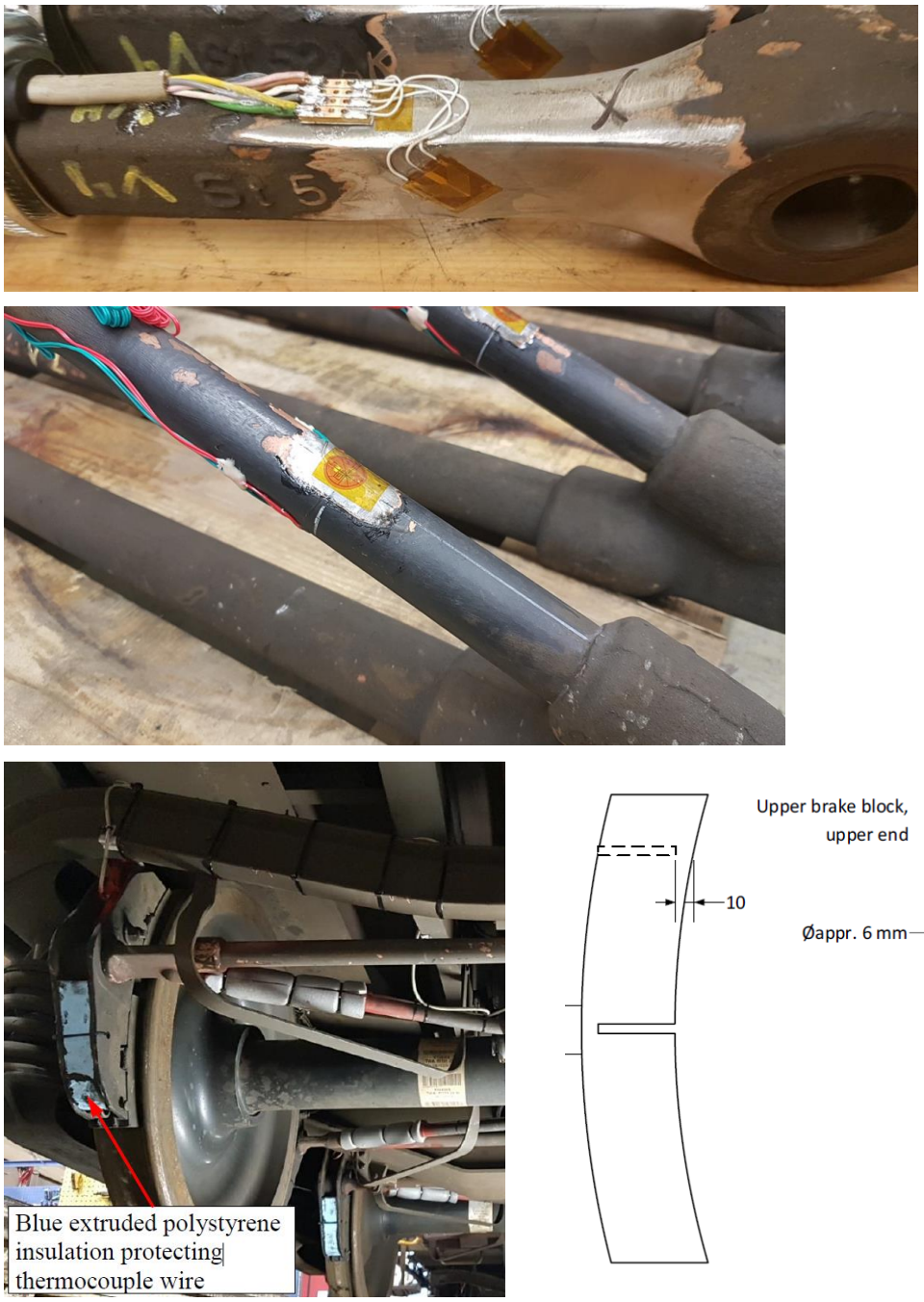

Figure 6 Examples of instrumentation[16]. Top: hanger link with strain gauge rosette, Middle: Brake triangle with strain gauge rosette. For these components strain gauge rosettes were also mounted on the opposite side of the cross section. Bottom: Photo of brake block with thermocouple wiring and schematic location of thermocouple in upper part of the brake block.

[16] I. Brottare, Brake performance tests of brake blocks in winter conditions, *AFRY Test Center*, Report No 6213414:01, 2021-05-03

3. METHOD OF DATA ANALYSIS

3.1. Part 1: Braking distances

Firstly, the nominal data according to the test plan, as noted in Excel sheets on the train during testing, were imported to Matlab. These data provided the following information for the individual stop braking cycles: stop number of the day, date and time, test site no, track distance mark, average track gradient (always nil for test sites), initial speed at braking, nominal main pipe braking pressure, outdoor temperature and braking distance. For each test run, information is also provided on prevailing snow whirling conditions employing the UIC snow whirling index, as defined in Appendix G of UIC 541-4[17]. The classification scheme available to the on-train engineers is presented in Appendix G.

Acquired time data were then imported. Here, each individual brake cycle was identified by a graphical on-screen procedure based on 1) finding the approximate time period using time information as provided on the Excel sheets, and 2) manually introducing one mark prior to start of braking and one mark after the end of each brake cycle. After completion of this procedure a more exact numerical analysis of the brake data was carried out to assess stop braking distance and other information pertaining to each stop braking test.

The chosen start of braking was taken as the time point (and related distance mark) when the brake cylinder pressure starts to increase, as manifested by a distinct pressure peak in the brake cylinder pressure, see example in Figure 7 at time 4.7 s. This procedure was chosen instead of an alternative method to make detection based on decrease in the main pipe pressure, since this would give a less distinct starting point and thus could introduce an error in braking distances.

The end of the braking cycle should ideally be taken as the time (and related distance mark) when the train was at full stop. However, on one of the first days of testing with unloaded wagons during the 2019–2020 test campaign, it was found that small wheel flats had formed on the wheels on some wagons of the test train. The reason for this was the increasing block-wheel coefficient of friction at lower speeds, intrinsic to the LL type blocks. Consequently, it was decided that the locomotive driver should abort the braking at a speed of approximately 30 km/h, which has the effect that the main brake pipe pressure starts to increase and that the brake cylinder pressure slowly decreases, see Figure 7. The same braking procedure was again employed for the 2020–2021 test campaign. Depending on the overall conditions, this operating procedure meant that the train deceleration towards lower speeds was modified by the lowered brake block normal force and that the train rather frequently did not come to a full stop at end of the brake cycle. Therefore, an extrapolation scheme is needed to numerically estimate a stopping distance of the train that could be used for comparison of braking performance. A more elaborate discussion on this is given in the report on the 2019–2020 test campaign (reference given in footnote 1 on page 5). The extrapolation scheme introduced in that report[18] is utilized also here. The extrapolation scheme employs extrapolation for all stops that have a lowered cylinder pressure at end of the braking cycle.

[17] UIC CODE 541-4, Composite brake blocks – General conditions for certification and use, 5th edition, *UIC*, November 2018.

[18] It was denoted Version E4 in the report from 2019–2020.

It builds on curve fitting of the speed signal to find the instant in time with maximum deceleration.

To this end, the stopping distance is found for stops that have a lowered cylinder pressure at end of the braking cycle by:

1. integration of the speed signal up to the time point of maximum deceleration that occurs during the period of decreasing cylinder pressure, yielding the braking distance $S_{fullbrake}$
2. integration of extrapolated speed variation based on constant (maximum) deceleration until stop, yielding the braking distance S_{extrap}
3. Total braking distance is found as $S_{stop} = S_{fullbrake} + S_{extrap}$

The stop braking distances are corrected for differences in initial speed by employing a correcting factor, being the square of the ratio between actual initial speed and nominal speed (100 km/h), in accordance with UIC leaflet 544-1[19]. The correction should according to the leaflet only be used for braking cycles with speed deviations lower than 4 km/h. In the present report the correction factor has, however, been used for all braking cycles, irrespective of initial speed deviations.

All brake cycles for unloaded wagons are performed at the same nominal pneumatic settings with a main pipe reduction of the pressure to 3.3 bar, with a resulting brake cylinder pressure of about 1.3 bar, corresponding to full service braking of the (unloaded) train. For the initial four stops with loaded wagons on the first day of testing, full service braking is also performed with a resulting brake cylinder pressure of about 3.5 bar.

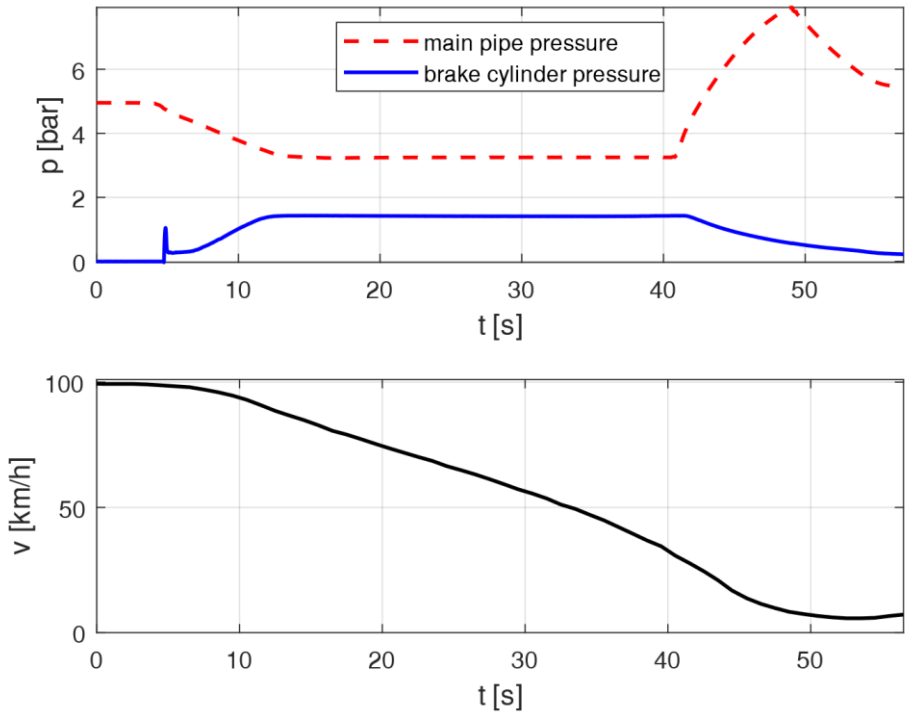

Figure 7 Example history of main pipe pressure, brake cylinder pressure and speed.

[19] UIC CODE 544-1, Brakes – Braking power, 4th edition, *UIC*, October 2004.

3.2. Part 2: Braking forces, braking energies and friction coefficients

Here, the sampled force data from the data acquisition system are analysed. In addition to the analyses performed in Part 1, also measured forces in brake triangles, denoted F_t, and hanger links, F_h, are exploited. These additional data allow for a detailed analysis of the friction conditions at brake block inserts. Based on force and moment equilibrium equations, the brake block normal forces and brake block friction forces are calculated for all brake block inserts using angles of hanger links, brake triangles and other geometrical information.

The time delay until a particular brake block insert starts to contribute "significantly" to the total braking power is also assessed. Here, some different assumptions were investigated on how to define the meaning of a "significant" part of each brake cycle, but finally the analysis was performed based on the build-up of the instantaneous friction force.

3.3. Part 3: Brake block temperatures, ice build-up and bedding-in

Brake block temperatures were measured only in the brake blocks on one side of wagon 3, as previously described. For each temperature signal from a thermocouple, both the initial temperature prior to a stop braking test and the temperature increase introduced by the test were established. The temperature signals occasionally show distortions in the form of fast oscillations. An automatic screening scheme was introduced to avoid errors that could be introduced from analysis of corrupt data. In a second step, a manual method was employed to possibly establish the temperature increase also for the automatically removed temperature data that nonetheless could contain high-quality temperature data for relevant time periods.

The degree of ice and snow build-up on the brake blocks were graded from videos. These were sometimes captured before leaving Boden in the morning and sometimes upon arrival at Haparanda at lunch-time. In addition, videos were frequently captured upon coming back to Boden in the evening. The grades are quantified according to the following:

- Grade 0: No ice and snow on blocks.
- Grade 1: Ice or snow on blocks but only away from the frictional contact (*i e*, away from the wheel).
- Grade 2: Ice or snow on blocks and also near-to the frictional contact, but the ice and snow can be observed not to be in-between block and wheel.
- Grade 4: Ice and snow are covering the brake blocks completely.
- Grade 5: Ice and/or snow can be observed in-between block and wheel.

Note that that Ice-grade 4 actually means that the status of the block-wheel contact cannot be judged or graded. Ice and snow may be present at the contact interface but it is impossible to distinguish if that is the case.

In addition to air temperatures and ice build-up, metrological information from weather stations at locations near to the test sites for brake testing (see Figure 3) has been acquired. The locations of the test sites have been added to the map using GPS data from some chosen brake cycles. The data include the following metrics:

1. Air temperature T_{air} [°C]
2. Surface temperature T_{surf} [°C]
3. Air dew point temperature $T_{air,dew}$ [°C]
4. Surface dew point temperature $T_{surf,dew}$ [°C]
5. Air humidity RH [%]
6. Wind speed, average v_{wind} [m/s]
7. Wind speed, maximum $v_{wind,\ max}$ [m/s]
8. Snow precipitation P_{snow} [mm/30 min]
9. Rain precipitation P_{rain} [mm/30 min]
10. Melting P_{melt} [mm/30 min]

Based on air temperature and snow precipitation, a metric that describes the possibility for snow drift D_{snow} could be calculated based on a report developed for assessing risks of winter problems in road traffic[20]. According to the report, snow is prone to drifting if all of the following conditions are fulfilled:

1. Snow has fallen during the 14 recent days. The snow precipitation[21] shall be at least 2.0 cm (solid form) under a period of 24 h.
2. **During** the last snowfall with at least 2.0 cm snowfall the air temperature (half-hour readings) has been higher than +0.5 ºC at the most 6 times (3 h totally, does not have to be in succession).
3. **After** the last snowfall with at least 2.0 cm snowfall, rain (half-hour readings) has occurred no more than 3 times (1.5 h totally, does not have to be in succession).
4. **After** the last snowfall with at least 2.0 cm snowfall, the air temperature (half-hour readings) has been higher than +0.5 ºC at the most 12 times (6 h totally, does not have to be in succession).

Metrological data were received for the past four years. This also allows for a statistical comparison between different winter seasons, see Section 5.4.

[20] S. Möller, Calculation model for VädErsKombi (in Swedish), version 1.00, VTI notat 38-2003, *The Swedish national Road and Transport Research Institute*, Linköping Sweden, 2003

[21] A requirement on wind speed given in the report has been neglected. It is assumed that the running train provides the required speed for drifting of the snow.

The degree of bedding-in of brake block friction surfaces was quantified using photos of the block friction contact areas. The wagons with organic brake blocks had previously been in traffic with the same sets of brake blocks. For this reason they were 100 % bedded-in. It can be mentioned that some areas with thermally degraded organic binder material was present on the contact surfaces. For documentation purposes the areas of organic composite blocks that showed signs of thermal degradation were quantified using the same scheme as used for quantifying not bedded-in areas of the contact, see below. It is unclear how these areas contribute to the braking performance of the blocks.

The sinter brake blocks that were fitted on the test wagons were the same ones that were used during the 2019–2020 test campaign. Efforts were made to fit the blocks on wheels having a wheel diameter that deviated as little as possible from the diameter during the previous tests. For the sinter brake blocks, one entire week prior to the test campaign was dedicated to bedding-in of the blocks running from Borlänge to Kil employing a mix of stop braking cycles and continuous braking applications (while maintaining the speed using the locomotive). The wagons were unloaded during these bedding-in runs.

The quantity of non bedded-in area of all brake blocks were assessed by the following procedure, see also Figure 8:

1. Contact areas of brake blocks are faced upwards and photos are taken.
2. Photos are catalogued in a database to link with their positions on the wagons.
3. Photos are imported into the Matlab environment, see Figure 8a.
4. The block exterior of the contact surface is marked manually using mouse cursor positions in the Matlab environment, see Figure 8b. First and last points are at the block external part, see blue circle. In similar fashion are unworn block areas also introduced, see dark grey coloration. Bedded-in areas are shown as light grey.
5. Adjustment of photo view Figure 8c to nominal block rectangular shape (rotation and warping), see Figure 8d, in order to ensure non-biased data that would otherwise be introduced by the point-of-view angle at which the photo was taken.
6. Calculation of block bedding-in state comparing area (*i e* number of pixels in different areas)

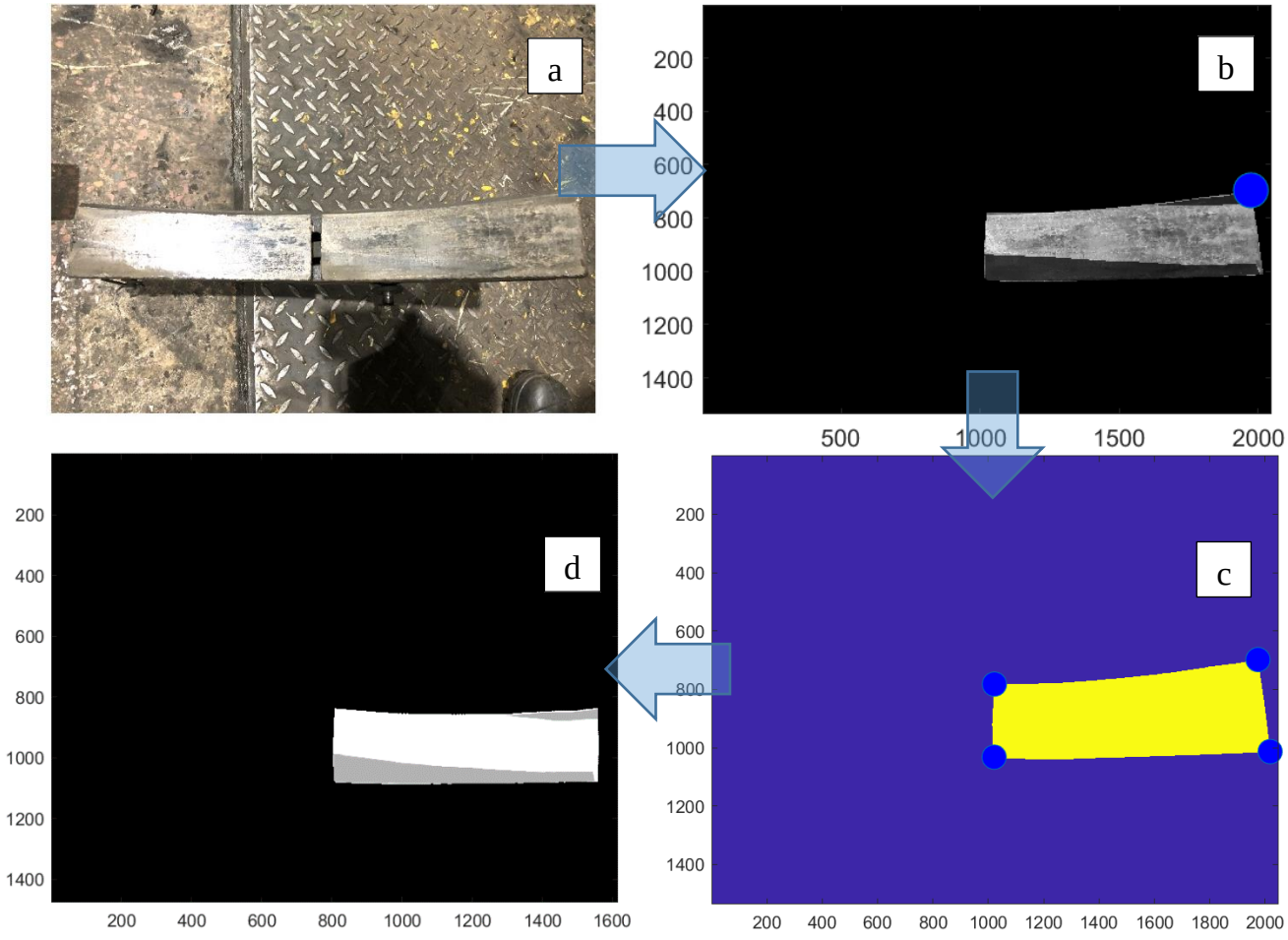

Figure 8 Example of bedding-in state quantification of brake block from photo. In (a) the photo is shown as imported to Matlab software with its wagon number and position given in the header. In (b) the block exterior of the right block has been introduced using graphical inputs (light grey area) and in addition the non bedded-in areas have been marked (dark grey areas). In (c) block corners are identified and in (d) the block has been rotated and warped into a near rectangular shape allowing for calculation of bedded-in area and of the entire (nominal) contact area.

4. RESULTS AND DISCUSSION

In Part 1 the focus is on braking distances for brake cycles having the wagons equipped with uniform brake block types. In Part 2 the focus is on measured forces and braking energies. Part 3 focus on block temperatures, ice build-up, and bedding-in of blocks. Note that the organic composite blocks are perfectly bedded-in from prior usage, whereas the sinter blocks show various bedding-in states, as detailed in Part 3.

As previously explained only the four first stops were for loaded wagons. The wagons were then equipped with organic composite brake blocks. The results from these four stops will be mentioned only briefly in the following section on braking distances. All other results are for unloaded wagons.

The three different driver instructions that were employed at the tests are summarized in Table 1 (see also Chapter 2). It was found that for the test train the *normal brake conditioning* (Driver instruction 1) resulted in a speed decrease of about 16 km/h whereas the *enhanced brake conditioning* (Driver instruction 2) results in a speed decrease of 24 km/h. The initial train speed was 100 km/h.

Table 1 Summary of employed driver instructions. The locomotive is unbraked during all tests, *i e*, also during brake applications.

Driver instruction	**Denomination**	**Brake usage**
1	normal brake conditioning	Brake application every 10 minutes with main brake pipe pressure lowered by 0.6 bar. Brakes applied for 13 s.
2	enhanced brake conditioning	Brake application every 15 minutes with main brake pipe pressure lowered by 1.0 bar. Brakes applied for 10 s.
3	provocative brake conditioning	Northbound or southbound: employ “Driver instruction 2” up to midways (includes first stopping test). After this, make no further brake applications except for the second stopping test.
4	frequent stop braking	Every 15 minutes a braking test is performed to stop. No additional brake applications.

4.1. Part 1: Braking distances

The braking distances measured for the test train can be compared to nominal braking distances based on the UIC leaflet 544-1, see Appendix A which gives the details of considerations for the case with unloaded wagons. The calculated UIC nominal braking distance is introduced in some of the figures in the following.

4.1.1. Stop braking of loaded wagon with organic composite brake blocks

For the four tests with loaded wagons, a histogram of braking distances is shown in Figure 9. The four tests were performed for UIC snow whirling conditions W3–W4 and temperatures between -13 ºC and -11 ºC. The average braking distance was 526 m and the standard deviation 39 m. The braking distances were very short, and it was found that the tests gave wheel flats on one axle. For this reason, testing on fully loaded wagons was abandoned for

the rest of the test campaign. The resulting braking distances can be compared to a nominal braking distance of 683 m, as calculated for the short test train[22] based on information in UIC 544-1 (c.f. Appendix A in which the detailed calculation is performed for the unloaded case).

The fourth of the four stops was the shortest with a braking distance of 480 m. This braking distance implies a braked weight percentage of each of the wagons of 140%. The braking of the loaded wagons constitutes very powerful braking.

It needs to be pointed out that wheel flats on three axles resulted after these initial tests with loaded wagons. The wayside wheel impact load detector (WILD) at Niemisel registered, after the fourth (and last) stop braking of the day, that unacceptable forces were resulting from axle 1 of wagon 1 and of axles 3 and 4 of wagon 4[23]. There were no flats after the third stop braking (normal forces registered at the Kalix WILD). In the evening, the tread damage on the wheels, see example in Figure 10, were rounded by a manual effort using an angle grinder. This means that the wheel treads had some deviations remaining from the flats upon restarting the tests with unloaded wagons on the following day. It is presumed that there were increased vibration levels of these wagons during the continuation of the tests.

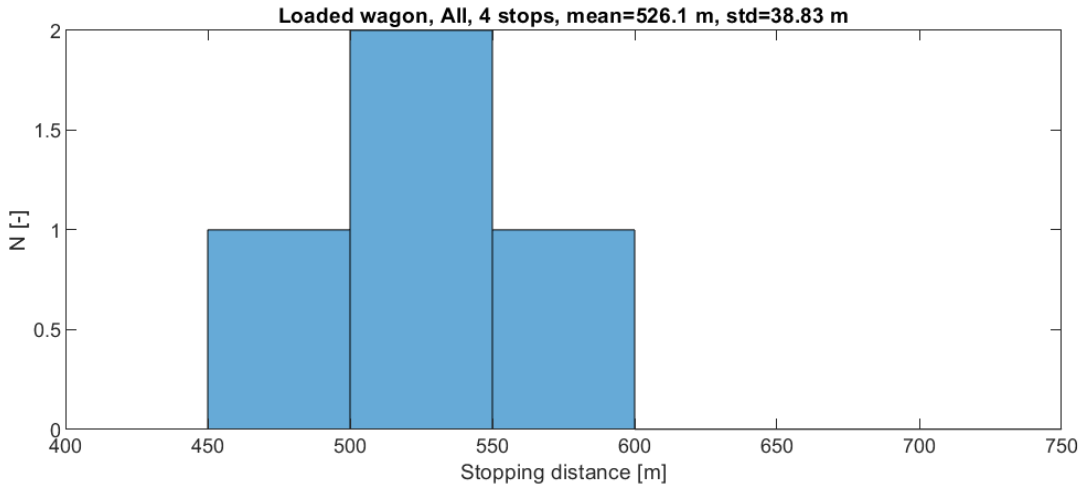

Figure 9 Histogram of braking distances for loaded wagons with organic composite brake blocks at full service braking.

[22] The assumed braking efficiency of the five wagons is 90%

[23] The peak force of axle 1 of wagon 1 was 408 kN (mean load 75 kN), whereas axles 3 and 4 of had peak forces 272 kN and 187 kN respectively (mean loads 77 and 71 kN, respectively).

Figure 10 Example of wheel tread damage resulting from braking with loaded wagons. In top of picture is lower part of block with an icicle.

4.1.2. General on stop braking cycles (unloaded wagons)

A total of 131 stop braking cycles were performed by the test train having unloaded wagons and for full service braking (71 stops with organic composite and 60 stops with sinter blocks[24]). These are analysed in the following.

The initial speeds v_{init} of the studied brake cycles are shown in Figure 11. The average initial speed is 100 km/h and the standard deviation is 1.4 km/h. As described earlier, stop braking distances are corrected for differences in initial speed by employing a correcting factor being the square of the ratio between actual initial speed and nominal speed (100 km/h), in accordance with UIC leaflet 544-1. The average brake cylinder pressures for the time duration of full braking pressure[25] are given in Figure 12. There is a variation of pneumatic pressures between the wagons. However, considering an average brake cylinder pressure for the five wagons on finds that the average pressure is 1.24 bar with standard deviation 0.03 bar for the tests with organic composite blocks. For sinter blocks the same average is 1.26 bar with standard deviation 0.03 bar.

[24] 11 of these are tests for which the wagons carry no instrumentation carried out in April 2021. As previously described, three of the stops with organic composite blocks were not analysed because of deviating conditions (two at low initial speeds and one with partial service braking).

[25] Numerically implemented as when cylinder pressure is higher than 90% of maximum braking pressure for that braking cycle

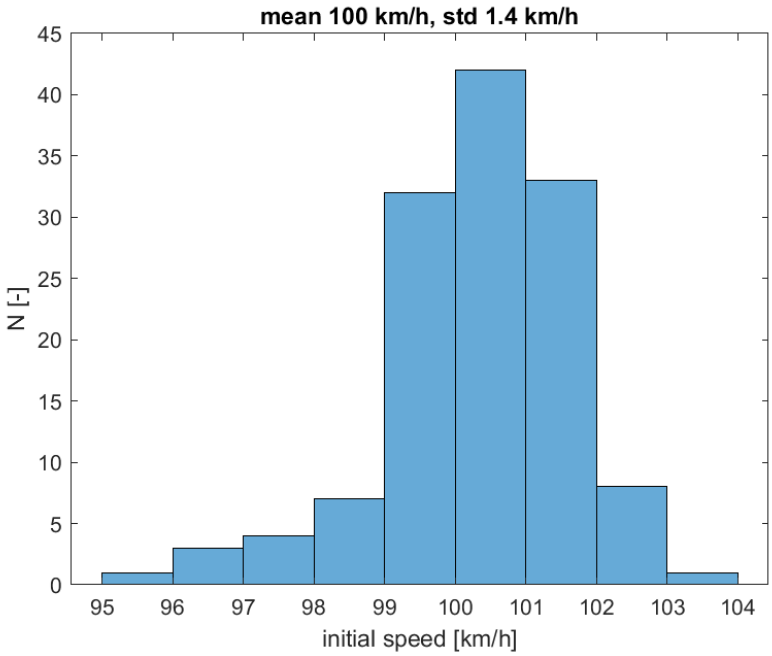

Figure 11 Initial test speeds for the studied stop braking cycles.

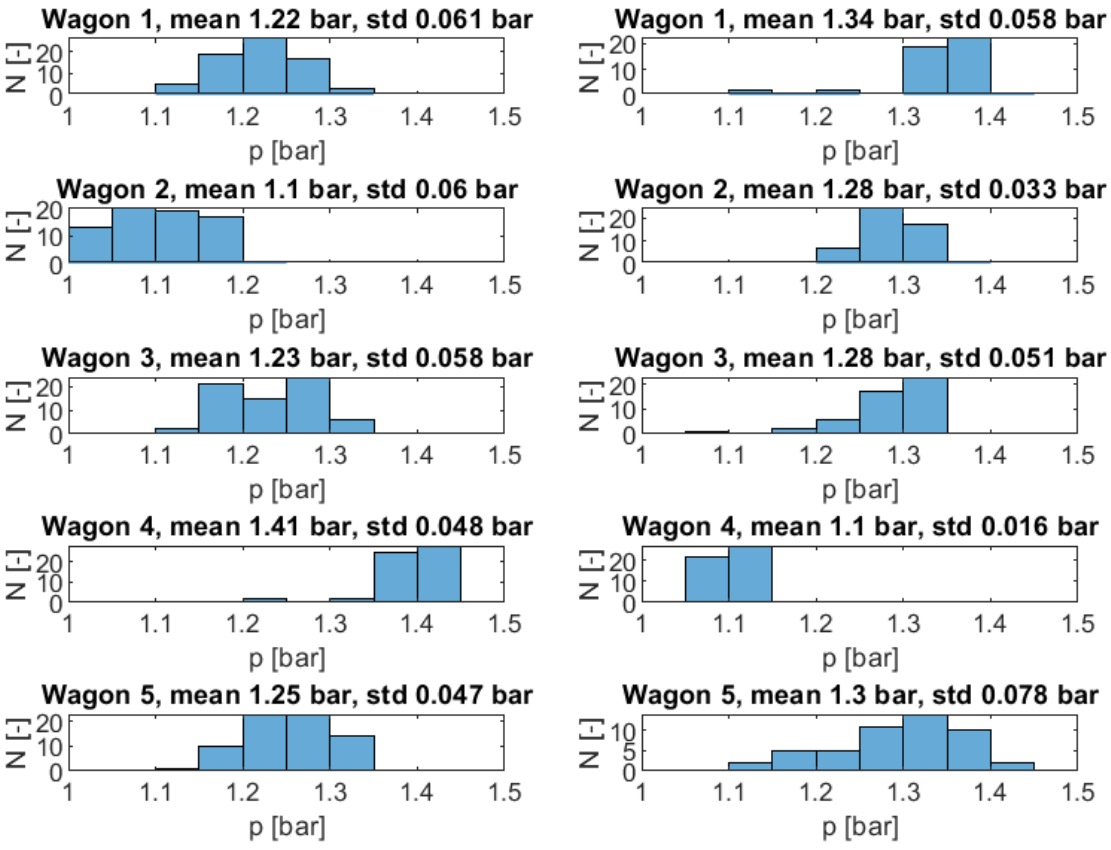

Figure 12 Average brake cylinder pressures during the time with full braking pressure for the studied 203 stop braking cycles. Left column is for organic composites and right column is for sinter blocks.

4.1.3. **Braking distances – general**

A first overview of the braking distances for the entire test campaign with uniform blocks on the test wagons is given in Figure 13. It is clear from the graph that brake cycle no 48 for braking with unloaded wagon and sinter blocks features a braking distance that substantially deviates from the other ones. This brake cycle (braking test number 84 out of all tests), has a stopping distance of 1550 m. It is the second last brake cycle that was performed in sequence in accordance with Driver instruction 3 “provocative brake conditioning”. From the sampled data it was found for this specific test that 1) the brake cylinder pressures on all wagons were normal, 2) the brake triangle forces and hanger link forces in wagons 2 and 4 did not increase in relation to the increase in brake cylinder pressure, 3) the hanger link forces in wagons 2 and 4 did increase in relation to the increase in brake triangle force (even at low force levels). From videos of the ice build-up on the wagons, it was found that large amounts of ice were present on most of the brake block holders and blocks both prior to, and after the tests this day. In addition, snow and ice were present between blocks and wheels in the form of thick layers. Based on this information it is clear that prior to, or at, the initiation of the braking for this particular test, large amounts of ice between block(s) and wheel(s) came off on wagons 2 and 4. The amount of ice could not be compensated for by the stroke of the brake cylinders. Thus, the cylinders went to their maximum extension position and no braking force could after this be transferred to the brake rigging system and hence not to the brake triangles.

Since this sequence of events is not really an effect of the braking performance of the brake blocks it is chosen to disregard this test for the remaining assessments. However, this brake test for which two wagons basically became deprived of their brakes, constitutes a dangerous and extreme case of prolonged braking distances. Detailed information regarding this individual stop braking is given in Appendix B.

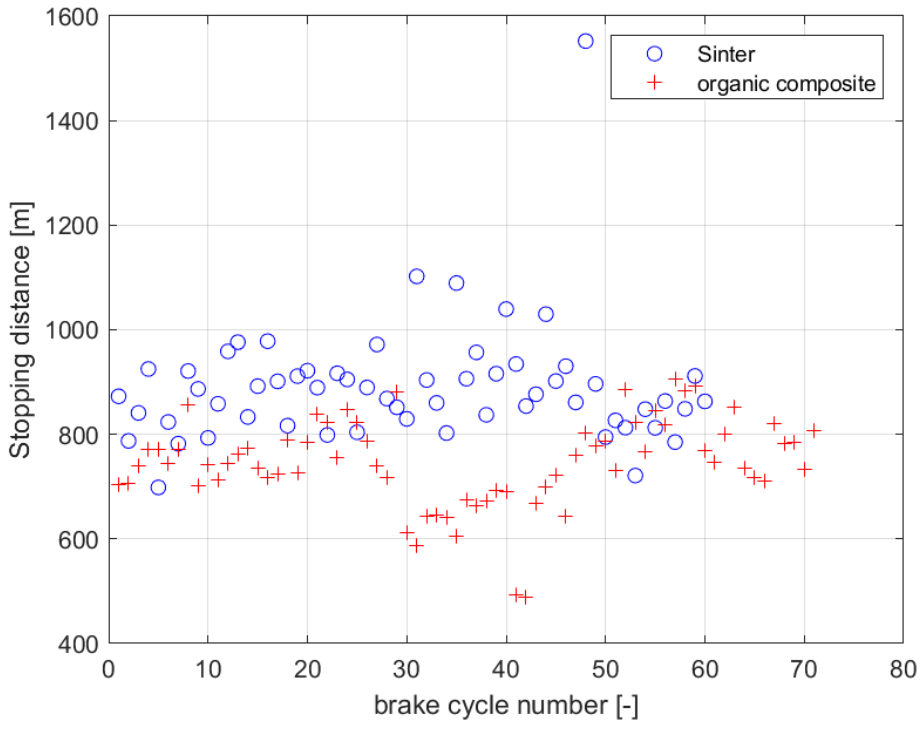

Figure 13 Braking distances for both types of brake blocks as function of brake cycle for each block type.

4.1.4. **Braking distances – organic composite brake blocks**

The organic composite brake blocks were tested under locomotive driver instructions 1–3 and also using the frequent stop braking scheme (Driver instruction 4). The results from all of these tests are visualized in the form of histograms in Figure 14. There is a clear difference in results for R0 and W1–W5 conditions, see snow whirling classification provided in Appendix G. For R0 conditions (no whirling snow), the average braking distance is 695 m with a standard deviation of 76 m whereas for W1–W5 the average is 761 m (*i e*, a 10% increase) with standard deviation 80 m (*i e*, a 5% decrease). In Figure 15 the average and standard deviation of the braking distances are shown as a function of the UIC winter conditions. However, since several different driver instructions are present in the data, these overviews do not give a full picture of winter braking performance for the blocks.

In Figure 16, the same stopping distances are split into groups so that the results for each of the different driver instructions can be seen. The results are rather similar for driver instructions 1–3, with slightly shorter braking distances for driver instruction 1 than for instruction 2 and 3.

For driver instruction 1, denoted "normal brake conditioning", the average braking distances are rather consistent, and no increase can be seen when winter conditions change from reference conditions R0 up to W5 conditions. Moreover, the standard deviation is seen to be larger for R0 conditions than for the others.

For driver instruction 2, denoted "enhanced brake conditioning", there are no data for neither R0 nor W1–W2 conditions. The braking distances for W3 and W5 categories are longer than for driver instruction 1 and so are the standard deviations. Here, categories W3–5 show a large standard deviation and the top of the bar (showing average value with added standard deviation) indicates braking distances that are somewhat longer than the nominal braking distance estimated using information according to the UIC standard (see Appendix A for details).

For driver instruction 3, the so-called "provocative brake conditioning", the results point towards somewhat increased braking distances as compared to the ones for driver instructions 1 and 2. The braking distances indicated for the W3–5 category are longer than for driver instruction 2 by some 3 %. Remembering that this type of conditioning actually means the absence of conditioning brake applications for longer durations, this indicates that the blocks are not very sensitive to such driver behaviour.

The tests for driver instruction 4 are seen to result in substantially shorter stopping distances than the other driver instructions, especially the brake cycle for winter condition W3 that show a stopping distance of 489 m.

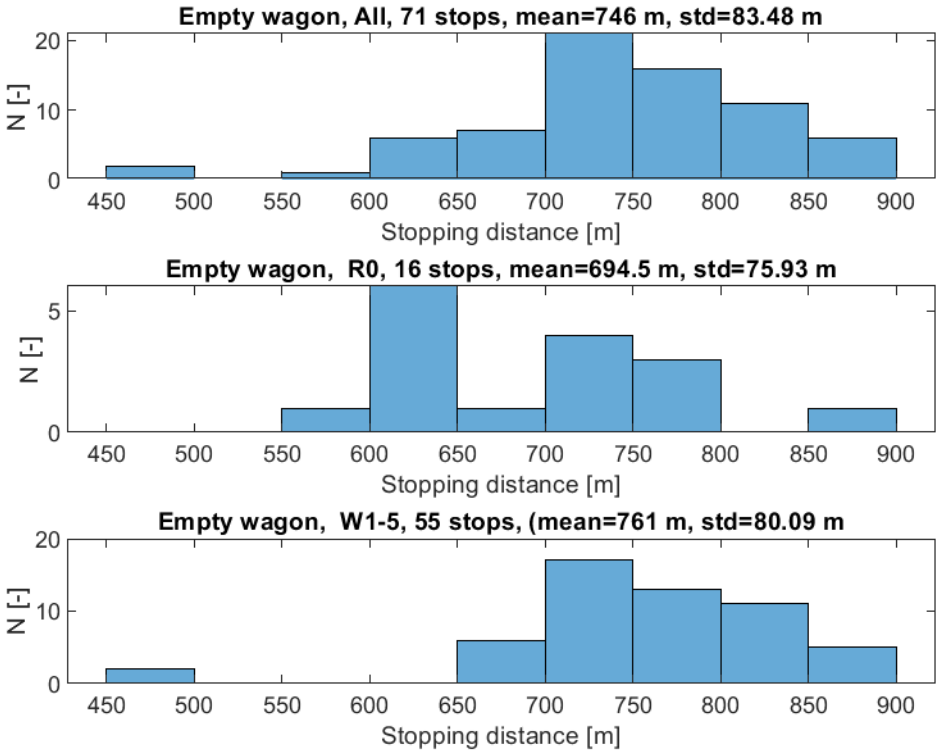

Figure 14 Histogram of braking distances for organic composite brake blocks. All braking cycles (top), braking cycles in conditions R0 (middle) and in conditions W1-W5 (bottom).

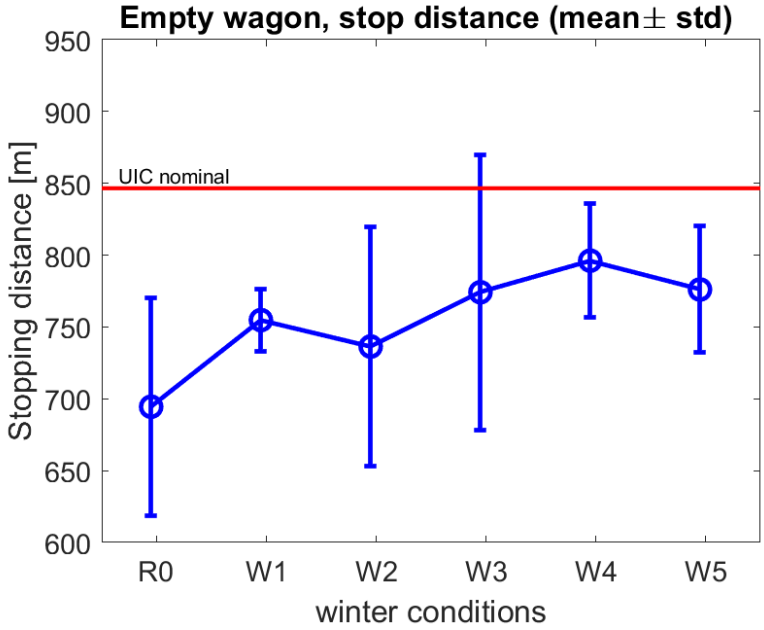

Figure 15 Results for organic composite brake blocks. Graph over average stopping distance indicated by circles, with bar indicating standard deviation, as a function of UIC winter conditions.

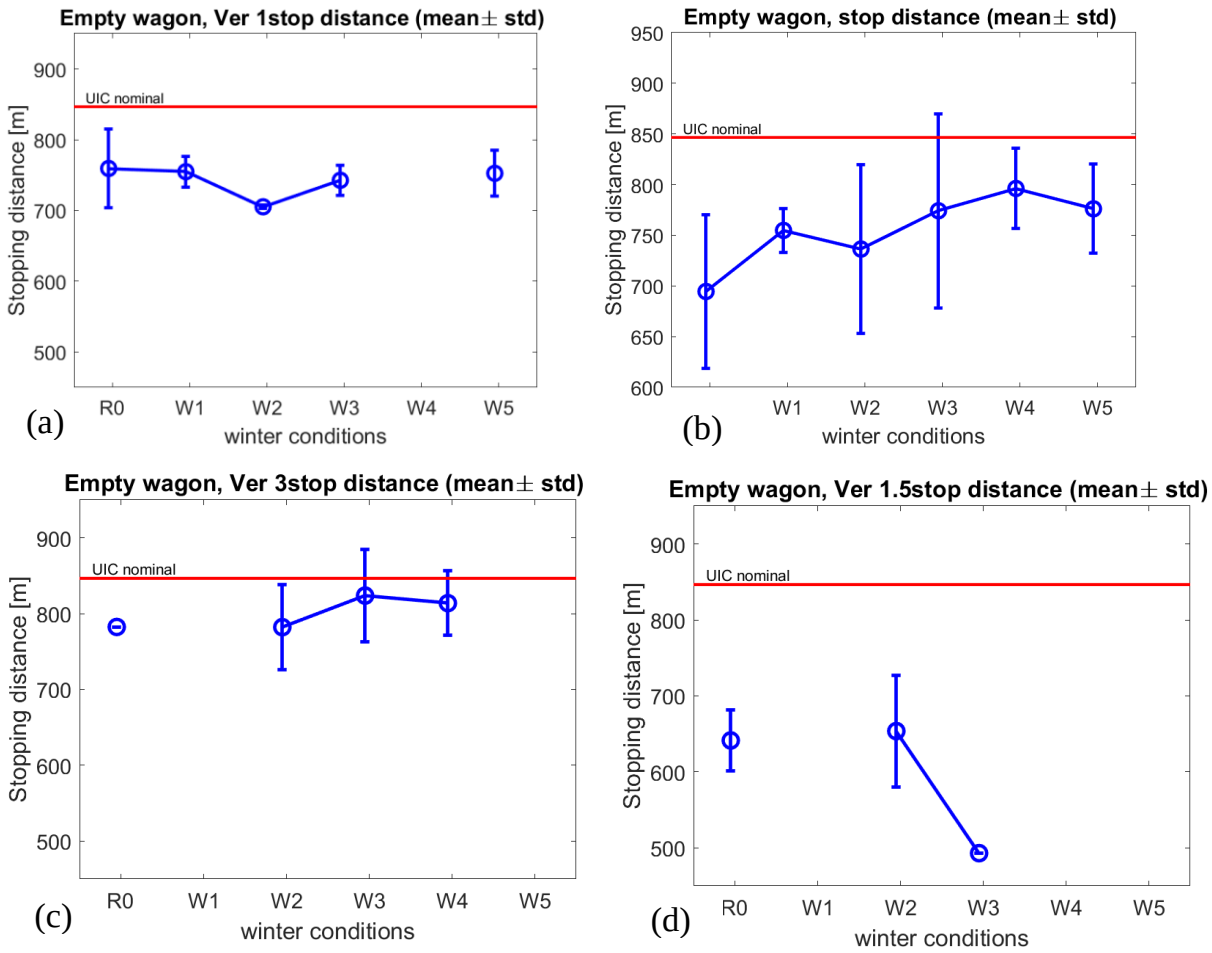

Figure 16 Results for organic composite blocks. Graphs over average stopping distance indicated by circles, with bar indicating standard deviation, as a function of UIC winter conditions. Figure (a) is for driver instruction 1, (b) is driver instruction 2, (c) is driver instruction 3, and (d) is driver instruction 4.

The same stop braking tests are presented in a slightly different way in Figure 17, which allows for straightforward comparison of driver instructions and winter conditions in the form of reference conditions R0, mild conditions (W1-2) and severe conditions (W3-5). One can (again) here see that driver instruction 1 results in short and consistent stopping distances. It is surprising that driver instruction 2, for which data only is present for the group UIC winter indices W3–5, result in substantially longer stopping distances and also a substantially larger spread in the distances. The longest stop distance is 860 m for the instruction 2 as compared to 780 m for instruction 1 for the same group of winter indices. Noteworthy is that the longest braking distance for reference conditions (R0) is 860 m.

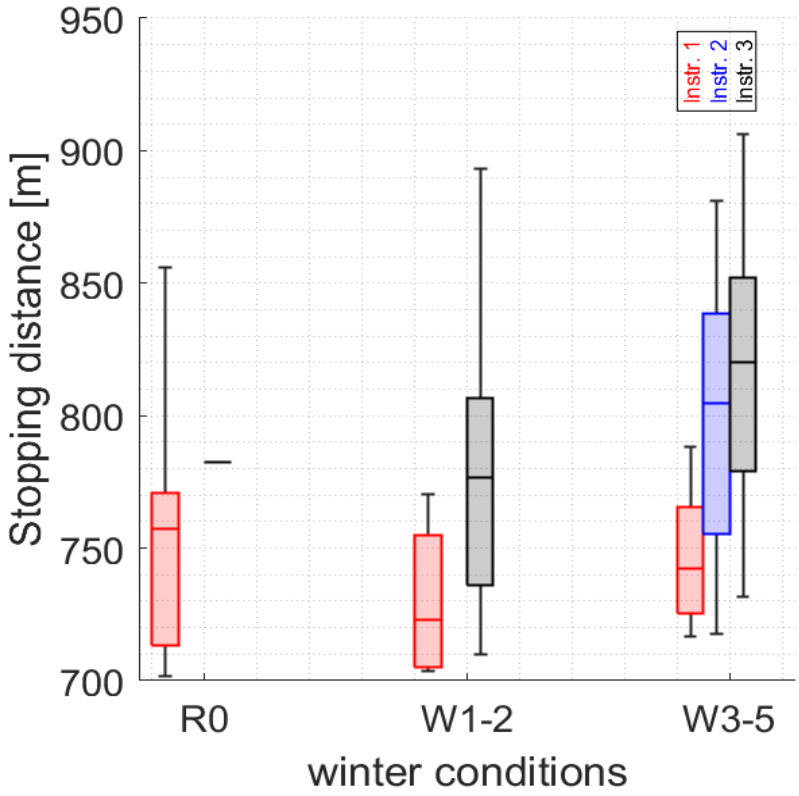

Figure 17 Overview of results for organic composite blocks for driver instructions 1–3 (indicated by colours: red for driver instruction 1, blue for instruction 2 and black for driver instruction 3) and three groups of winter conditions. Resulting stopping distances are indicated by box plots: the median (center line in box), the lower and upper quartiles (box exteriors), any outliers (computed using the interquartile range) marked by circles (in the present figure there are none) and the minimum and maximum values that are not outliers indicated by whisker endpoints.

4.1.5. **Braking distances – sinter blocks**

The sinter blocks were tested under driver instructions 1–3, but not for the frequent stop braking scheme (driver instruction 4). Note that, as motivated previously, the only stop braking with extremely long braking distance with sinter blocks, caused by loss of braking on two wagons, has not been included in this section.

The results are visualized in the form of histograms in Figure 18, including data for all three driver instructions. There is a difference between R0 and W1–W5 conditions. For R0 conditions, the average braking distance is 838 m (organic had 695 m) with a standard deviation of 52 m, whereas for W1–W5 the average is 898 m (organic had 761 m), a 10% increase as compared to R0, and with standard deviation 80 m (a 5% decrease as compared to R0). In Figure 19, the average and standard deviation of the braking distances are shown as a function of the UIC winter conditions. It can be noted that the data generally indicate that the braking distances are longer than the ones given by the nominal UIC braking distance. However, since several different driver instructions are present in the data, these overviews do not give a full picture of winter braking performance for the blocks.

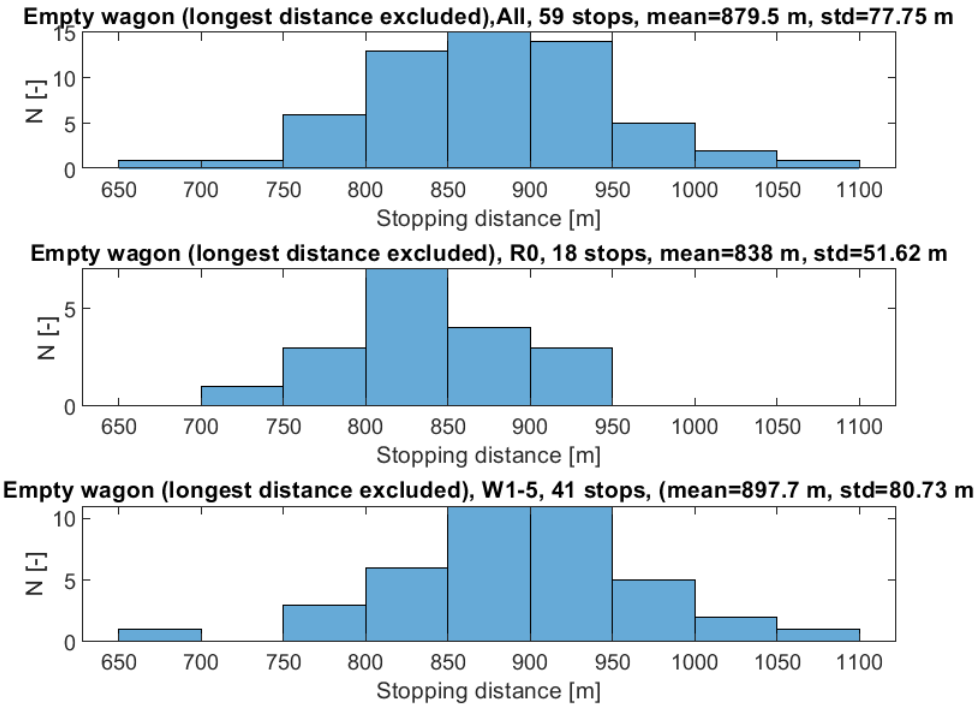

Figure 18 Histogram of braking distances for sinter brake blocks. All braking cycles (top), braking cycles in conditions R0 (middle) and in conditions W1-W5 (bottom).

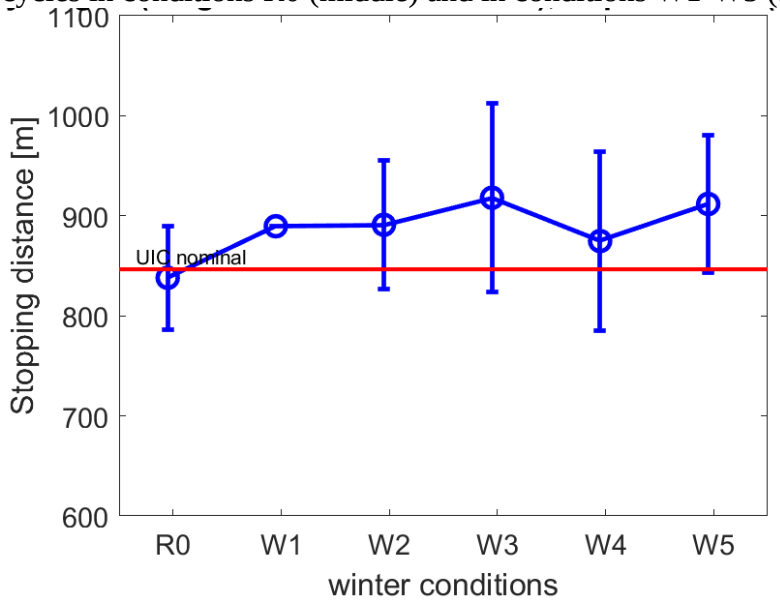

Figure 19 Results for sinter brake blocks. Graph over average stopping distance indicated by circles, with bar indicating standard deviation, as a function of UIC winter conditions (bottom).

In Figure 20, the same stopping distances are split into groups so that the results for each of the three driver instructions can be seen.

For driver instruction 1, denoted “normal brake conditioning”, the average braking distances are rather consistent, and only minor changes in average braking distances can be seen when winter conditions change from R0 (reference conditions) up to W4 condition (no data present for W5). The standard deviation is somewhat larger for W3 and W4 conditions than for R0 conditions.

For the driver instruction 2, denoted “enhanced brake conditioning”, there are no data for neither W1 nor for W4–W5 conditions. The braking distances for W2 and W3 categories are longer than for driver instruction 1, but standard deviation shown for W2 is about the same. In general, driver instruction 2 seems to give braking distances that are somewhat longer than the nominal braking distance estimated using information according to the UIC standard (see Appendix A for details).

For driver instruction 3, the so-called “provocative brake conditioning”, the results show longer braking distances as compared to those for driver instructions 1 and 2. They are also substantially longer than the nominal braking distance estimated using information according to the UIC standard (for W3 adding mean and standard deviation values equals 1060 m, which is 25% longer than UIC nominal distance). Remembering that this driver instruction actually means the absence of conditioning brake applications for longer durations, this indicates that the blocks are rather sensitive to such driver behaviour. In addition, one should remember that also the extremely long braking distance (1550 m) caused by loss of braking of one wagon did occur during testing for driver instruction 3, but data from this particular brake cycle are not part of the current analyses as explained before.

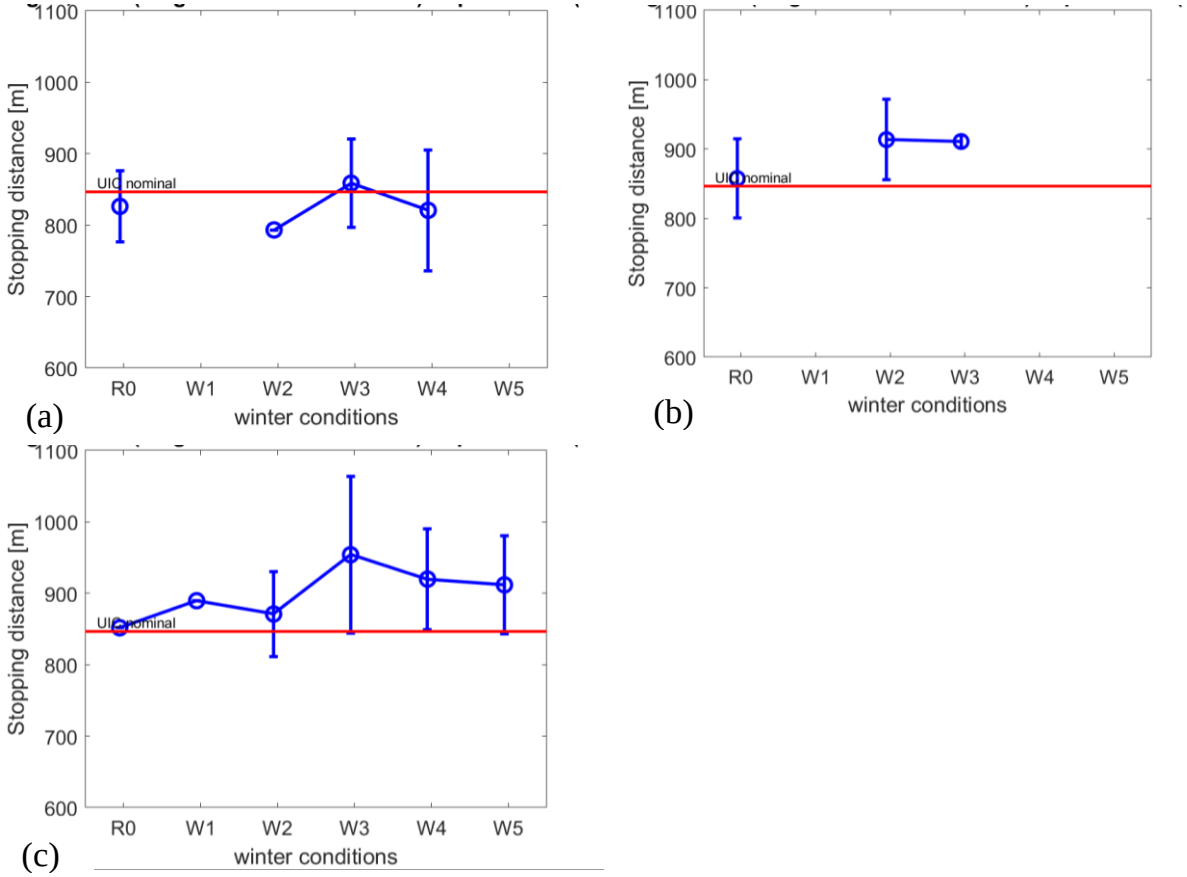

Figure 20 Results for sinter blocks. Graphs over average stopping distance indicated by circles, with bar indicating standard deviation, as a function of UIC winter conditions. Figure (a) is for driver instruction 1, (b) is for driver instruction 2, (c) is for driver instruction 3 (no tests available for driver instruction 4 on sinter blocks).

The same stop braking tests are presented in the form of box plots in Figure 21. Here, one can (also) see that driver instruction 1 results in short stopping distances, however with a larger difference between upper and lower quartiles (and also extreme values) for both R0 and W3–5 categories. In this presentation, driver instruction 2 stands out in the W1–2 category with substantially longer upper quartile braking distances than for driver instruction 1. For the group with UIC winter indices 3–5, driver instruction 3 can be seen to result in substantially longer stopping distances than the two others, with an extreme braking distance of 1100 m, which is 29% longer than UIC nominal braking distance. Moreover, the shortest braking distance found during testing for driver instruction 3 and W3–5 is only slightly shorter than UIC nominal braking distance. Again, this indicates that the sinter blocks are sensitive to the absence of conditioning brake applications for longer durations.

It should be noted that the sintered blocks were not fully bedded-in at the tests. The relationship between bedding-in ratio and braking performance is studied in Results "Part 3", see Chapter 5.

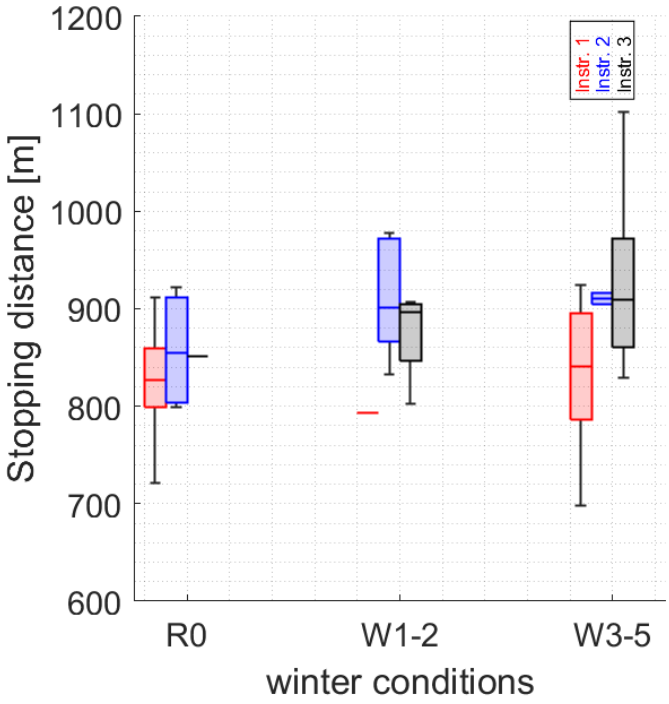

Figure 21 Overview of results for sinter blocks for driver instructions 1–3 (indicated by colours: red for driver instruction 1, blue for instruction 2 and black for driver instruction 3) and three groups of winter conditions. Resulting stopping distances are indicated by box plots: the median (center line in box), the lower and upper quartiles (box exteriors), any outliers (computed using the interquartile range) marked by circles (in the present figure there are none) and the minimum and maximum values that are not outliers indicated by whisker endpoints.

The usage of driver instruction 3 means that driver instruction 2 (brake applications every 15 min) is used up to the first stop braking test, after which no additional brake applications are employed up to the second stop braking test. For this reason, for each stop braking test, the time from the end of the brake application preceding the stop braking and the starting time of the stop braking test was determined. The relationship between time since the previous brake applications and the stopping distance is visualized in Figure 22. Near each mark (representing one stop braking test) also the UIC winter condition index and the air

temperature at the test are indicated. Further, the grade of grey of the marker indicates the numbering of the stop braking (for the ones in driver instruction 3). Not included in the figure is (as for the entire chapter) the stop braking having an extreme distance of 1550 m. For completeness sake, it can be noted that it was performed 3 min after the previous brake application, at –8 °C air temperature, and was brake cycle number 23 out of the 24 ones performed for driver instruction 3.

One can observe that four tests showed stopping distances longer than 1000 m; two of these four occurred a really long time after the previous braking application (over 30 min) and two occurred about 10 min after the previous brake event. For the two former ones, the air temperatures are very low (–24 °C and –21 °C) and they are both from the second brake test of the day (second stop on day 2 and on day 3). The two latter are both for milder temperatures (–12 °C and –10 °C) and are for the third stopping test of the day (of day 3 and 5)[26].

The fifth longest stopping distance 970 m resulted for the second test when employing driver instruction 3 and started 27 min after the previous brake application. For comparison, the first test (thus performed according to driver instruction 2) had a stopping distance of 880 m, implying an increase by 10%. As previously stated, the sinter blocks seem to be sensitive to long absence of conditioning brake applications and somewhat prolonged braking distances may occur already after the first period of absence.

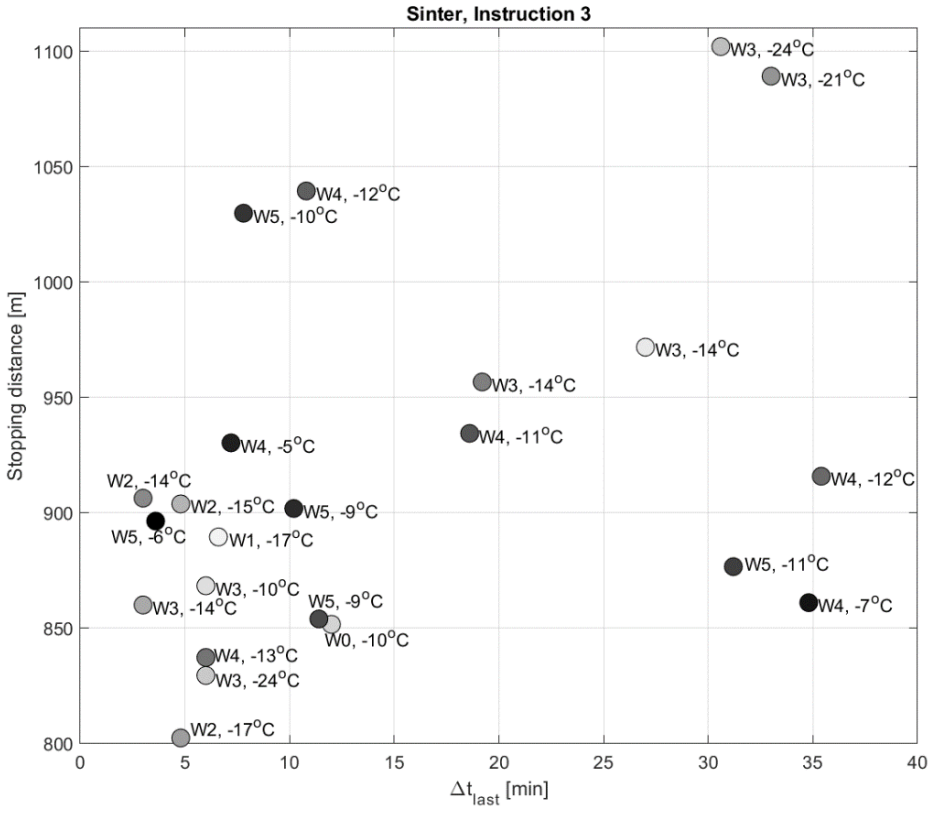

Figure 22 Stopping distance as function of time since previous brake application. At each marker, the air temperature and UIC winter condition grading are presented. In addition, the grey scale of each circle face (fill) indicates the time sequence of the tests. The first test performed for driver instruction 3 has a fully white face and the last one has a completely black one.

[26] The disregarded braking distance of 1550 m was the third stop of day 6.

4.1.6. **Investigation of explanatory relationships.**

Regression models are explored using visualization of response surfaces and by linear regression modelling employing so-called stepwise regression. In the latter, terms are added or removed in an automatic stepwise regression procedure[27]. After an initial fit, the procedure examines a set of available terms and adds the best one to the model if the statistics for the analysis of variance for adding the term gives a p-value 0.05 or less. If no terms can be added, it examines the terms currently in the model, and removes the worst one if removing it has a p-value equal to or greater than 0.10. It repeats this process until no terms can be added or removed.

The result from this stepwise regression analysis is that the braking distances show no dependencies on air temperature or UIC winter condition indices when using a quadratic model[28] for driver instructions 1–3 for organic composite brake blocks. For driver instruction 4 with frequent braking, a minor dependency on temperature can be found with a slight increase in braking distance with a lowering of temperature, however identified over a rather narrow range of temperatures.

In order to find a possible dependency on air temperature for the organic composite blocks, the behaviour within three groups of UIC indices were then studied; firstly R0, secondly W1–W2 and thirdly W3–5. Again, no dependencies could be identified for driver instructions 1–3.

For sinter blocks, no linear models[29] could be identified for driver instructions 1 and 3. For driver instruction 2, the identified model is visualized in Figure 23. The model can also be represented by a 3D surface as shown in Figure 24, in which also the individual braking distance results have been introduced. Here the tendency is that a combination of high UIC winter indices and low temperatures lead to longer braking distances.

In order to investigate how braking distances depend on air temperature for the sinter blocks, the behaviour within three groups of UIC indices was studied; firstly R0, secondly W1–W2 and thirdly W3–5. Dependencies could only be identified for driver instructions 2, for R0 and W1–2 conditions, see Figure 25. There is a trend for increasing braking distances with a lowering of temperatures for both of these conditions.

[27] Matlab function ”stepwiselm” is exploited.

[28] Model contains an intercept term, linear and squared terms for each predictor, and all products of pairs of distinct predictors.

[29] Only an intercept was identified. No dependency on variables

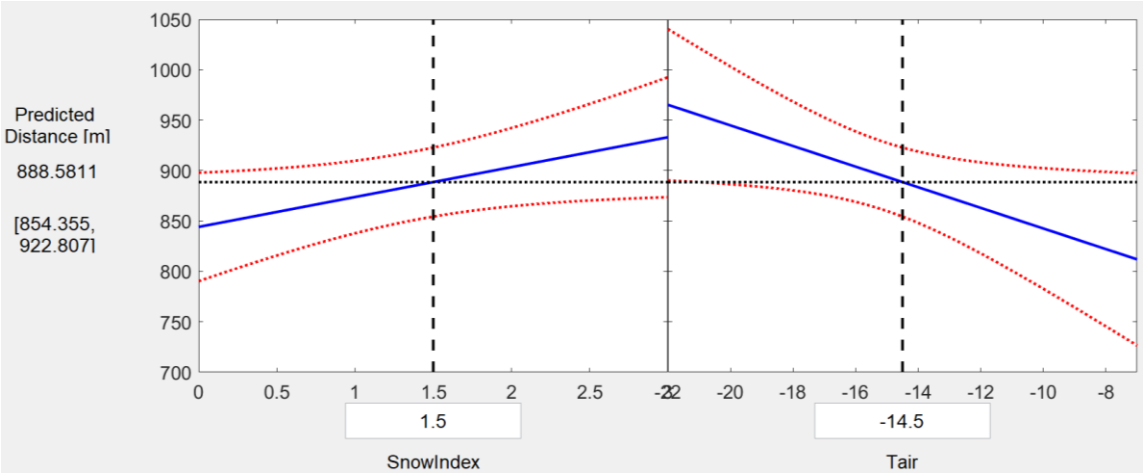

Figure 23 Sinter blocks. Visualization of dependencies for stopping distance [m] on vertical axis for driver instruction 2 as function of *Snowindex*, UIC winter index, and *Tair*, air temperature [° C]. Subplots show dependencies on separate influencing parameters. Fit is plotted in blue and 95% simultaneous confidence bands for the fitted response surface are indicated as two red (dotted) curves on each plot.

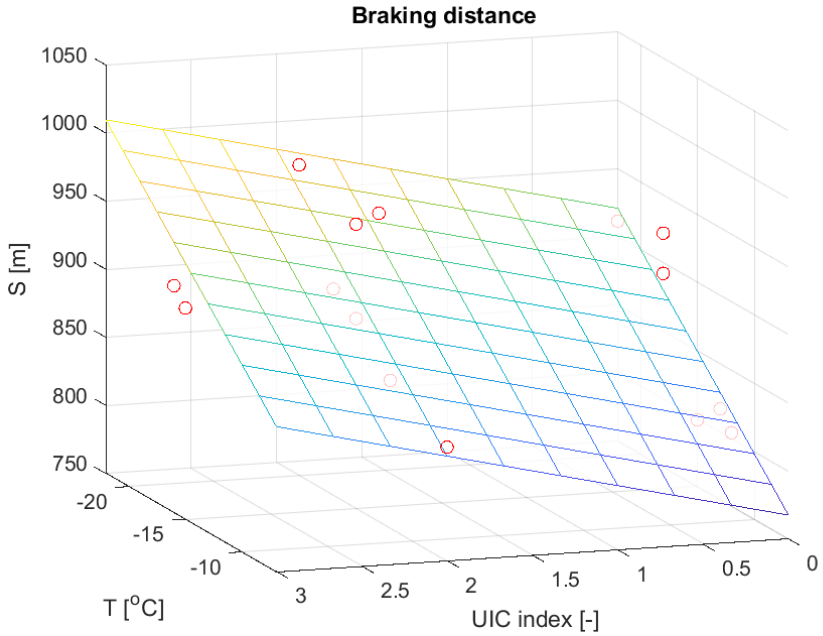

Figure 24 Braking distance results for sinter blocks as function of air temperature and UIC winter index along with the fitted regression surface.

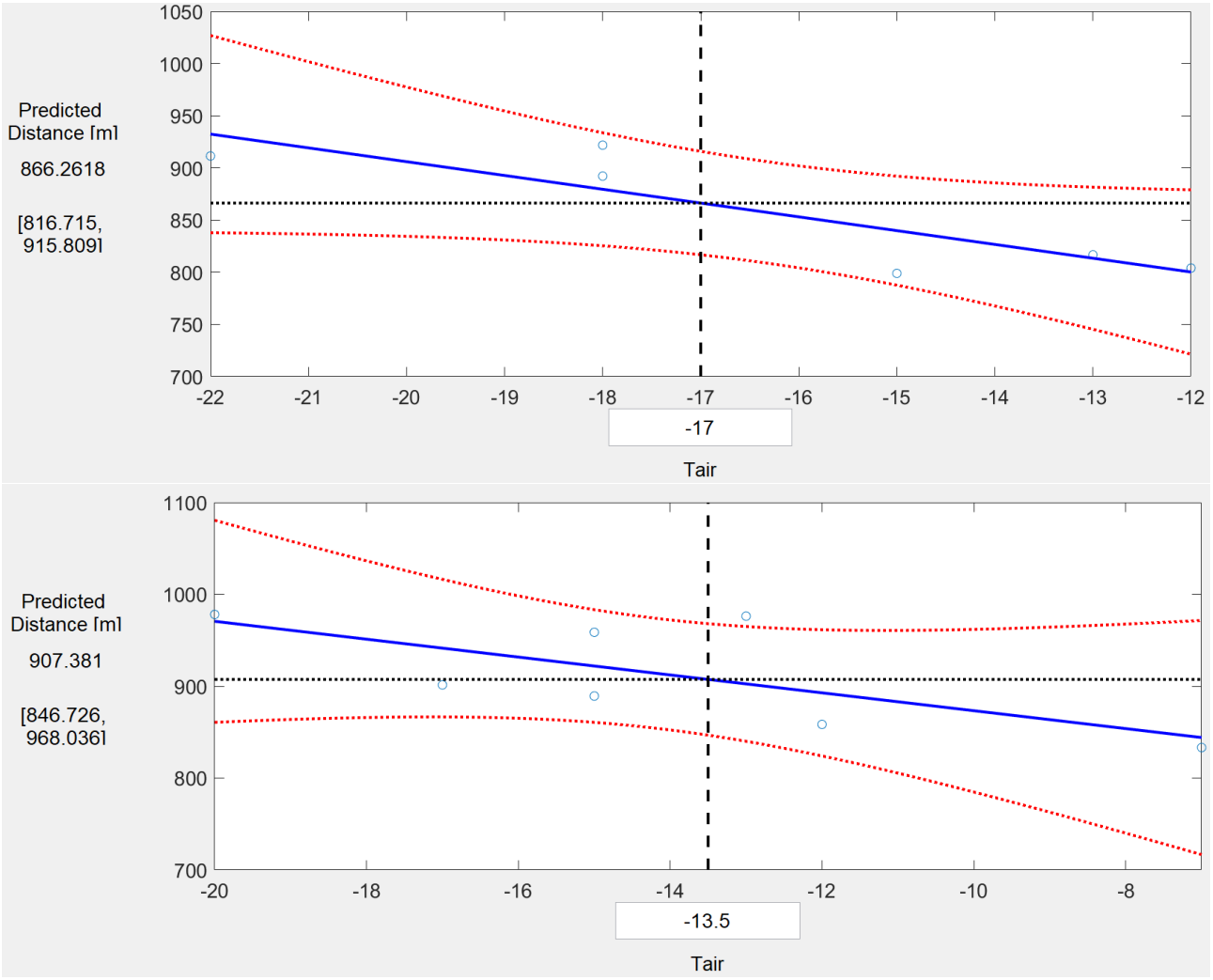

Figure 25 Sinter blocks. Visualization of dependencies for stopping distance S [m] on vertical axis for driver instruction 2. Results for driver instruction 2, with R0 conditions (top) and W1-2 conditions (bottom). Fit is plotted in blue and 95% simultaneous confidence bands for the fitted response surface are indicated as two red (dotted) curves on each plot. Experimental data are marked as circles.

4.2. Part 2: Braking forces, braking energies and friction coefficients

Results from unloaded (empty) wagons are presented in the following, excluding only stops from lower speed, reduced braking and the test having the extreme 1550 m stopping distance.

4.2.1. Block normal forces

Brake block friction forces and brake block normal forces are found from measured brake triangle forces and hanger link forces. A histogram over resulting brake normal forces are presented in Figure 26. For each of the block types, the force distributions are very similar for driver instruction 1 and 2. The distributions resulting from driver instruction 3 show a somewhat larger propensity towards higher forces for the organic composite blocks whereas the propensity is towards lower forces for the sinter blocks. For each of the driver instructions, the average forces on the sinter blocks are always somewhat higher than the force on the organic composite blocks (2.7% higher for driver instruction 1, 6.1% for instruction 2 and 1.3% for instruction 3). No compensation is normally made for these differences.

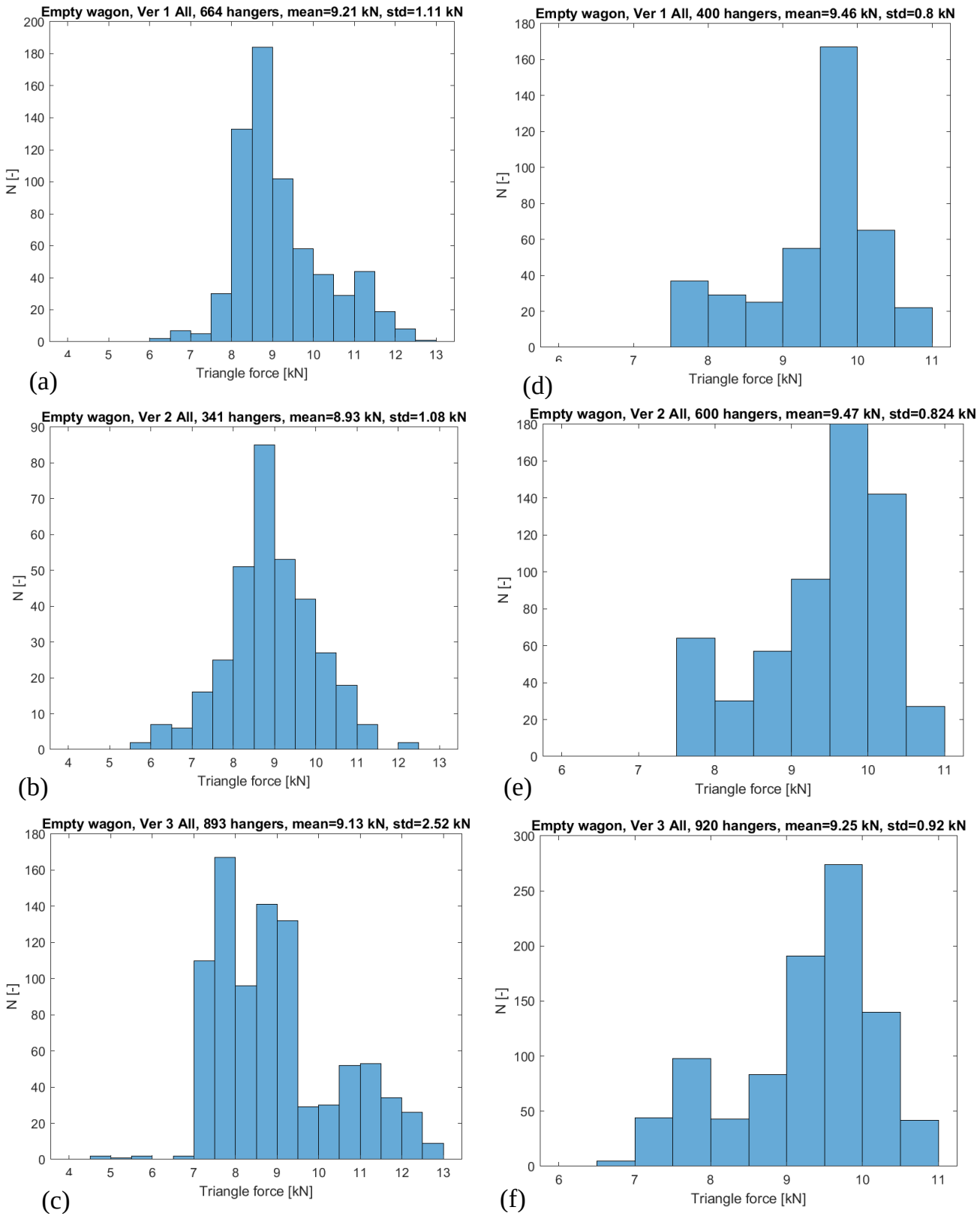

Figure 26 Histograms of average normal forces of individual brake blocks. The average is taken over the time for which the brake cylinder produces the full braking effort. Results for organic composite blocks are the left column, denoted (a)–(c), and results for sinter blocks are in the right column, denoted (d)–(f). Note the different scaling on the force axes. Driver instruction 1 is in top row, instruction 2 in middle and instruction 3 at bottom.

4.2.2. Block friction forces

Focussing on the differences in braking capacity for the studied block materials under winter conditions, the braking performance in the form of friction forces is studied. The presented value for each stop braking is the average force during the time for which the brake cylinder pressure is above 90% of the maximum pressure. Results are available for each block hanger link of wagons 2 and 3, and the first bogie in wagon 4. The results are here presented separately for the situation when the hanger link is in tension (hanger located in front of the wheel, when considering the train travel direction) and in compression (hanger located at the back of the wheel).

The results are presented (Figures 27 and 28) in box charts for driver instructions 1–3 (indicated by colours), and by winter conditions (indicated by position). Driver instruction 1 is to the left (red), instruction 2 is in the middle (blue) and instruction 3 (black) is to the right for each group of winter conditions. Results are given for R0 conditions and for the group W1–2 and finally the W3–5 group.

The results for organic composite blocks are shown in Figure 27. A first observation is that the median values for driver instruction 1 (data represented by red colour) are almost identical for the three winter groups, and also for tension and compression. The interquartile ranges (difference between upper and lower quartile) are also very similar. Some hanger links showing very low energies (outliers marked by circles) can be seen below all lower whiskers. For driver instruction 2, there are only data for the W3–5 group. Here the median value is about the same as for driver instruction 1 for links in tension, but is smaller for links in compression. In addition, the interquartile range is larger than for driver instruction 1, especially for links in compression. The hanger links in compression seem to underperform for driver instruction 2.

For driver instruction 3, the median values are lower than for the two other instructions when more severe winter conditions prevail (W3–5), especially in compression, but the difference is minor for conditions W1–2. The median value is (strangely) somewhat higher for R0 conditions. Note however that the results for R0 conditions are for one single braking test. The interquartile ranges are large for all UIC winter groups.

The results for sinter blocks are shown in Figure 28. The friction forces for instruction 1 show no data for the R0 category, since brake distance tests for R0 conditions were performed with a train having no instrumentation. A first observation is that the friction forces for the sinter blocks in general are lower than the ones for the organic composite blocks, with only a few median values reaching 1.5 kN, which is a common median value for the organic blocks. This indicates an overall weaker braking performance of the sinter blocks. The results for the hanger links in compression show rather similar results to those in tension for all driver instructions, which implies consistent braking performance for the two block positions. Driver instruction 3 has a substantial influence on values for W3–5, with the median energy being reduced in compression, and for both tension and compression the interquartile ranges increase and very low friction forces are common.

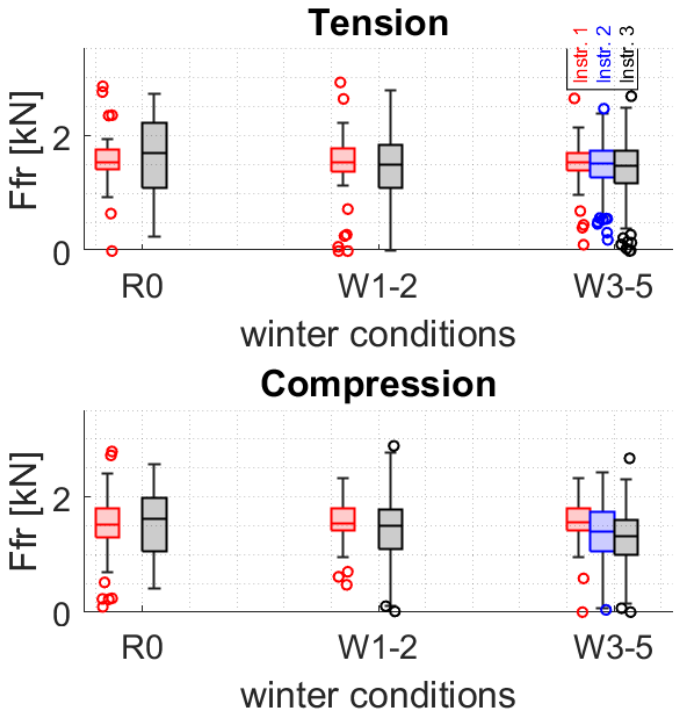

Figure 27 Overview of results for organic composite blocks for driver instructions 1–3 (indicated by colours: red for driver instruction 1, blue for instruction 2 and black for driver instruction 3) and three groups of winter conditions. Resulting friction forces are indicated by box plots: the median (center line in box), the lower and upper quartiles (box exteriors), and outliers (computed using the interquartile range) marked by circles and the minimum and maximum values that are not outliers indicated by whisker endpoints.

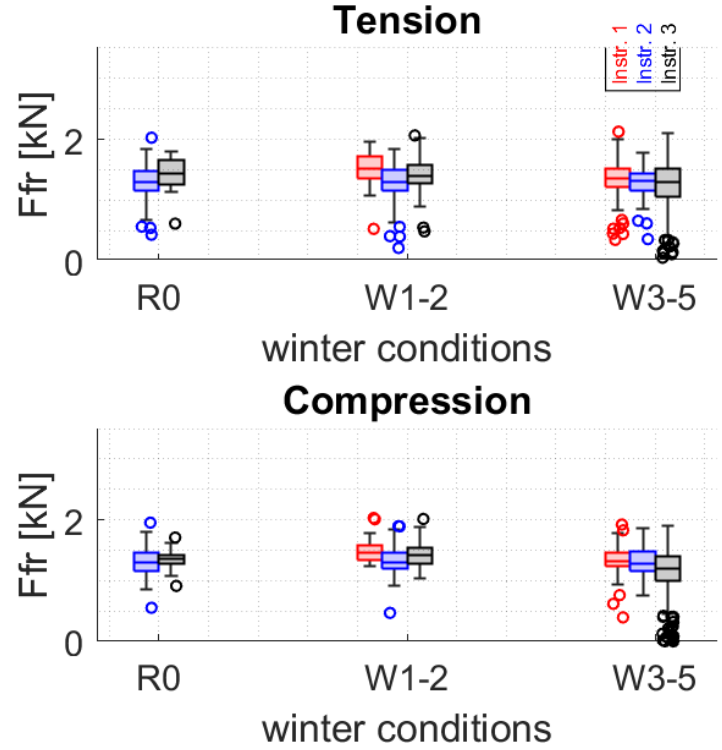

Figure 28 Overview of results for sinter blocks for driver instructions 1-3 (indicated by colours: red for driver instruction 1, blue for instruction 2 and black for driver instruction 3) and three groups of winter conditions. Resulting friction forces are indicated by box plots: the median (center line in box), the lower and upper quartiles (box exteriors), any outliers (computed using the interquartile range) marked by circles and the minimum and maximum values that are not outliers indicated by whisker endpoints.

Linear regression modelling employing stepwise regression is performed on data as previously performed in Section 4.1.6. The individual friction forces are investigated regarding UIC snow index, air temperature and whether the hanger is in tension (+1) or compression (-1). A linear model is employed in the stepwise regression procedure.

For organic blocks, the results are presented in Figure 29 for the three different driver instructions. For driver instruction 1, the stepwise fitting procedure identifies an increase in friction force with decreasing temperature, and a (slight) increase in the force with UIC winter index. No dependency on hanger link loading mode is found (tension/compression). For driver instruction 2, on the other hand, the force is only identified to be depending on the hanger loading mode. The load is lower in compression (indicated as "-1") as compared to tension (+1). Finally, for driver instruction 3, the model predicts a decrease in friction force with increasing UIC snow index, and that the force is lower in compression than in tension.

For the sinter blocks, the results are presented in Figure 30. For driver instruction 1, the identified model predicts decreasing braking force with increasing UIC snow index and with lowering of the temperature. For driver instruction 2 it is the loading mode of the link that is the important variable, whereas for driver instruction 3, all three studied variables are important.

The identified relationships are rather similar for the two block types. For driver instruction 1, the loading mode (tension or compression) is not important for predicting friction forces, whereas for loading driver instruction 2 it is the only identified variable. The difference between these two driver instructions thus seems to introduce a shift in what conditions that affect the friction forces. For driver instruction 3, both UIC snow index and loading mode is important for both block types. For the sinter blocks also the air temperature is of importance.

An increase in UIC snow index or a decrease in air temperature are generally found to lower the friction force, with the exemption being organic blocks in combination with driver instruction 1 for which the opposite is found. When the hanger link loading mode is identified, it is always the hanger links in compression that produce lower force levels and the ones in tension that produce higher forces.

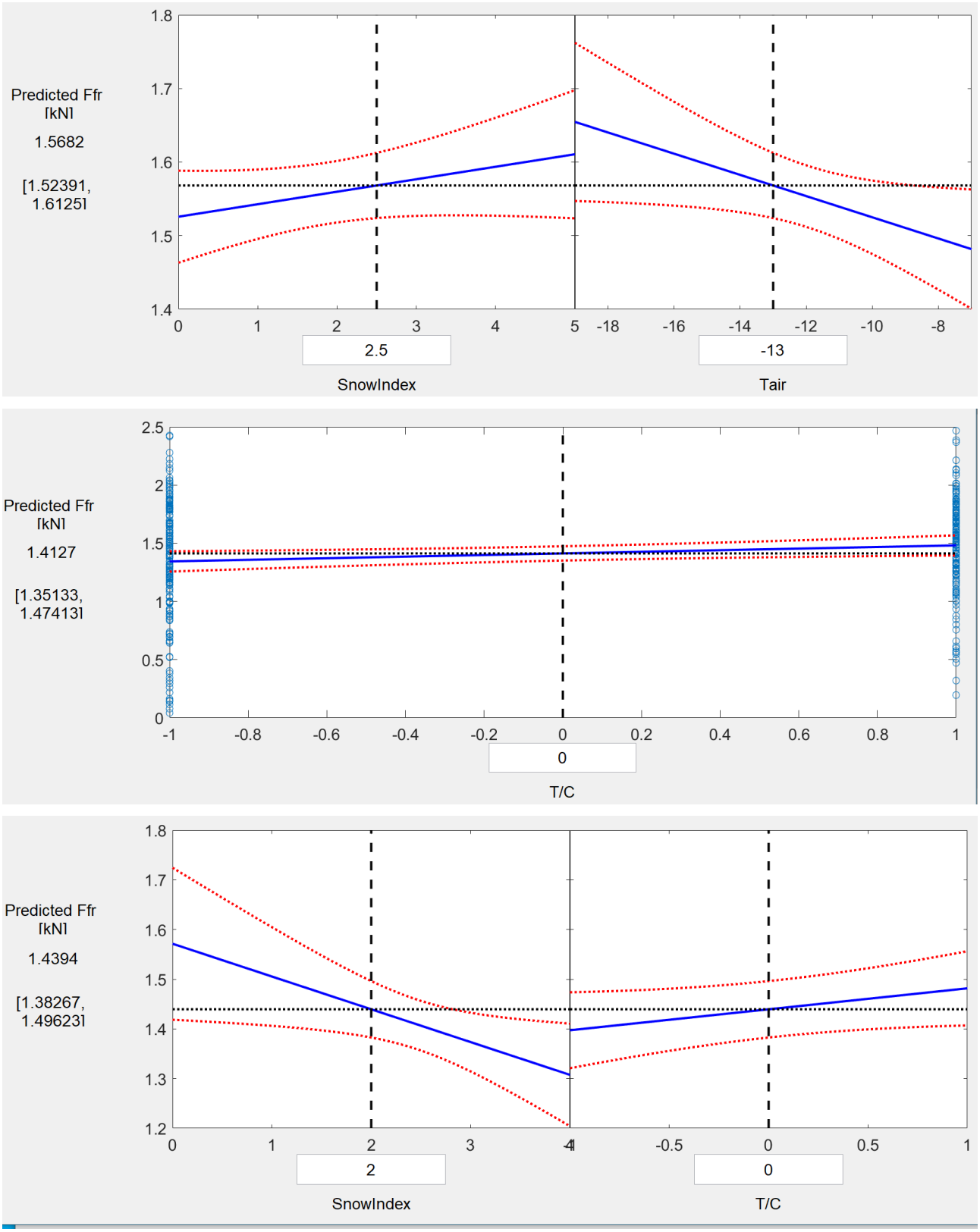

Figure 29 Organic composite blocks. Visualization of dependencies for block friction force [kN] . Results for driver instruction 1 (top), instruction 2 (middle) and instruction 3 (bottom). Fit is plotted in blue and 95% simultaneous confidence bands for the fitted response surface are indicated as two red (dotted) curves on each plot.

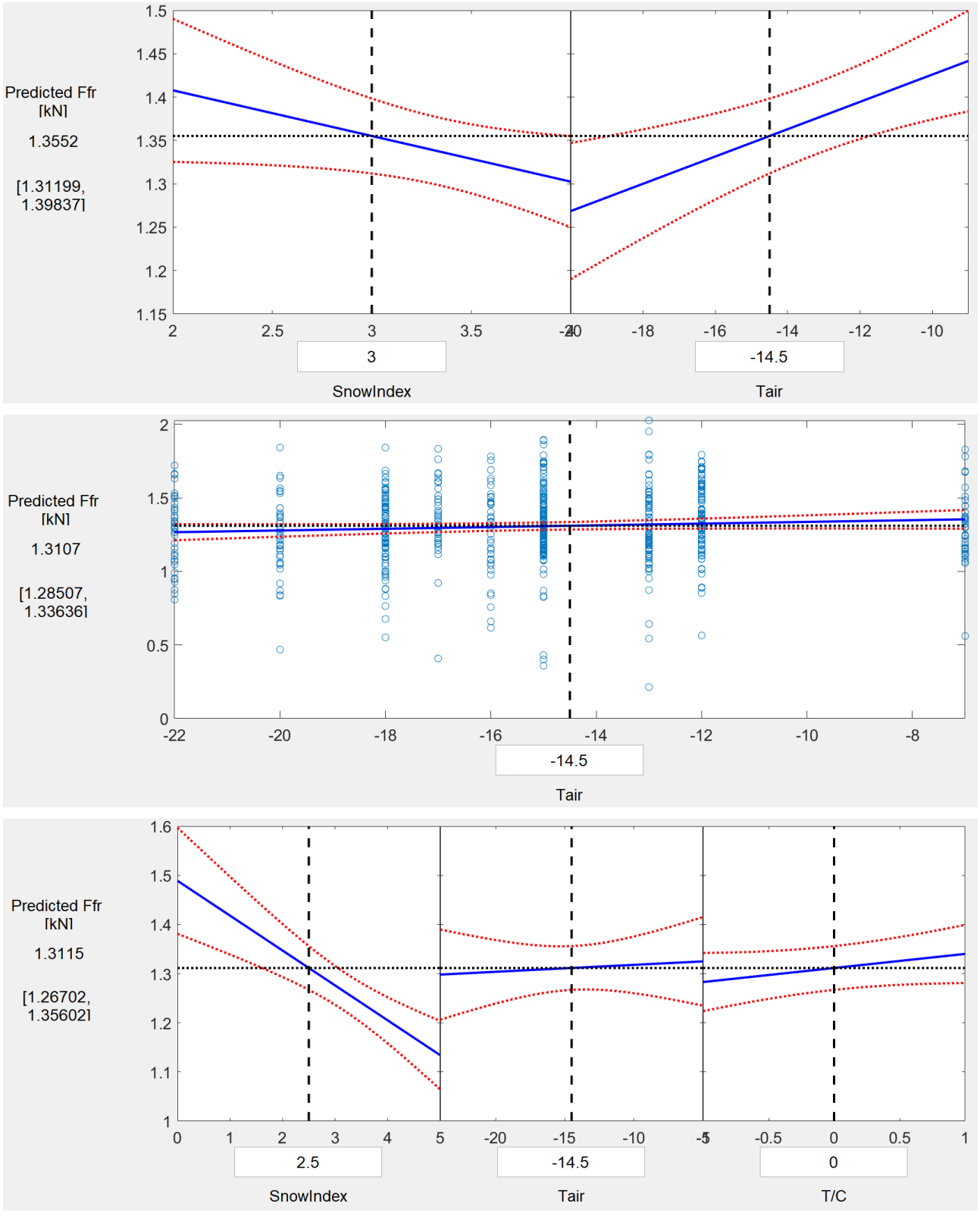

Figure 30 Sinter blocks. Visualization of dependencies for block friction force [kN]. Results for driver instruction 1 (top), instruction 2 (middle) and instruction 3 (bottom). Fit is plotted in blue and 95% simultaneous confidence bands for the fitted response surface are indicated as two red (dotted) curves on each plot.

4.2.3. **Block coefficient of friction**

During the period of full braking pressure, the average[30] friction coefficient has been calculated for each block hanger link of wagons 2 and 3, and the first bogie in wagon 4. The results are again presented in the form of box charts separately for the situations when the hanger link is in tension and in compression.

The results for organic composite blocks are shown in Figure 31 and for sinter blocks in Figure 32. The two figures are at a quick glance very similar (although we here have friction coefficient) to the ones in the previous section that shows the results for the friction forces. This is not surprising since the nominal brake normal forces are the same for all tests. The discussion on similarities and differences between results made in the previous section is thus not repeated here.

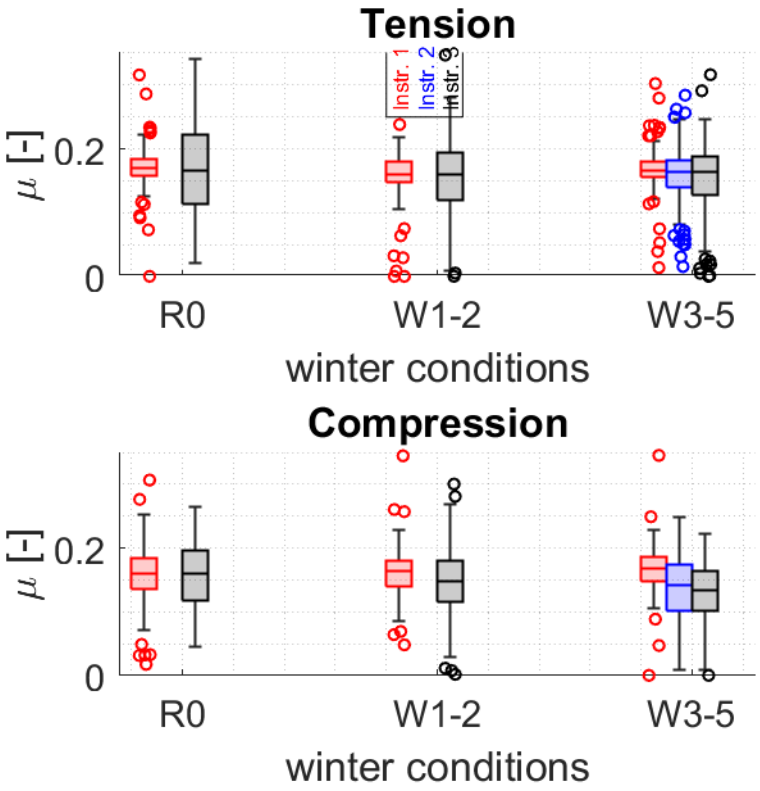

Figure 31 Overview of results for organic composite blocks for driver instructions 1–3 (indicated by colours: red for driver instruction 1, blue for instruction 2 and black for driver instruction 3) and three groups of winter conditions. Resulting coefficient of friction values are indicated by box plots: the median (center line in box), the lower and upper quartiles (box exteriors), any outliers (computed using the interquartile range) marked by circles and the minimum and maximum values that are not outliers indicated by whisker endpoints.

[30] The average is based on braking distance.

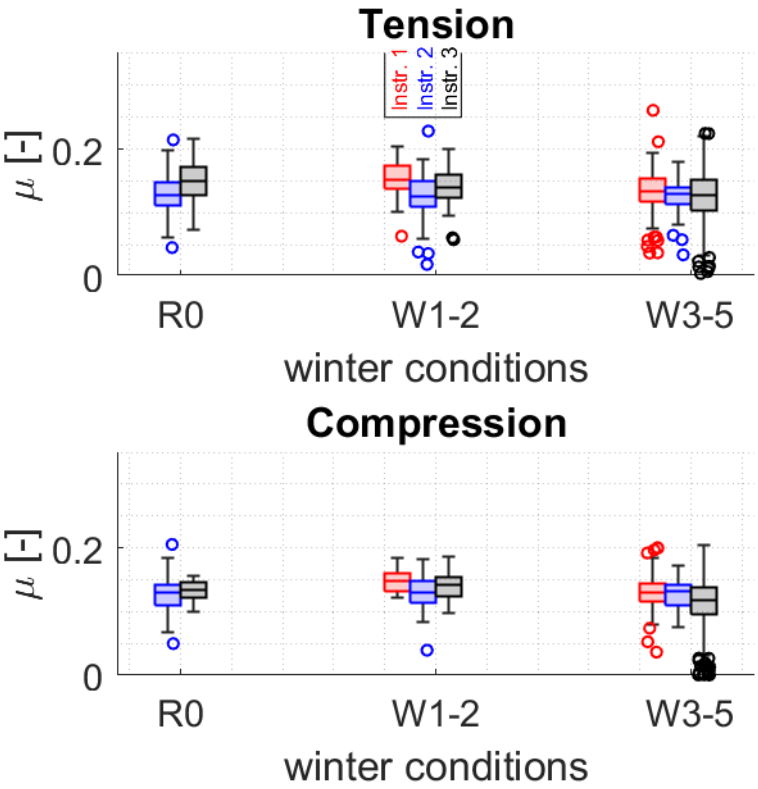

Figure 32 Overview of results for sinter blocks for driver instructions 1-3 (indicated by colours: red for driver instruction 1, blue for instruction 2 and black for driver instruction 3) and three groups of winter conditions. Resulting coefficient of friction values are indicated by box plots: the median (center line in box), the lower and upper quartiles (box exteriors), any outliers (computed using the interquartile range) marked by circles and the minimum and maximum values that are not outliers indicated by whisker endpoints.

4.2.4. Time delay to onset of braking for individual block inserts

The braking performance is now studied with respect to the time delay until the onset of the brake friction force for the individual brake block inserts. Here, it has been chosen to employ a criterion based on brake friction force, assessing the time delay value as the time from start of the pneumatic pressure rise in the brake cylinder until the time at which the friction force reaches 50 % of the maximum friction force. The considered maximum force amplitude is the largest registered force for the entire stop for any block insert for the considered wagon and braking.

The resulting time delays are first presented in the form of box charts, see Figure 33 for an overview for organic composite blocks and Figure 34 for sinter blocks. For the organic blocks and driver instructions 1 and 2, the median time delays for hangers in tension are below 10 s, except for driver instruction 2 of W3–5 and for the link in compression it is about 13 s. Driver instruction 3 has a somewhat longer median time delay than the two others, but only by some seconds. For sinter blocks and driver instructions 1–2, the median values are generally higher than for the organic composite blocks, with the delays in compression being between 18 and 30 s, which is substantially longer than the 10 to 13 s for organic blocks. Also for driver instruction 3, the median time delays are substantially longer than for organic blocks, with,

e g, W3–5 showing 27 to 33 s as compared to 13–15 s for organic blocks. Longer median delays points towards reduced braking performance for the sinter blocks.

In general, the interquartile ranges (difference between upper and lower quartile) are substantially larger for sinter blocks than for organic blocks, pointing towards more unreliable braking performance, not knowing the onset of the brake friction forces of the train.

The time delay of the onset of the friction force has a direct effect on the average friction force that is calculated, since the friction force is the average value during the time for which the brake cylinder pressure has at least 90 % of its maximum pressure. An example of the identified relationships between friction force and UIC snow index, air temperature and time to onset of the friction force is given in Figure 35 (block holder loading mode was ignored by the step-wise regression modelling). The time delay can be seen to have a strong effect on the calculated friction force, a much stronger effect than the dependency on UIC snow index, and stronger than the dependency on air temperature.

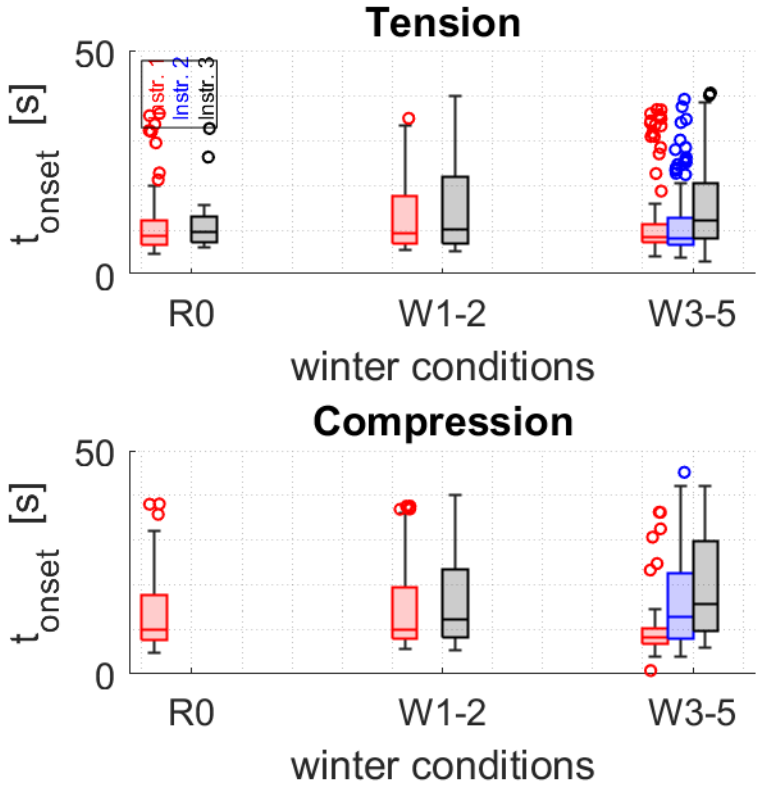

Figure 33 Overview of results for organic composite blocks for driver instructions 1–3 (indicated by colours: red for driver instruction 1, blue for instruction 2 and black for driver instruction 3) and three groups of winter conditions. Resulting time delays till onset are indicated by box plots: the median (center line in box), the lower and upper quartiles (box exteriors), any outliers (computed using the interquartile range) marked by circles, and the minimum and maximum values that are not outliers indicated by whisker endpoints.

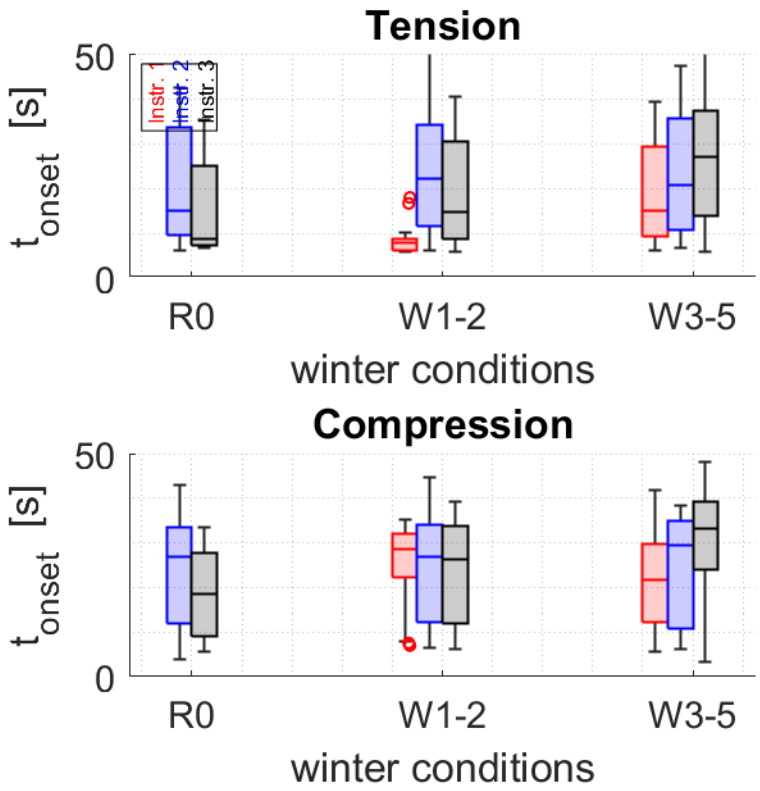

Figure 34 Overview of results for sinter blocks for driver instructions 1-3 (indicated by colours: red for driver instruction 1, blue for instruction 2 and black for driver instruction 3) and three groups of winter conditions. Resulting time delays till onset are indicated by box plots: the median (center line in box), the lower and upper quartiles (box exteriors), any outliers (computed using the interquartile range) marked by circles and the minimum and maximum values that are not outliers indicated by whisker endpoints.

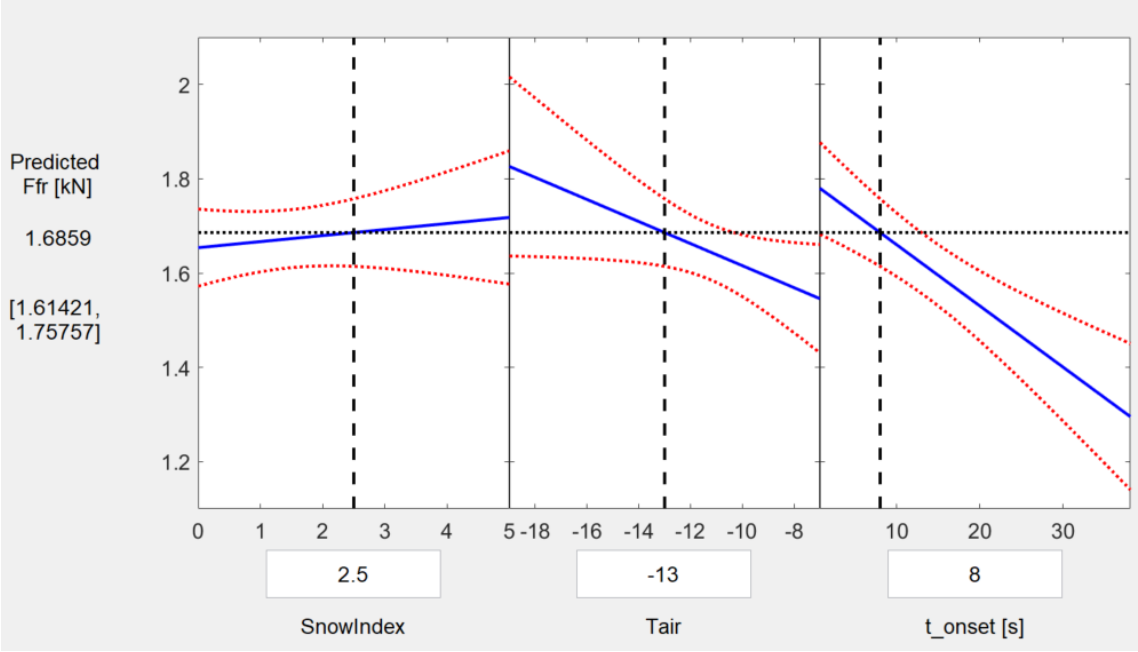

Figure 35 Organic composite blocks and driver instruction 1. Example of dependencies of block friction force [kN] on vertical axis. Fit is plotted in blue and 95% simultaneous confidence bands for the fitted response surface are indicated as two red (dotted) curves on each plot.

The time delays are in Figure 36 and Figure 37 analysed with respect to dependencies when it comes to UIC snow index, air temperature and hanger link loading (tension/compression) as in the previous section. These visualizations show the variations of the time delays for the centre of the parameter ranges. For this situation, the predicted values for organic composites are 13 to 15 s which is about 7 s shorter than for sinter blocks in the same condition. This difference is notable and important for braking performance. Longer or shorter delays could be found by changing the parameter settings.

A comparison with the linear regression modelling performed on the individual friction forces reveal that the time until onset of the friction force can be an important factor for explaining the difference in calculated friction forces in Section 4.2.2 (where it is the average force over the entire time period for which the brake cylinder pressure is high).

For organic blocks and driver instruction 1, the stepwise fitting procedure identified an increase in friction force with decreasing temperature, and a (slight) increase in the force with UIC winter index. The relationships on air temperature is contradictory to the one found for the time delays that predict a higher time delay with increasing force. In total, this implies that the friction force after the time delay must be increasing for lower temperatures.

For driver instruction 2, the force was identified to be depending on the hanger loading mode. A compressive state points towards a lower force, which is consistent with a predicted increase of the time delay. Finally, for driver instruction 3, the stepwise regression modelling predicts a decrease in friction force with increasing UIC snow index, and that the force is lower in compression than in tension. These variations are both consistent with the identified variations of the time delay having a high time until onset for high UIC snow index, and also for compression loading.

For the sinter blocks, the identified regression model for time delay can generally help explain the changes in magnitude of the predicted friction forces. An increase in time delay corresponds to a lowering of the friction force.

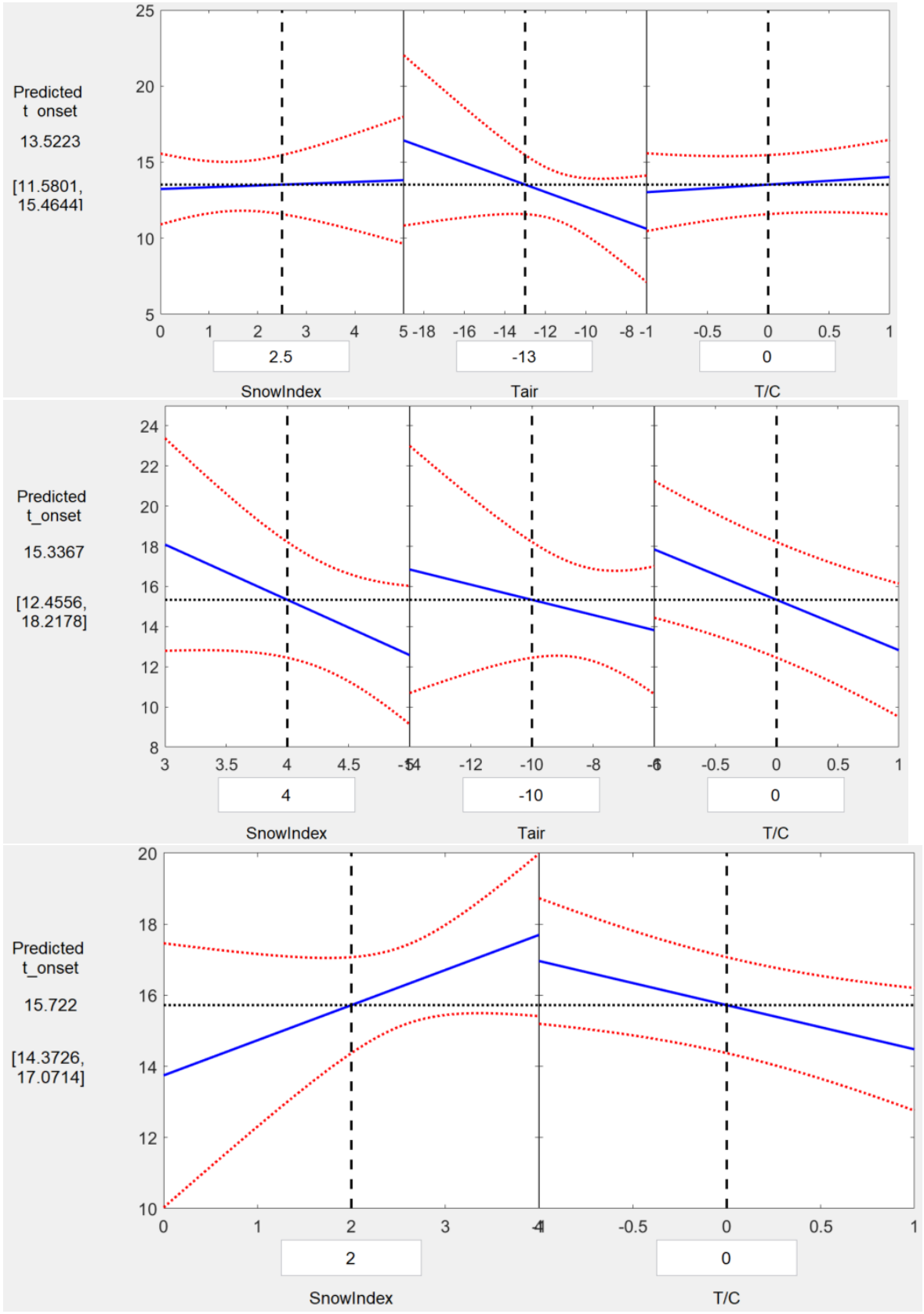

Figure 36 Organic composite blocks. Time delays until onset of friction force [s]. Results for driver instruction 1 (top), instruction 2 (middle) and instruction 3 (bottom). Fit is plotted in blue and 95% simultaneous confidence bands for the fitted response surface are indicated as two red (dotted) curves on each plot.

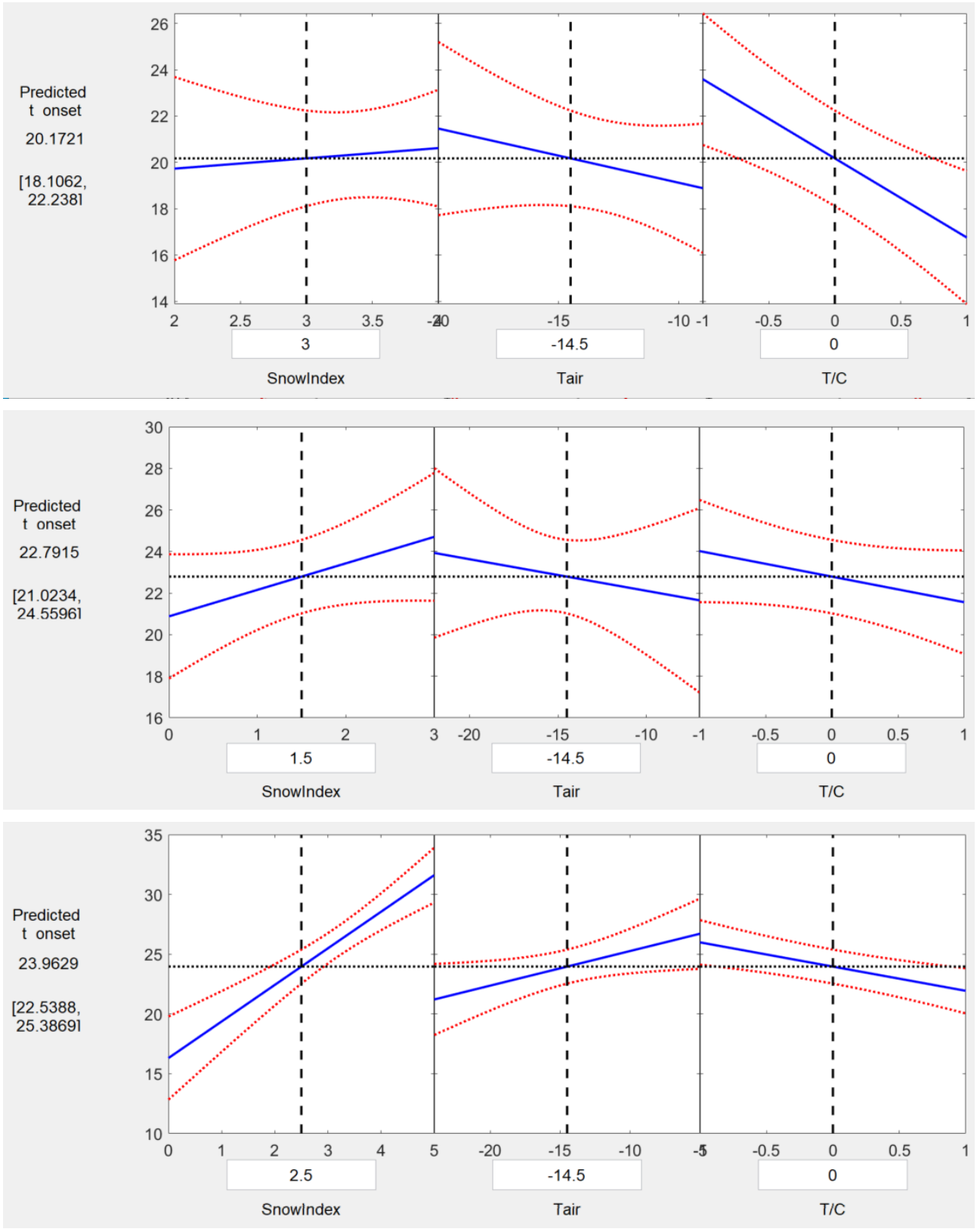

Figure 37 Sinter blocks. Time delays until onset of friction force. Results for driver instruction 1 (top), instruction 2 (middle) and instruction 3 (bottom). Fit is plotted in blue and 95% simultaneous confidence bands for the fitted response surface are indicated as two red (dotted) curves on each plot.

5. PART 3, BLOCK BEDDING-IN, BLOCK TEMPERATURES AND ICE BUILD-UP ON BLOCKS

5.1. Bedding-in state of brake blocks (sinter only)

The organic blocks were, as explained previously, perfectly bedded-in at the start of the tests. For this reason, this section will only be analysing the bedding-in of the sinter blocks. The resulting bedding-in ratios for the assessed blocks on wagons 2–4 are visualized in Figure 38, both as assessed prior to testing and after the tests. Acknowledging that there are differences between the two assessments, only blocks having consistent assessments (within 10%) are used in the following studies.

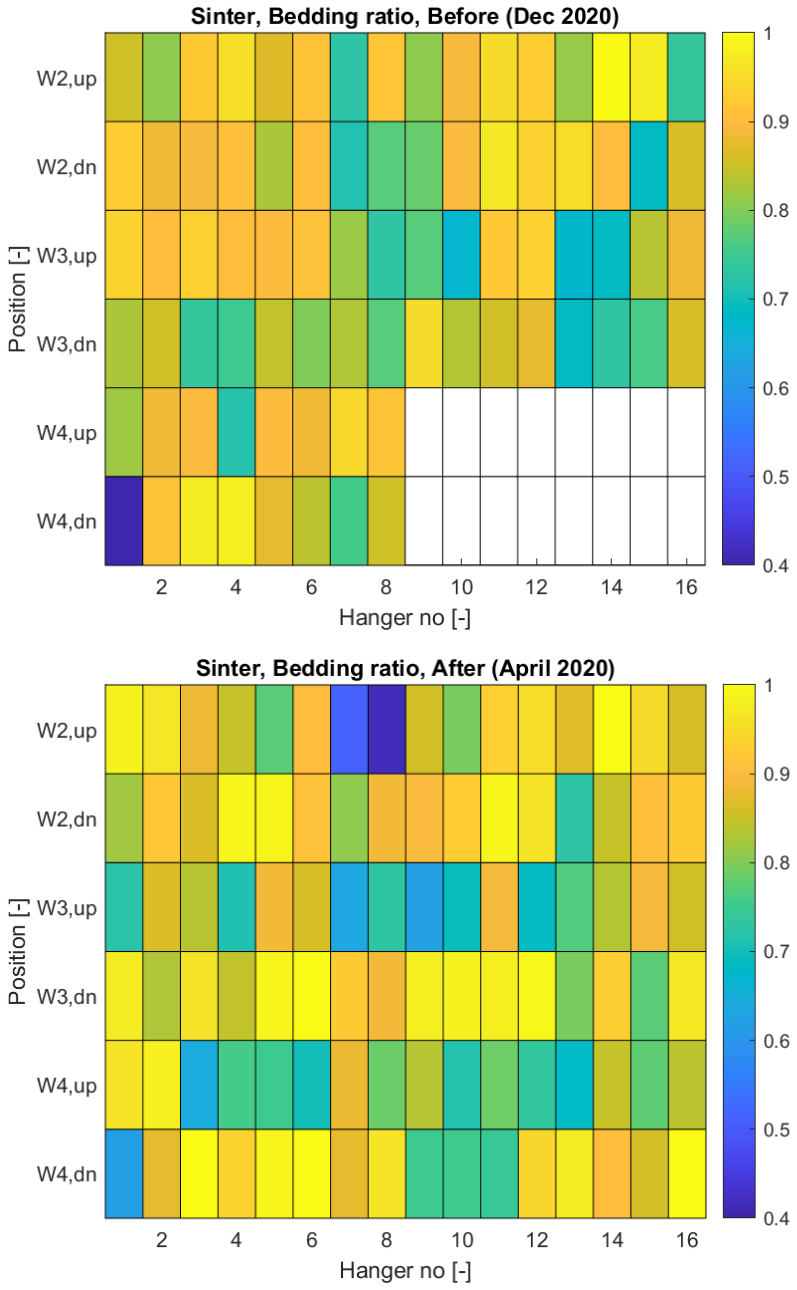

Figure 38 Sinter blocks. Visualization of ratio of bedded-in contact area prior to tests (top) and after tests (bottom)

The relationship between the friction force, block bedding-in ratio and winter conditions is shown in the box plots in Figure 39. For driver instruction 1 and 2 in the upper two figures, the friction force for the least bedded-in blocks (in the hangers) have lower median values for hanger links loaded in both tension and compression for winter condition R0 and W1–2. However, the interquartile distances are generally smaller, indicating a more predictable braking performance. For winter conditions W3–5, the median value in tension for the least bedded-in category is as large as for the other two categories, still with a lower interquartile distance. The mean value in compression is substantially larger for the less bedded-in brake blocks, however with a larger interquartile distance.

For driver instruction 3 in the lower two figures of Figure 39, it is more of a mixed picture for R0 winter conditions, with only one data point for the least bedded-in category. For W1–2, the median forces in tension does not seem to depend on the bedded-in state, while in compression the least bedded-in category shows higher median force than the more bedded-in blocks. For W3–5, the median force in tension for the least bedded-in category is somewhat below the other two (with a smaller interquartile range) but in compression the median value is again higher (with a small interquartile range). Noteworthy is also the low forces found as outliers (marked with circles) and the large total range of forces for the two higher bedding-in ranges. This indicates that the braking performance for these are inferior to the one of the least bedded-in block category.

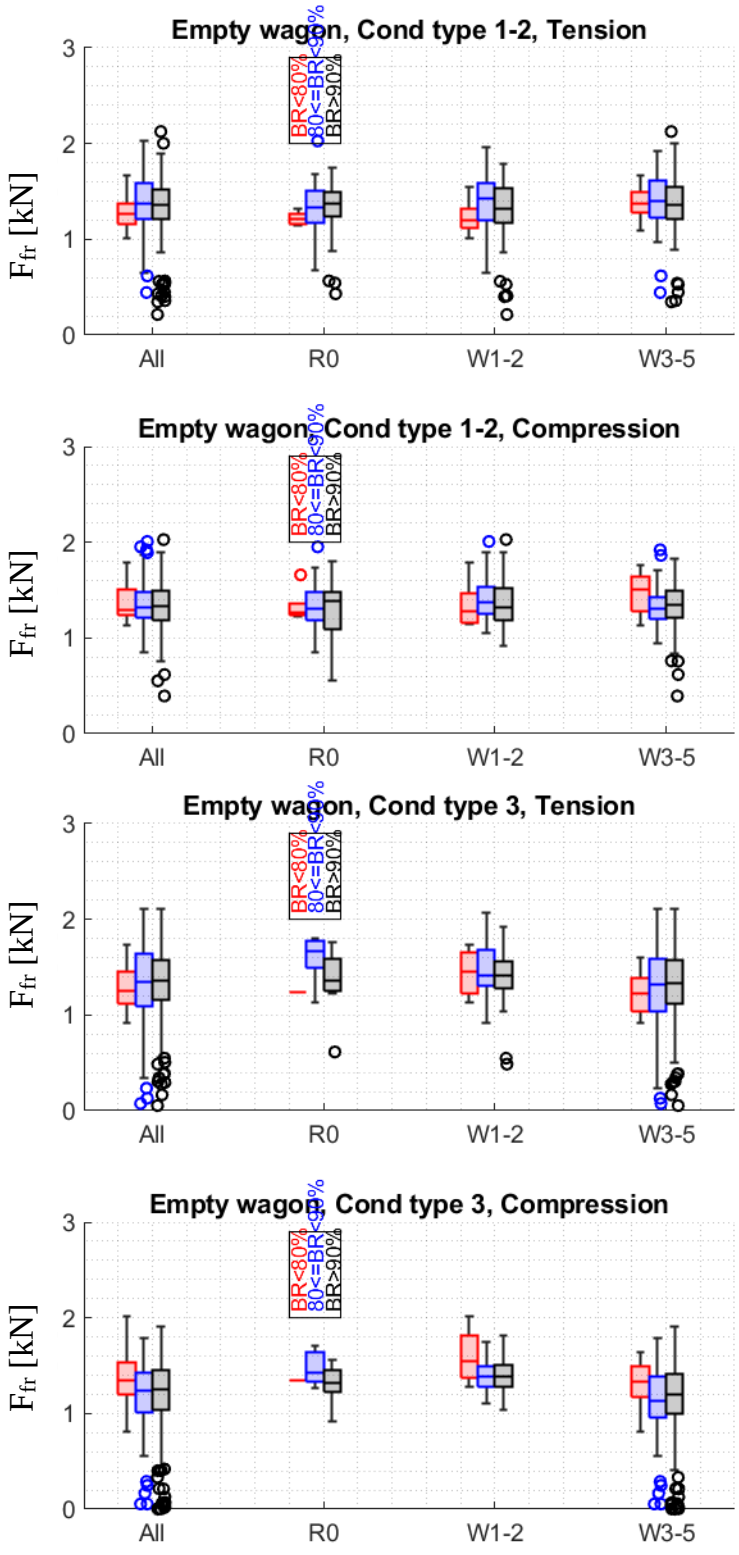

Figure 39 Sinter blocks. Results for block friction force for three block bedding-in ratios (indicated by colours: red for bedding-in ratio below 80%, blue for bedding-in ratio from 80 % to 90 % and black for bedding-in ratio higher than 90%) and three groups of winter conditions. Results for driver instructions 1–2 are given in the two upper figures and results for instruction 3 are in the two lower ones. Forces are indicated by box plots: the median (center line in box), the lower and upper quartiles (box exteriors), any outliers (computed using the interquartile range) marked by circles and the minimum and maximum values that are not outliers indicated by whisker endpoints.

5.2. Block temperatures

An overview of the increase in block temperatures are shown in Figure 40 for all tests. The first four stop braking tests are for loaded wagons with organic blocks and the following ones up to test 36 are for unloaded wagon and organic blocks. Tests 37 to 85 are for unloaded wagon with sinter blocks and after that follows braking with unloaded wagons with organic composite blocks. White squares indicate faulty data. In addition, sensor 1 for the sinter tests unintentionally measures air temperature since the thermocouple leads got extracted from the hole drilled in the upper block of hanger 1. Test 80 had a too short data sampling sequence and the maximum temperatures could not be established as for all the other tests[31], which forced exclusion also of these data.

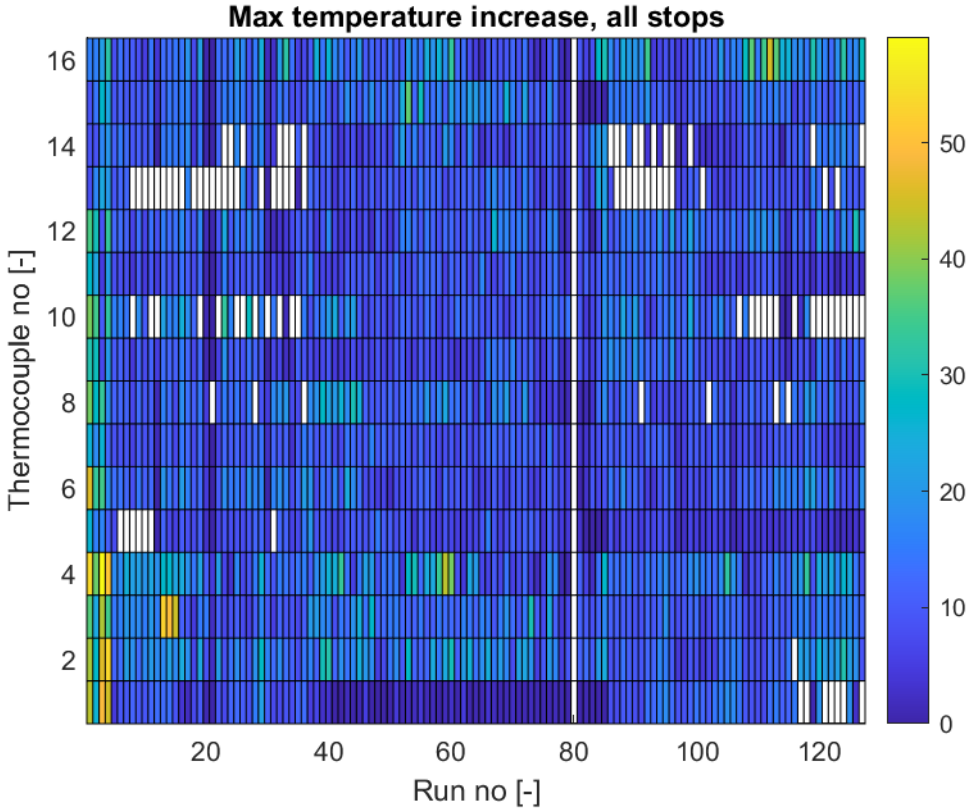

Figure 40 Overview of increase on block temperatures for organic composite blocks (loaded wagons for run no 1–4 and unloaded for runs 5–36 and 86–137) and sinter blocks (runs no 37–85). Temperature [10 °C] is given by colour bar to the right

The increase of the temperatures in the blocks are presented in the form of box charts in Figure 41. Median increase in temperatures introduced by tests are similar for the three driver instructions (around 10 °C) and often also similar with respect to the interquartile ranges. Larger differences can be found when focussing on lowest temperatures, where very low increases in temperatures results after braking with organic blocks, e,g, for driver instruction 3 for W1–5, and for driver instruction 2 for W3–5. For braking with sinter blocks it is only driver instruction 3 in for conditions W3–5 that produces temperature increases below 5 °C. A low temperature increase follows from the block having a low frictional heat input near the thermocouple.

[31] The maximum temperature for a stop braking is often registered after the train has stopped.

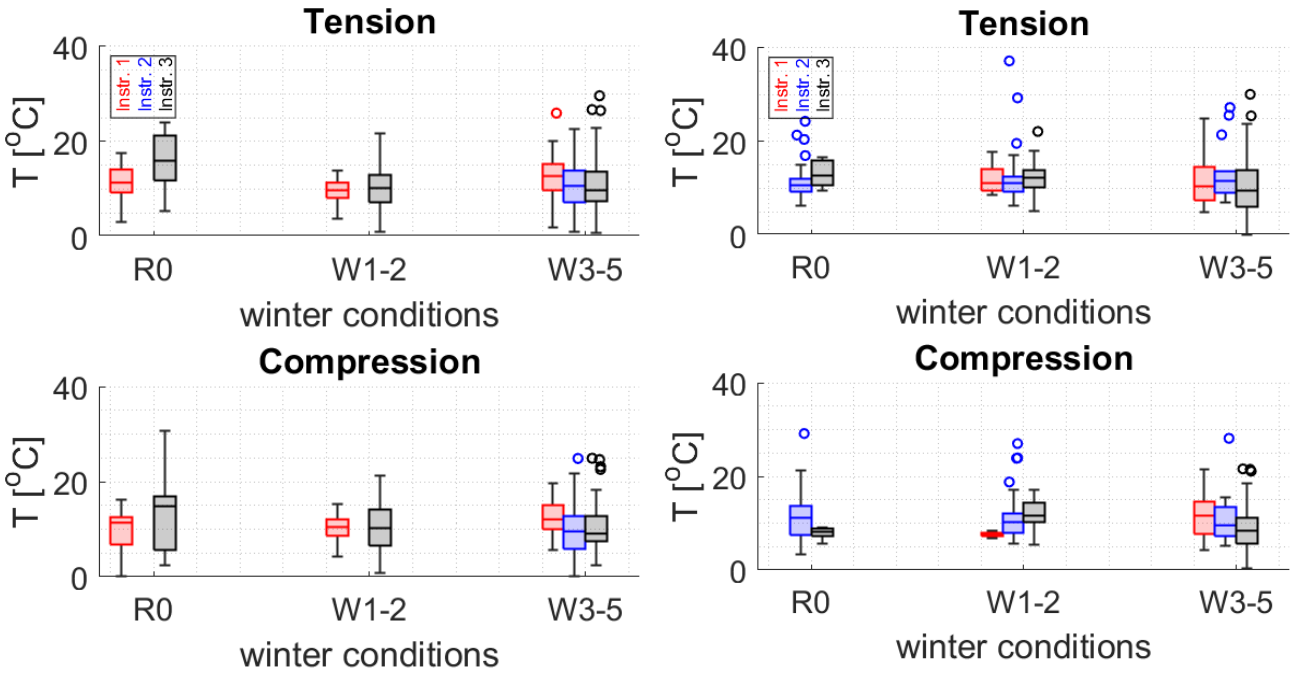

Figure 41 Overview of results for organic composite blocks (left) and for sinter blocks (right) for driver instructions 1-3 (indicated by colours) and three groups of winter conditions. Resulting temperature increase of brake blocks are indicated by box plots: the median (center line in box), the lower and upper quartiles (box exteriors), any outliers (computed using the interquartile range) marked by circles and the minimum and maximum values that are not outliers indicated by whisker endpoints.

The block temperatures are now analysed with respect the influence from UIC snow index, air temperature T_{air} [ºC], hanger link loading (tension/compression) and work W [kJ] performed by the friction force, see Figure 42 and Figure 43. These visualizations show the variations over the ranges of the variables for which they are fitted and only for the identified relevant variables for each case.

For the organic blocks in Figure 42, the temperatures are all found to be strongly dependent on the friction force work, which is reasonable since the work is responsible for the heat generation: an increase in work results in increasing block temperature. The UIC snow index is also influential in all three driver instruction cases, but with a rather minor effect on temperatures. However, it is a conflicting influence as instructions 1 and 2 result in increased temperatures with increase in winter index, whereas instruction 3 predicts a decreasing temperature. Minor effects are also found for driver instruction 1 for air temperatures and hanger link loading mode and for driver instruction 3 for hanger link loading mode.

For the sinter blocks in Figure 43 there is again a strong influence from the friction work, but the confidence intervals of the predictions are much wider than for the organic blocks, pointing towards larger variations in the block temperatures. For the sinter blocks also other factors have an almost equal influence as the work: 1) for driver instruction 1 an increase in UIC snow index results in a strong decrease in block temperature, 2) for driver instruction 2 both air temperature and hanger link loading mode are important, and 3) for driver instruction 3 both snow index and air temperature have strong influence.

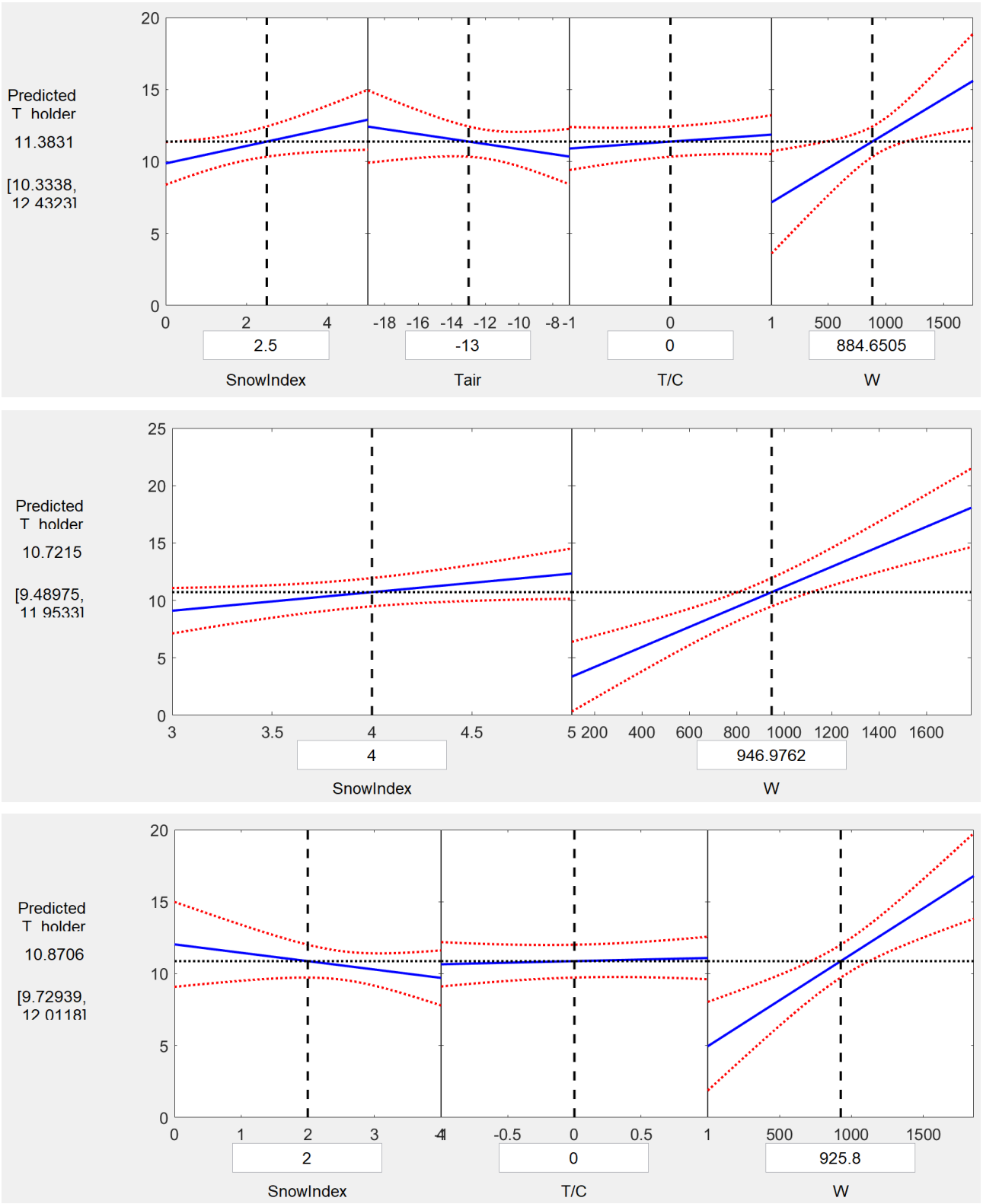

Figure 42 Organic composite blocks. Visualization of dependencies of block temperature increase [°C] on vertical axis. Results for driver instruction 1 (top), instruction 2 (middle) and instruction 3 (bottom). Fit is plotted in blue and 95% simultaneous confidence bands for the fitted response surface are indicated as two red (dotted) curves on each plot.

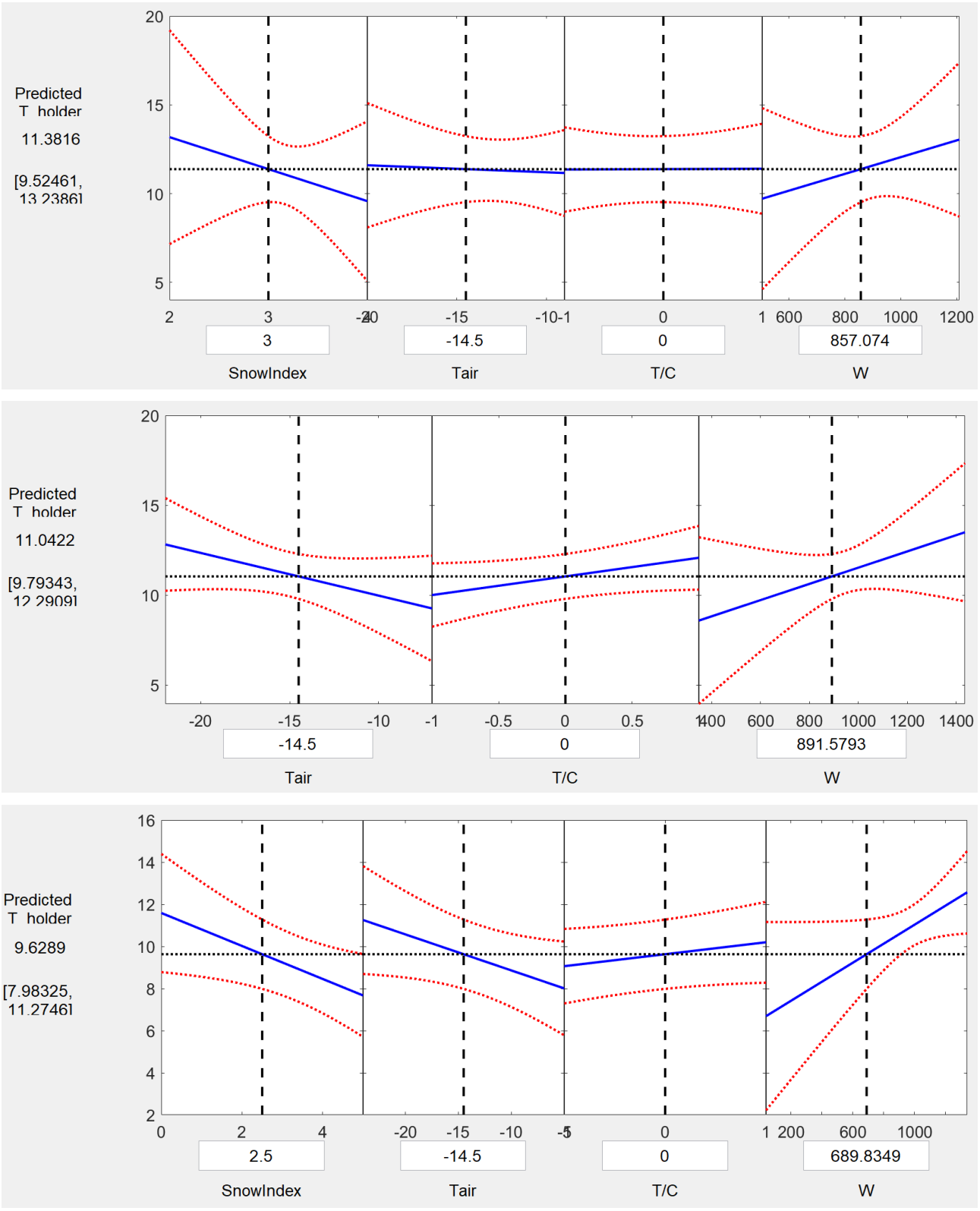

Figure 43 Sinter blocks. Visualization of dependencies of block temperature increase [°C] on vertical axis. Results for driver instruction 1 (top), instruction 2 (middle) and instruction 3 (bottom). Fit is plotted in blue and 95% simultaneous confidence bands for the fitted response surface are indicated as two red (dotted) curves on each plot.

For the sinter blocks, an effort has been made to investigate the increase in brake block temperatures as compared to the bedding-in states of the blocks[32]. The results for driver instructions 1–2 are presented in Figure 44 and results for driver instruction 3 are in Figure 45. For driver instructions 1–2, the smallest increase in temperature is about 5°C. Also, the results imply that the highest temperatures are found for blocks with bedding-in ratio in the range 80–90 % and the lowest generally being for the range 65–80 %, with 80-90 % bedding -in ratio showing intermediate values. This difference is more pronounced at the bottom position for conditions W3–5.

For driver instruction 3, the minimum temperatures for R0 and W1-2 are rather similar to the ones for driver instructions 1–2. However, for W3–5 the minimum temperatures are close to 0 °C, for both positions, indicating that some of the blocks are not subjected to frictional heating at all.

[32] Such a study is not possible for the organic composite blocks since they are perfectly bedded-in.

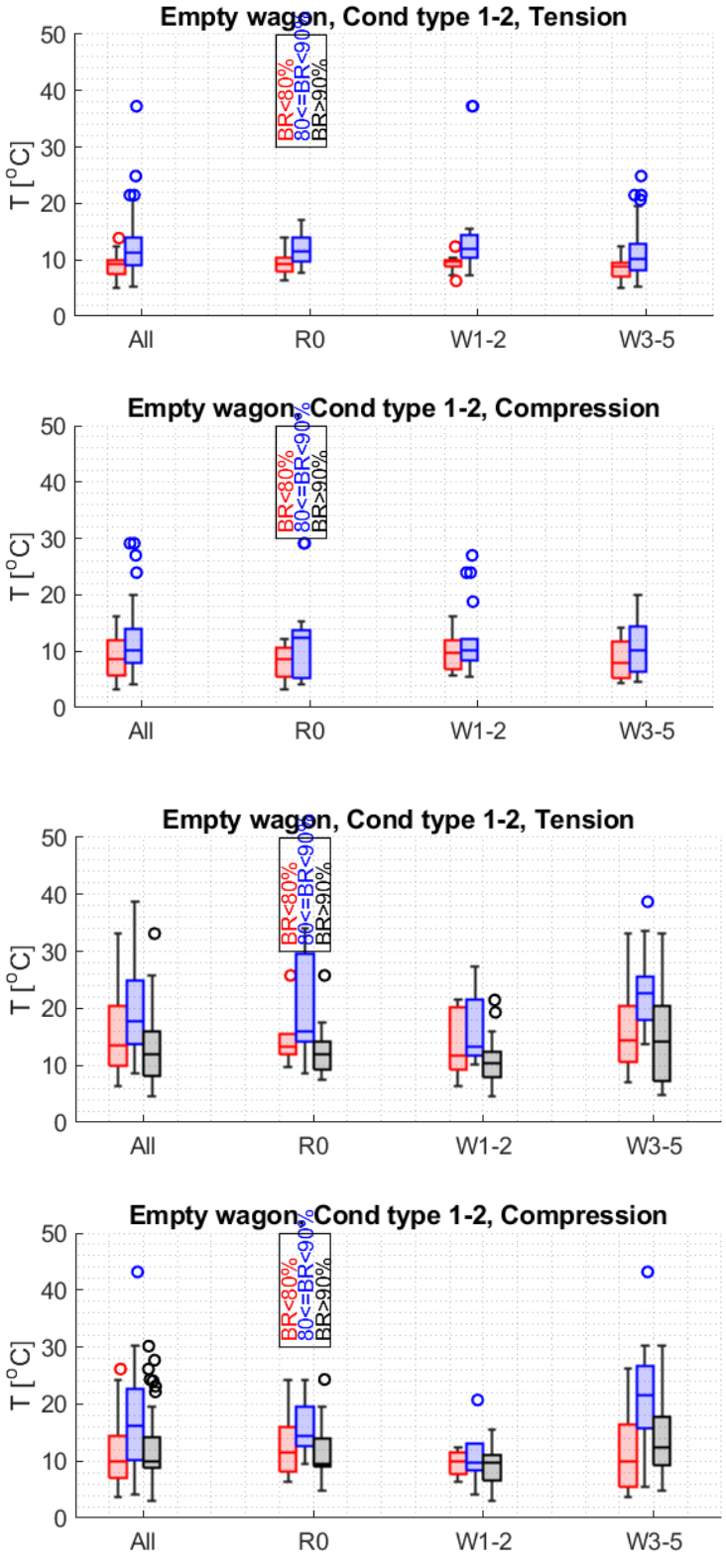

Figure 44 Overview of increase on block temperatures for sinter blocks for driver instruction 1–2. Blocks at top in upper two figures and blocks at bottom in bottom two figures.

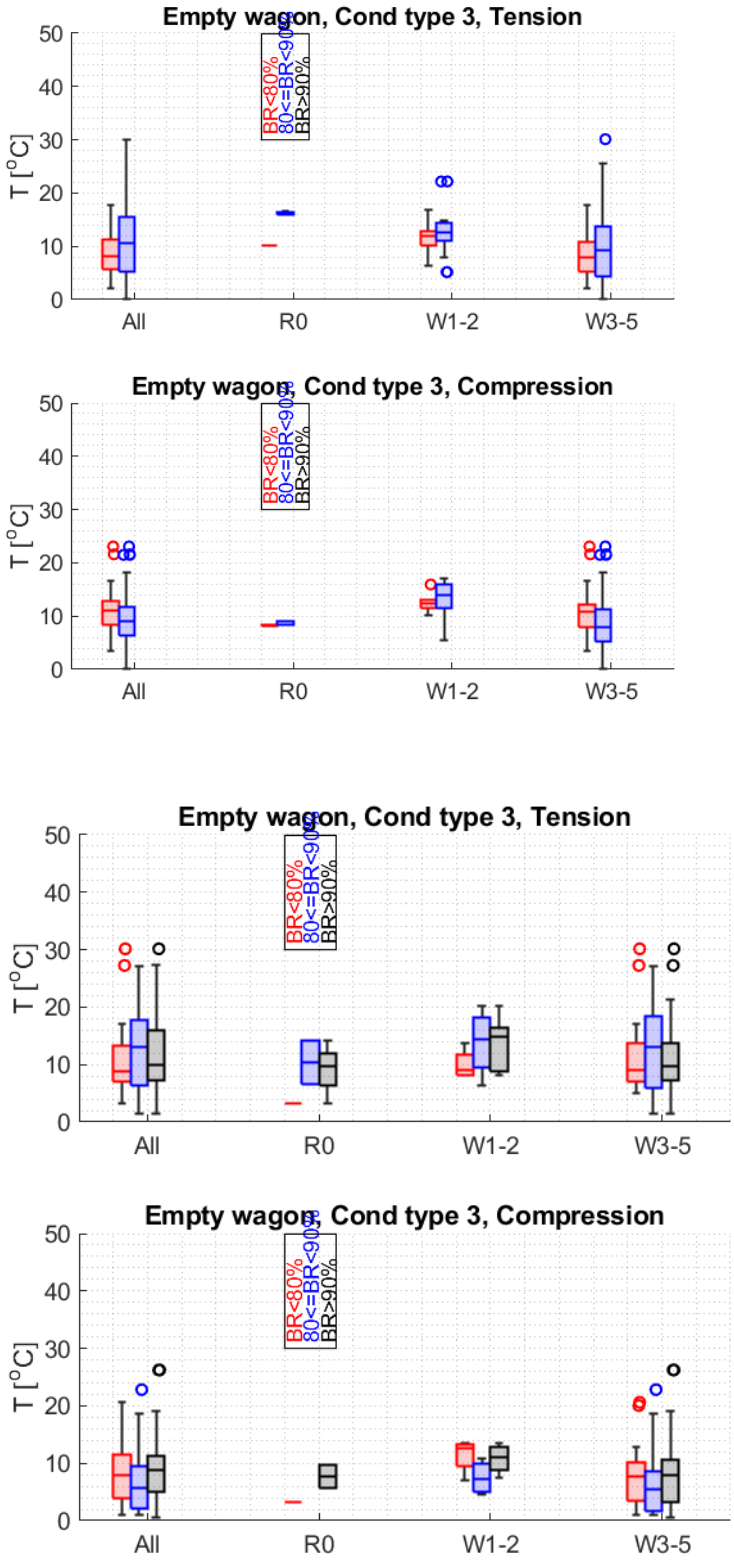

Figure 45 Overview of increase on block temperatures for sinter blocks for driver instruction 3. Blocks at top in upper two figures and blocks at bottom in bottom two figures.

5.3. Ice build-up in blocks

The build-up of ice is given in Appendix C for the five wagons for each of the test days on each block material. One general reflection is that for both block types, the blocks in the block holders are for several days completely covered in ice and snow. This means that the actual status of the block to wheel contact could not be inspected. However, for several inspections, it was observed that snow and ice was present between block and wheel for both types of blocks.

In Appendix D an attempt is made to visualize the relationship between changes in build-up of ice and snow and measured block temperatures on wagon 3. Time-data are provided for the entire test campaign for each of the 8 hanger positions. The reason for labelling the positions using two hanger link numbers is that it is not known for which side of the train that the inspections of ice and snow was performed.

Organic composite blocks

At the tests with organic blocks, they were observed to be covered in ice and snow (ice grade 4) at most of the inspections. The situation with ice covered blocks and holders becomes stable after a few inspections when testing using driver instruction 1–2 (when air temperatures were below –5 °C). At one occasion, ice/snow could be seen to be present between block and wheel (hangers 5–6). Block maximum temperatures are mostly higher than 0 °C after braking tests, and temperatures are scattered between air temperature and +47 °C (then ignoring the first four brake tests when the wagons were loaded[33]). Occasions with maximum block temperatures being close to the initial temperature occur for all studied periods with different driver instructions. A low temperature increase implies that very little (friction induced) heat has been introduced near the thermocouple. The block initial temperatures, *i e*, prior to tests, are normally higher than the air temperature but they are normally lower than 0 °C for driver instructions 1–3. Despite these differences and the high maximum block temperatures, the ice/snow build-up does not change during testing using driver instructions 1 and 2.

For driver instruction 4 (labelled as 1.5 in the figures), there is a build-up of ice and snow on about half the hanger positions. Despite the vigorous brake testing with a stop test performed every 15 min, substantial build-up of ice and snow nevertheless occur on the blocks upon a drop in air temperature to about –6 °C. For hanger with substantial ice build-up, the maximum block temperatures are normally low. It should here be noted that the tests with driver instruction 4 started with basically ice-free blocks.

For driver instruction 3, the ice/snow coverage is shifting from inspection to inspection, from several occasions with ice build-up between block and wheel, to blocks being completely ice covered, to a situation with no ice/snow at the block–wheel contact. The variations seem to be more dependent on air temperature and block initial temperature than on maximum block temperatures after tests: when the air temperature or block initial temperature are near 0 °C there is a reduction in ice build-up, but the ice/snow seem to be stable or re-build for temperatures around –10 °C. Again, it can be found that for hanger with substantial ice build-up the maximum block temperatures are normally low.

[33] The highest temperature for loaded wagons was 57 °C.

Sinter blocks

For the sinter blocks, substantially less ice/snow is present on the blocks when employing driver instructions 1 and 2 than when using organic composite blocks. The block–wheel contact can be inspected and no ice/snow can be seen at the contact between block and wheel, even though ice and snow is present on the sides of the blocks and also towards the contact with the wheel tread. The initial block temperatures are similar to those found for braking with organic blocks and so are the maximum temperatures after braking tests.

For driver instruction 3, there seem to be a trend towards increasing ice/snow on the blocks during this entire testing period, even if the air temperature actually is increasing towards the end of the period (going from about –20 °C to –5 °C). There are several inspections for which there are ice/snow between blocks and wheels. Measured block temperatures related to these inspections are often low. However, since there is an uncertainty regarding what side of the wagon that was inspected for ice and snow, and the fact that thermocouples are only on one side of the wagon, discrepancies can be found.

5.4. Comparison of winter seasons 2016–2017 up to 2020–2021

The winter season 2020–2021 was quite a normal Swedish normal winter for the test area in the northern part of Sweden, almost as harsh as the winter 2018–2019, but certainly more harsh than the winter 2019–2020. In an effort to demonstrate the different metrological conditions for the past five winters, data has been compiled using the data provided by Trafikverket for station 2553, located at Niemisel near test site 2. The average monthly temperatures are shown in Figure 46. Note that winter testing was performed from January to March.

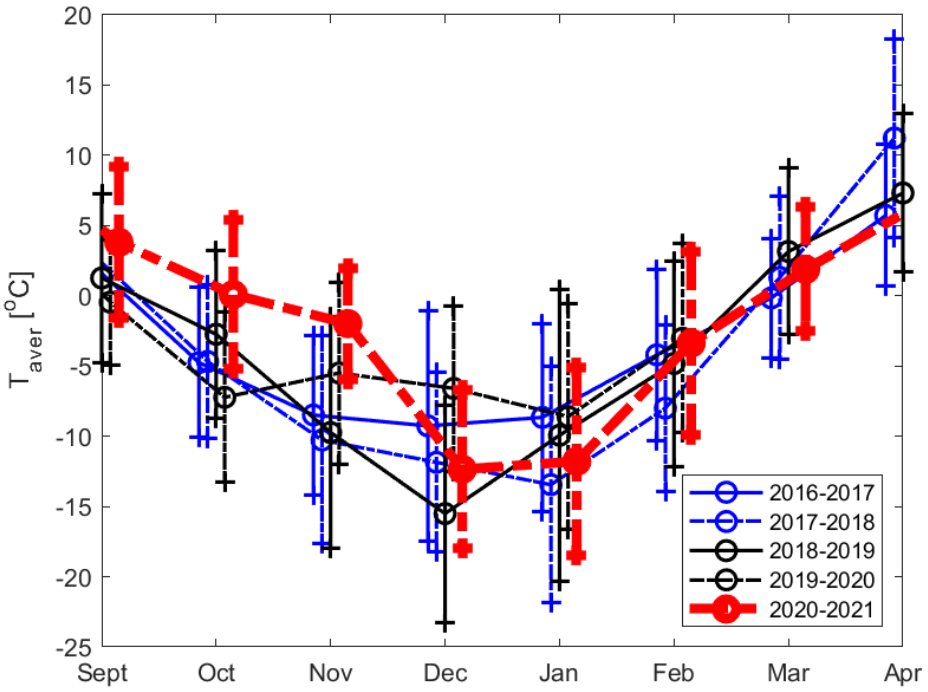

Figure 46 Overview of average temperatures indicated by circles during months July to May for the three past seasons. Vertical intervals indicate standard deviation of temperatures.

More detailed information on snow fall for the last three winters is provided in Figure 47, Figure 48 and Figure 49. The length of the winter season was 239 days (days from first snow to last falling of snow), which can be compared to 190 and 192 for the two earlier winter seasons. The total durations of snowfall (recalculated into days) are 32.9, 31.5 and 45.8 days for the three seasons. Thus, the winter 2020–2021 was longer and had more time of snowing than the others. In addition, the snow fall was more common at lower temperatures (between –15 ºC and –10 ºC) for the winter season 2020–2021 than for the two previous ones.

The total duration of periods of possible snow drift (developed for assessing risks of winter problems in road traffic, see Section 3.3) was calculated to be somewhat shorter for the entire winter 2020-2021 than for the winter 2019-2020, and almost half of that for the winter 2018-2019. Despite this, the winter testing conditions as registered on the test train were good during testing days, with substantial amounts of snow whirling around the wagons.

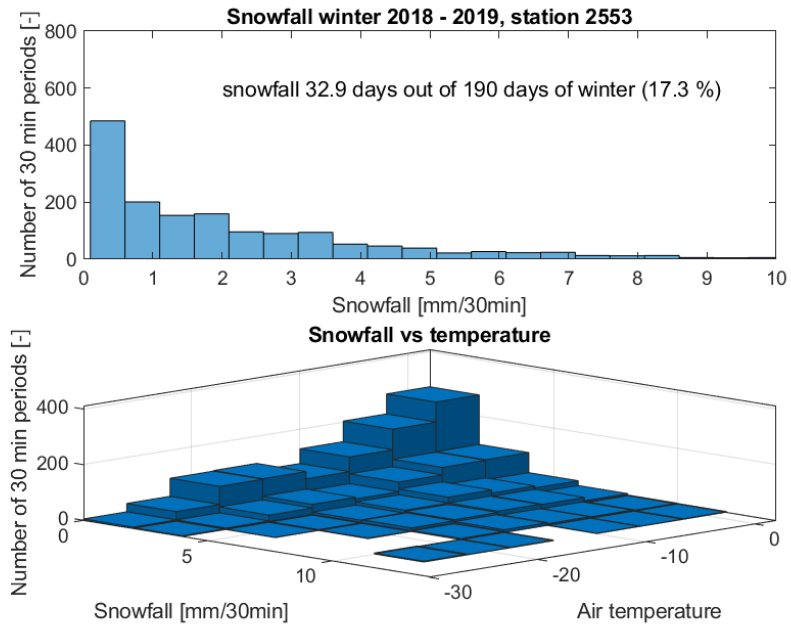

Figure 47 Histogram of snow fall detailed according to snowfall intensity and air temperatures for the winter season 2018–2019.

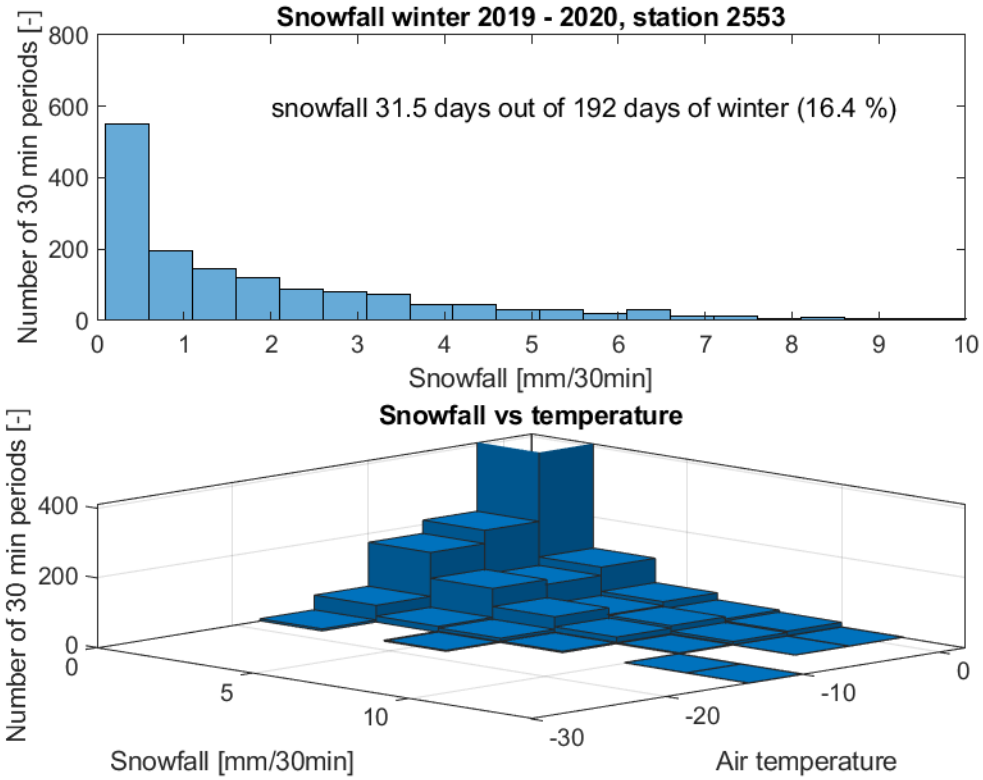

Figure 48 Histogram of snow fall detailed according to snowfall intensity and air temperatures for the winter season 2019–2020.

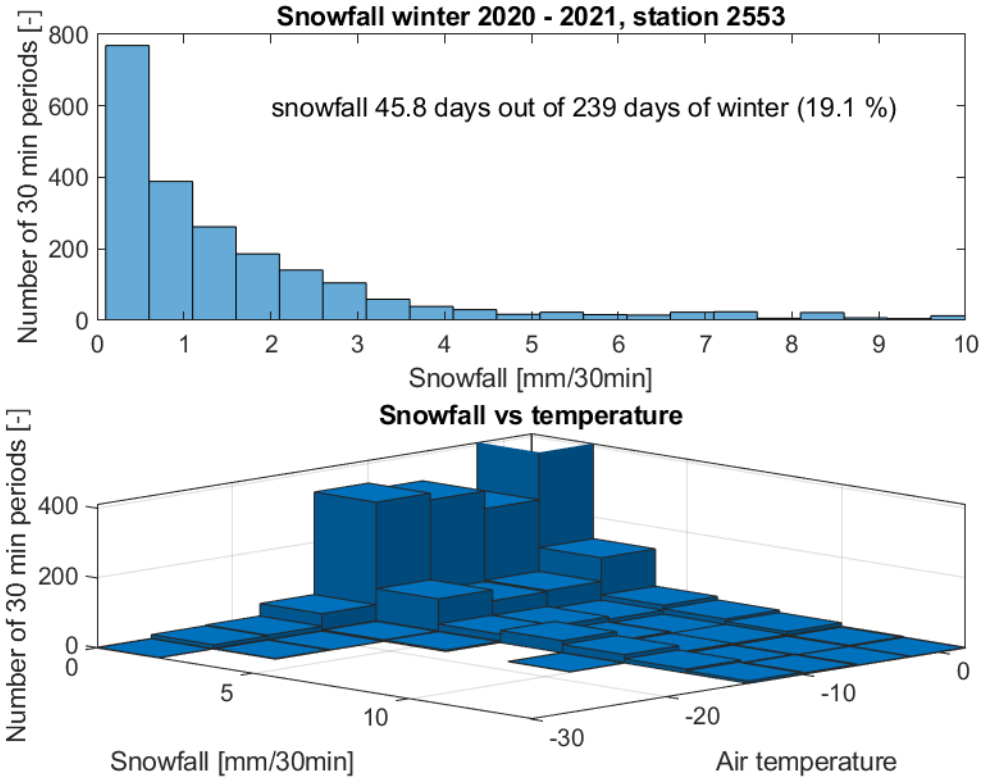

Figure 49 Histogram of snow fall detailed according to snowfall intensity and air temperatures for the winter season 2020–2021.

6. SUMMARY

The test campaign was performed in the most northern part of Sweden using a train having five tread braked and partially instrumented wagons, and an unbraked locomotive. Tests were performed for wagons that had either organic composite blocks or sinter blocks. A data acquisition system was installed that allowed for measurement brake pipe pressure, brake cylinder pressures on all wagons and on two and a half wagons also of braking forces (via instrumented hanger links and brake triangles). Temperatures in brake blocks were measured in all blocks on one side of one wagon. Results from the tests were analysed with respect to stop braking distances in the first part of the report, with a focus on braking forces in the second part, and with focus is on measured block temperatures, ice build-up on brake blocks, and bedding-in states of brake blocks in the third part. Some metrological data acquired from Trafikverket are also presented.

Focus is on how the locomotive driver uses the brakes *in-between* the stop braking tests with the purpose to condition the brakes through intermittent brake applications having short duration. For this reason, braking performance under three different driver instructions were studied. Here, "normal" and "enhanced" brake conditioning are in line with UIC guidelines for usage of LL brake blocks, with short brake applications every 10–15 min. A third type called "provocative brake conditioning" means a disruption on the brake applications by the driver so that the brake is nominally not used for about 0.5 hour.

The organic brake blocks were perfectly bedded-in towards the wheels already at the start of the testing since they had previously been in traffic on the wagons used at the tests. This was not the situation for the sinter blocks that had previously been used for testing on wagons during the 2019–2020 test campaign and were now installed on five new wagons with differing wheel diameters.

Four stops were performed using loaded wagons. However, the braking featuring organic composite blocks was very powerful and created wheel flats during these tests. Very short braking distances resulted, implying a braked weight percentage of up to 140% of the test wagons, which should be seen in the light of the nominal value being 100% braked weight percentage for wagons. The maximum allowed percentage for a wagon is 125% according to regulations. The wheel flats were machined (rounded) so that the wheel-rail contact forces were low enough to allow continued tests, thus avoiding a change of wheelsets. However, somewhat increased peak wheel–rail contact forces are still present after this operation and thus the vibration levels of the wagons are also somewhat increased. As side-note, not relating to safety concerns, the issue of wheel flat formation implies an overall increase in cost, and a reduction in reliability for freight traffic. These costs need to be taken by the train operator if no faults can be found on the wagon braking system[34].

In the following results are discussed for unloaded wagons.

6.1. Braking distances

When braking with sinter blocks, one brake cycle showed a very long stopping distance of 1550 m when braking according to Driver instruction 3 "provocative brake conditioning".

[34] Communicated by Lars Fehrlund, Green Cargo, at meeting 2021-10-04.

Based on measured information it was concluded that large amounts of ice between block(s) and wheel(s) came off on wagons 2 and 4 during or shortly before this test. The amount of ice could not be compensated for by the stroke of the brake cylinders and upon this the brake cylinders could not produce sufficient braking forces on the blocks. This means that the 1550 m braking distance resulted from a situation with two wagons braking at reduced capacity. Since this sequence of events is not really an effect of the braking performance of the brake blocks it was chosen to disregard this test for the remaining assessments. However, this brake test for which two wagons basically became deprived of their brakes does constitute a dangerous and extreme case of prolonged braking distances. It should be noted that this substantial build-up of ice and snow on the blocks and holders of these wagons occurred during three days of testing according to Driver instruction 3. An important question is if this type of build-up of ice and snow can occur during normal revenue traffic, but that question is outside the scope of the present report.

The analyses of stop braking tests reported in Part 1 show that the organic composite brake blocks are somewhat sensitive to driver instructions. However, no extreme braking distances are found, not even for driver instruction 3 “provocative brake conditioning”. Braking distances resulting from driver instruction 1 “normal brake conditioning” are the shortest, followed by driver instruction 2 “enhanced brake conditioning”. The longest stopping distances are for driver instruction 3. For driver instruction 1, the braking distances show no trend of increasing braking distances for situations with snow whirling. For driver instruction 2 there is a trend towards longer braking distance (increase by 9 % of average distance) for severe winter conditions W3–5 (with substantial amounts of whirling snow around the wagons) than found for instruction 1. Driver instruction 3 resulted in braking distances somewhat longer than those found for driver instruction 2 (11% higher average distance as compared to instruction 2). No braking distances are longer than 910 m and the average braking distance is below 820 m. The results can be compared to the nominal braking distance 850 m calculated according to UIC. With frequently performed stop tests (driver instruction 4), short braking distances were found, ranging from 500 m up to 730 m. When employing regression models, no trends could be identified for driver instructions 1–3. This indicates that the braking distance should not change due to changes in air temperature or in UIC winter indices.

The sinter blocks show braking distances that clearly depend on the employed driver instructions. Driver instruction 1 “normal brake conditioning” results in braking distances that only increase slightly when the winter conditions worsen. The mean braking distance is about the same as the one calculated according to UIC with a maximum braking distance of about 930 m. Driver instruction 2 “enhanced brake conditioning” leads to longer braking distances with average braking distances of about 910 m for W1–2 conditions. The longest braking distance is 980 m, which is 15% longer than the UIC nominal braking distance. For driver instruction 3 “provocative brake conditioning”, a trend of increasing braking distances with increasing UIC winter index is found. Average braking distances are for W1–2 and W3–5 are 910 and 960 m respectively, with extremes going up to 1100 m, which is 29% longer than UIC nominal braking distance. Regression modelling could not identify dependencies for driver instruction 1, nor for driver instruction 3. For driver instruction 2, the identified regression model indicated a tendency that a combination of high UIC winter indices and lower temperatures lead to longer braking distances.

6.2. Brake friction forces

The results for organic composite blocks show that median friction force values[35] for driver instruction 1 (data represented by red colour) are almost identical for the three winter groups, both for block inserts with hanger links in tension and compression. Some block inserts show very low energies for all conditions, indicating that they contribute poorly to the braking of the train. For driver instruction 2 and W3–5 conditions, there is a difference between hanger links in tension and compression. The results show that the hanger links in compression seem to underperform for driver instruction 2. For driver instruction 3, the median friction forces are lower than for the two other instructions when more severe winter conditions prevail (W3–5), with a more pronounced decrease in compression. Linear regression modelling for driver instruction 1, identifies an increase in friction force with decreasing temperature, whereas for driver instruction 2, it is only identified to be depending on the hanger loading mode, with lower forces in compression than in tension. For driver instruction 3, the model predicts a decrease in friction force with increasing UIC snow index, and that the force is lower in compression than in tension.

The results for sinter blocks show that the friction forces for the sinter blocks in general are lower than for the ones for the organic composite blocks, indicating an overall weaker braking performance which is in line with the longer braking distances. For driver instructions 1–2, hanger links in compression and tension show similar behaviour for all driver instructions, which implies consistent braking performance for the two block positions. For driver instruction 3 for W3–5, the median force is reduced in compression but not in tension. Several hanger links show very low values for both tension and compression. Linear regression modelling show that an increase in UIC snow index or a decrease in air temperature are generally found to lower the friction force. When the hanger link loading mode is identified by the linear regression modelling, it is always the hanger links in compression that produce lower force levels and the ones in tension that produce higher forces.

One aspect part of the braking performance is the time until onset of the instant friction force by the brake blocks in a hanger link. Employing a criterion where the time until the force has reached 50% of its maximum value reveals differences between organic composite blocks and sinter blocks. The time delay is found to be 10–13 s for driver instructions 1–2 when using organic composite blocks, but 18–30 s for sinter blocks. The longer time of build-up of the friction forces for the sinter blocks correlate well both with the above presented lower friction forces and also with the longer presented brake distances for the sinter blocks. Longer time delays until the friction force is building up to a significant value is reducing the braking performance for the sinter blocks.

6.3. Block bedding-in, block temperatures and ice build-up on blocks

The effect on bedding-in on the friction force for sinter blocks is mixed and depends on the conditions at hand. No clear trend can be seen regarding median values. However, the results indicate that the *variations* of the forces in the form of range between largest and smallest

[35] The calculated force is taken as the mean force over the time for which the brake cylinder pressure is close to its maximum pressure.

forces are lowest for the least bedded-in category and highest for the most bedded-in blocks. Also, the number of blocks for which the block forces are very low are also substantially higher for blocks with bedding-in ratios larger than 80%.

Brake block temperatures at the measuring point 10 mm below the block–wheel contact are rather similar for the two block types. Median increase in temperatures introduced by stop braking tests are similar for all three driver instructions, around 10 °C, and also interquartile ranges are similar. Differences are found when studying the lowest temperatures. For organic blocks, low increase in temperatures is found, *e g*, for driver instruction 3 for W1–5, and for driver instruction 2 for W3–5. For braking with sinter blocks it is only for driver instruction 3 and W3–5 that temperature increases below 5°C are produced. A low temperature increase follows from the block having a low frictional heat input (near) the thermocouple.

Linear regression analysis shows that block temperatures strongly depend on the friction work, which is reasonable since it is the cause of the heat generation. For the organic blocks the confidence intervals for the friction work are rather narrow for the predicted temperatures. Also the UIC snow index has a minor effect in all three driver instruction cases.

For the sinter blocks the confidence intervals of the temperature predictions relating to the friction work are much wider than for the organic blocks, pointing towards larger variations in the block temperatures. For the sinter blocks also other factors have an almost equal influence as the friction work, depending on the driver instruction at hand: 1) for driver instruction 1 an increase in UIC snow index results in a strong decrease in block temperature, 2) for driver instruction 2 both air temperature and hanger link loading mode are important, and 3) for driver instruction 3 both snow index and air temperature have strong influences.

7. CONCLUSIONS

For unloaded wagons with an axle load of 6.5 tonnes (and a brake weight of 6.5 tonnes) it is found that perfectly bedded-in organic composite blocks behave rather well both when employing “normal driver instructions” and “enhanced driver instructions” but also when using the “provocative driver instructions”. The stopping distances when using the normal driver instructions are the shortest, followed by the ones for the enhanced instructions. The longest stopping distances result from employing provocative driver instructions. Ice and snow do build-up on the blocks during testing to a high degree and this is occurring when braking under all three driver instructions, often in such amounts that the actual blocks cannot be seen.

On loaded wagons with an axle load of 15 tonnes it was found that the organic composite blocks provided very powerful braking and that wheel flats formed on some wheelsets. For this reason, testing with loaded wagons was only performed on one day using organic blocks. Issues with wheel flat formation imply an overall increase in traffic cost, and a reduction in reliability for freight traffic.

Unloaded wagons with an axle load of 6.5 tonnes equipped with sinter blocks behave rather well when employing “normal driver instructions” – the performance is in fact somewhat better than for the “enhanced driver instructions”, which was also the case for the organic composite blocks. Braking employing the “provocative driver instruction” causes occurrences of substantially prolonged braking distances. For one such stop, two wagons more or less lost their braking capabilities as an effect of massive amounts of ice and snow accumulated between blocks and wheels falling off at the test. This resulted in almost a doubling of the braking distance. No testing with loaded wagons with sinter blocks could be performed during the test campaign.

One reason for the lower braking performance of the sinter brake blocks as compared to the organic composite blocks is that the time until the friction force reaches a significant level is almost double. The blocks at the tests were not very well bedded-in with degrees of bedding-in between about 60% and 100%. One effect of a low degree of bedding-in is that it seems to help keeping the brake blocks frictionally active, a conclusion from the fact that they are less prone to really low friction forces and therefor do not show really low block temperatures at tests.

APPENDIX A: COMPARISON WITH NOMINAL BRAKING DISTANCE BASED ON UIC 544-1

The nominal braking distances of a complete train and also for a single wagon can be calculated using the information in the UIC leaflet 544-1, based on train mass data and braked weight percentages. The braked weight for each wagon can be calculated as $B_i = \lambda_{dyn,i} \times m_i$ where $\lambda_{dyn,i}$ is braked weight percentage and m_i = 26 tonnes is wagon mass[36]. For the train, having an unbraked locomotive, the braked weight percentage can be found as

$$\lambda_{test=} \frac{B_{loco} + \sum_{i=1}^{5} B_i}{m_{loco} + \sum_{i=1}^{5} m_i}$$

where B_{loco} = 0 (unbraked loco) and m_{loco} = 89 tonnes is locomotive dynamic mass. The wagon brake calculations provided in Appendix F shows that 100% braked weight percentage results for a dynamic efficiency of 0.83. However, since the wagons have an estimated average dynamic efficiency 0.88, see Appendix E, the braked weight percentages of the wagons increase to 106%. Based on this information it is found that the braked weight percentage of the train is $\lambda_{test} = 0.63$.

The braking distance s [m] can readily be calculated for a train or a single wagon at speed 100 km/h using UIC544-1 by

$$s = \frac{C}{\lambda_{train}\,[\%] + D}$$

For a train C = 61300 m and D = 8.9 whereas for a single wagon C = 52840 m and D = 10. This gives a braking distance for a train $s_{train} = 855$ m and for a wagon $s_{wagon} = 726$ m, which are, according to the norm, for a nominal filling time of t_{UIC} = 4 s.

The filling time of the brake cylinders for the test train has an average value of 7 s. Note that this value is until 90% if the maximum brake cylinder pressure[37] is reached and that another 1 s is required to reach the maximum pressure. Thus, the filling time for the test train is taken as 8 s.

A proposal based on the information in the DB document ”On the regulations of technical brake assessment of rail vehicles within the scope of the acceptance according to § 32 EBO - principles of brake evaluation based on UIC 544-1 (in German)“[38], is that the braking distance of our test train could tentatively be found based on the ratio between train length L_{test} and maximum length L_{max} as

$$s_{test} = s_{wagon} + (s_{train} - s_{wagon}) \times \frac{L_{test}}{L_{max}}$$

[36] Rotational inertia of wagon wheels is neglected.

[37] See Section 3.1

[38] Anhang IV ”zu den Regelungen für die bremstechnische Beurteilung von Schienenfahrzeugen im Rahmen der Abnahme nach § 32 EBO - Grundsätze der Bremsbewertung in Anlehnung an UIC 544-1“ Stand: Rev. 05, 07.11.2006

where L_{test} = 132m is the length of the test train (locomotive being 15.5 m long and five wagons each with length 23.3 m). The maximum train length considered is taken as L_{max} = 500 m which is the longest train length considered in the standard for freight wagons, yielding a stopping distance s_{test}=760 m.

Compensating for t_F = 8 s filling time of the brake cylinder as compared to t_{UIC} = 4 s in UIC standard[39]:

$s_{test,F} = (\frac{t_F}{2} - \frac{t_{UIC}}{2}) \times v_{nom+}\, s_{test}$ = 829 m

A final compensation is introduced because of the chosen time point for detecting the start of a stop braking employed in the reported analyses. It was taken as the time point when the brake cylinder pressure starts to increase[40]. This time point is about t_c = 0.8 s after the first decrease in the main pipe pressure, which forces a compensation of the braking distance to be considered when the train is running at its nominal speed. Thus, the stopping distance becomes:

$s_{test,F,s} = t_c \times v_{nom+}\, s_{test,F}$ = 852 m

The stopping distance of the test train thus has a nominal value of 852 m with the described compensation for 1) the high efficiency of the wagons, 2) the length of the test train, 3) the longer time delay of building up of the brake cylinder pressure, and 4) that the brake cylinder pressure is used for detection of brake initiation.

[39] This relationship is in the UIC standard strictly only applicable for slipped wagons (*i e* a single vehicle test where the wagon is released from a locomotive by a mechanical coupler) but it is here deemed reasonable to use for our test train which is relatively short.

[40] See Section 3.1

APPENDIX B: DETAILED INFORMATION REGARDING TEST 84 ON SINTER BLOCKS WITH VERY LONG BRAKING DISTANCE

Measured data are presented for the extreme stopping distance. Variation of speed and brake cylinder pressures are given in Figure 50. The duration of the brake cylinder pressures is normal for the tests. Variation of train deceleration as function on train speed intervals during braking is given in Figure 51 for all brake tests performed using driver instruction 3. The deceleration for the longest brake cycle can be seen to deviate substantially from the others with much lower retardation values. The triangle forces that act on the block holders are shown in Figure 52. Wagon 2 shows a marked decrease in applied force at about 65s, whereas wagon 4 shows a decrease at about 52s. The reason for these reductions in forces is that that brake blocks have travelled forward towards the wheel as a result of large amounts of ice being removed from the block contacts and hence the brake cylinders have reached their maximum stroke, not being able to provide force to the blocks.

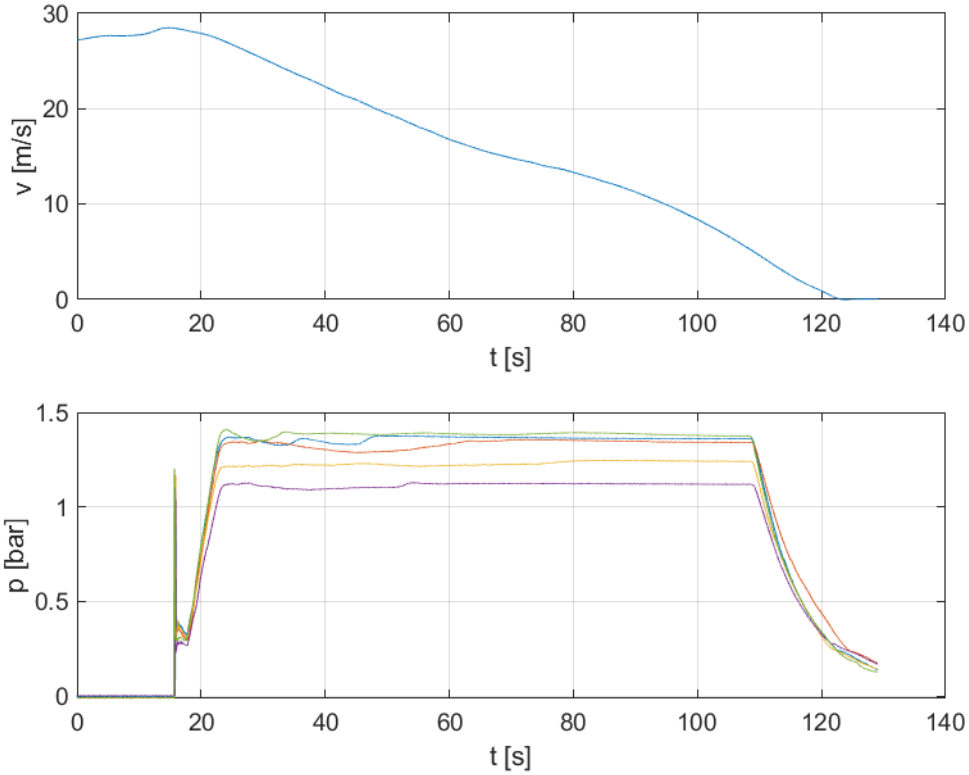

Figure 50 Time variation of train speed and brake cylinder pressures for the five wagons (each colour represents pressure in one wagon)

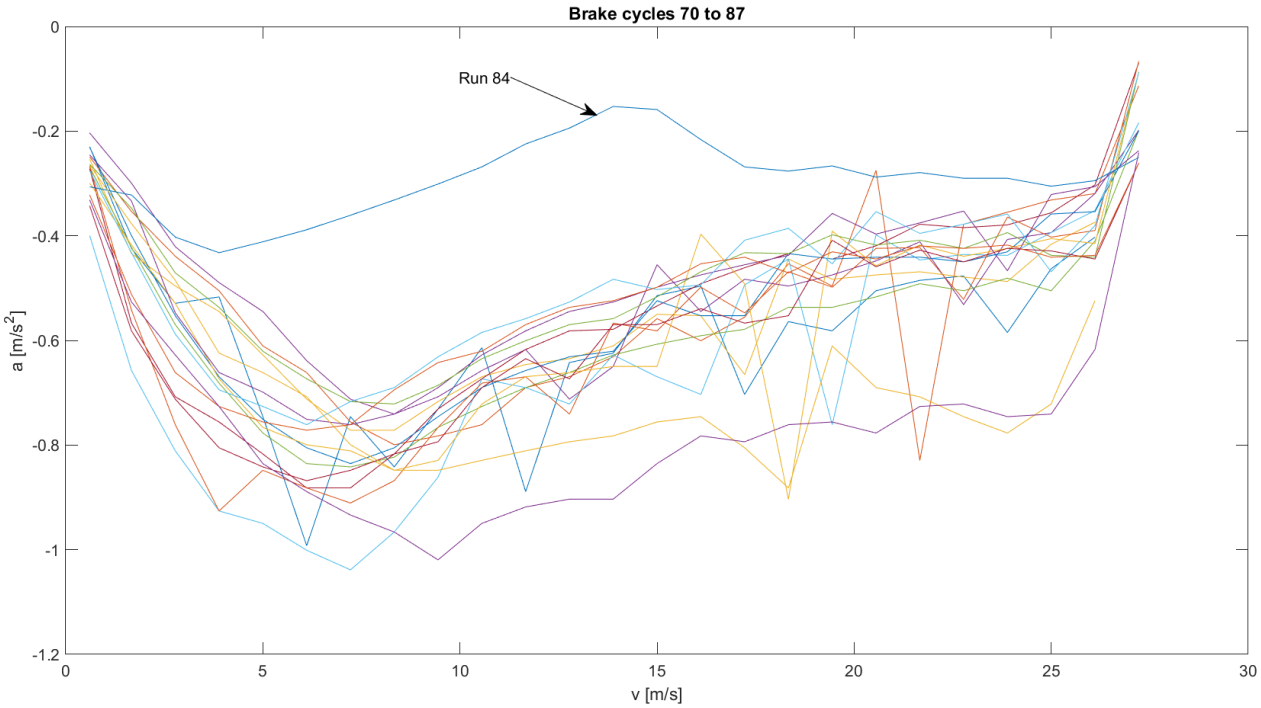

Figure 51 Variation of braking deceleration as function of speed for some stops with sinter brake blocks performed using driver instruction 3. The brake cycle with extreme braking distance is marked with Run 84 (sequence number of testing during the entire test campaign).

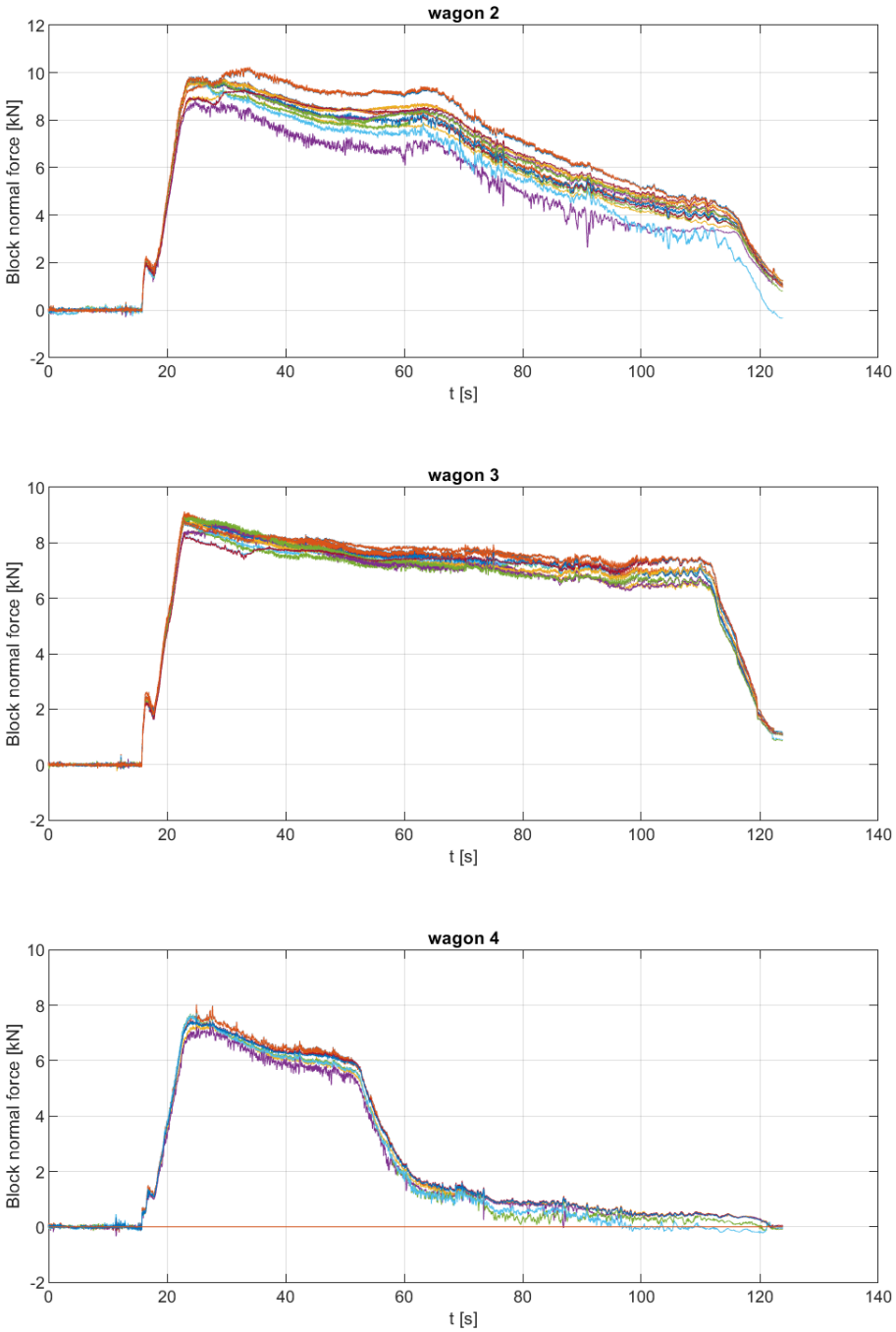

Figure 52 Time variation of brake triangle forces. Each colour represents data for one wagon

APPENDIX C ICE BUILD-UP ON BRAKE BLOCKS AND HOLDERS

For each wagon, data are presented for the entire test campaign as function of day of testing for that particular type of blocks.

Two figures are provided for each wagon, the upper one to judge if the blocks are covered in snow and ice, and the second one to judge whether snow and ice are present between block and wheel. The gradings shown in the figures are detailed at top of figures. In the lower figure, green patches mean that the blocks are not covered at all and the scale is not applicable.

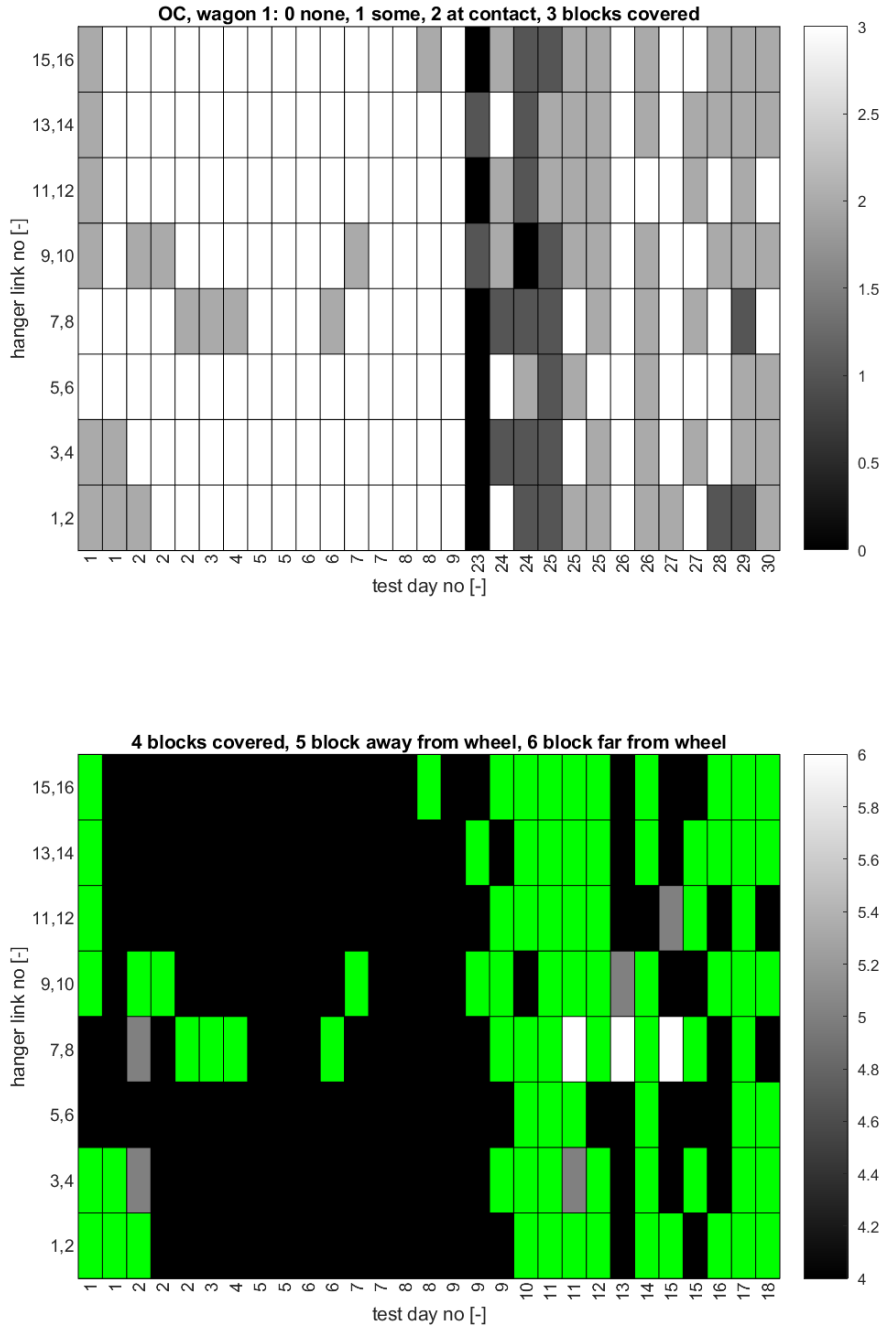

Figure 53 Ice build-up on blocks and holders for tests with organic composite blocks on wagon 1. The upper and lower figures show the same data, but have different values on the colour bars in order to give a clear view of the changes in ice build-up. An explanation of ice and snow build-up is provided at the top of each figure.

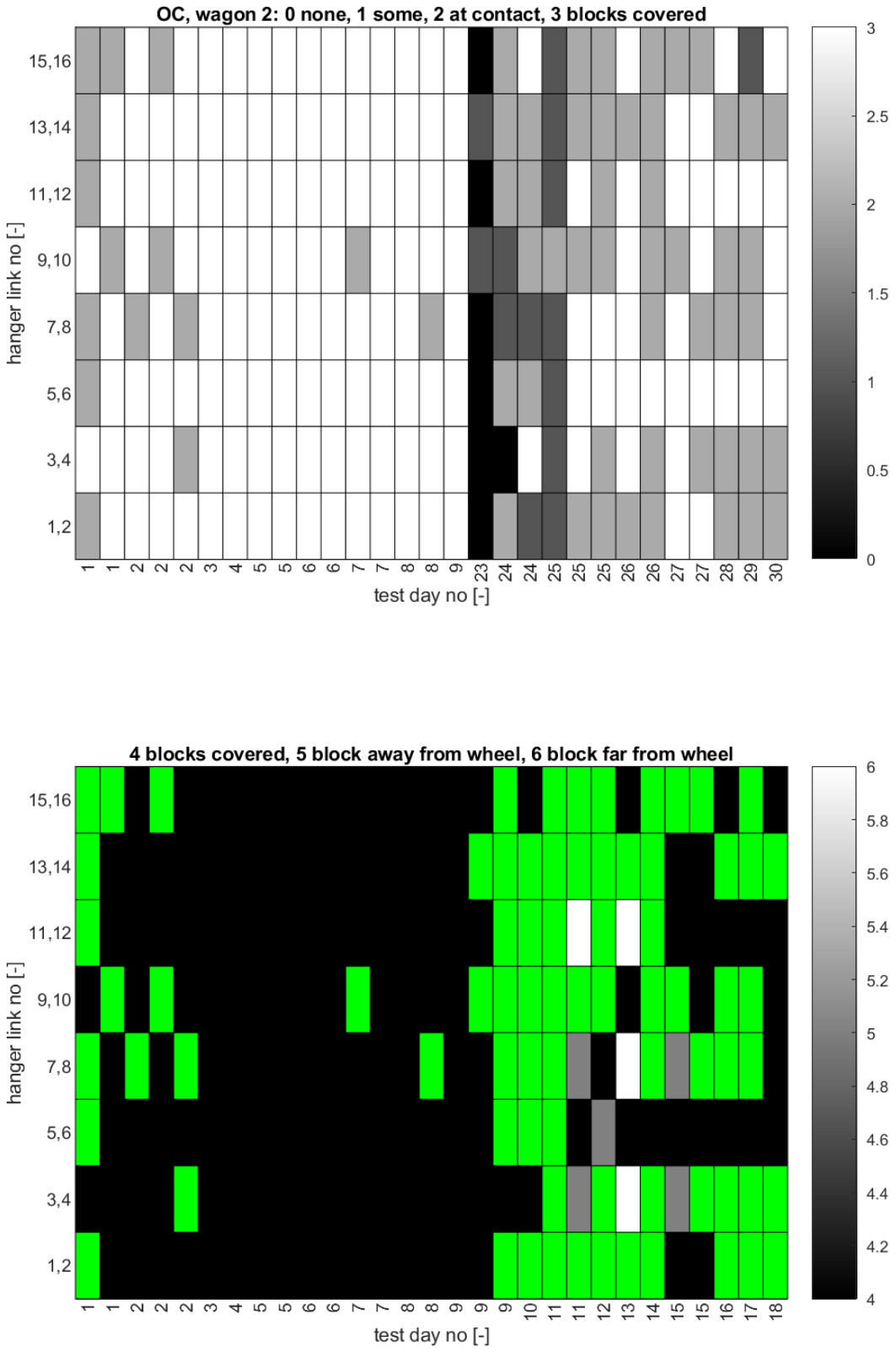

Figure 54 Ice build-up on blocks and holders for tests with organic composite blocks on wagon 2.

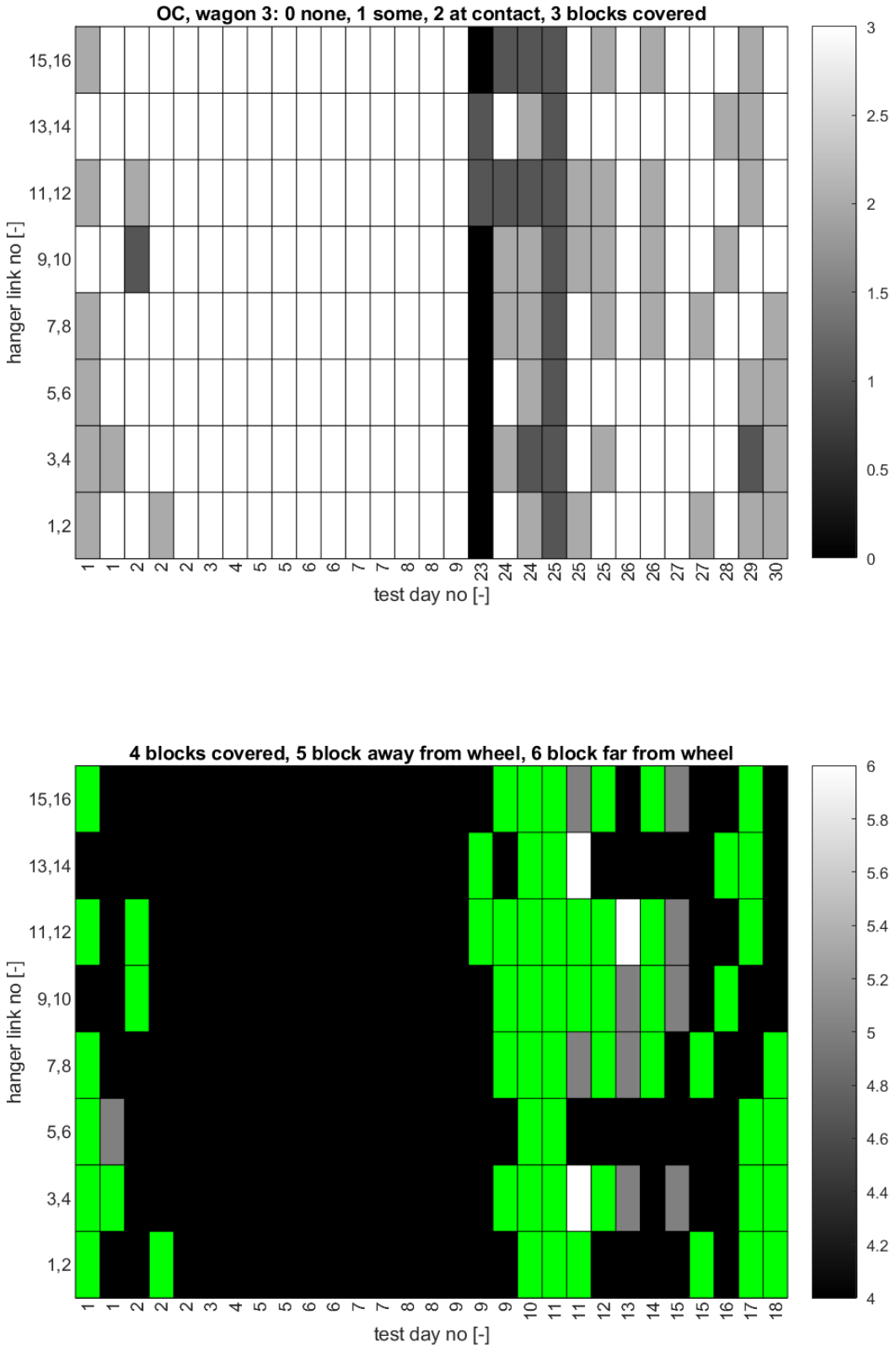

Figure 55 Ice build-up on blocks and holders for tests with organic composite blocks on wagon 3.

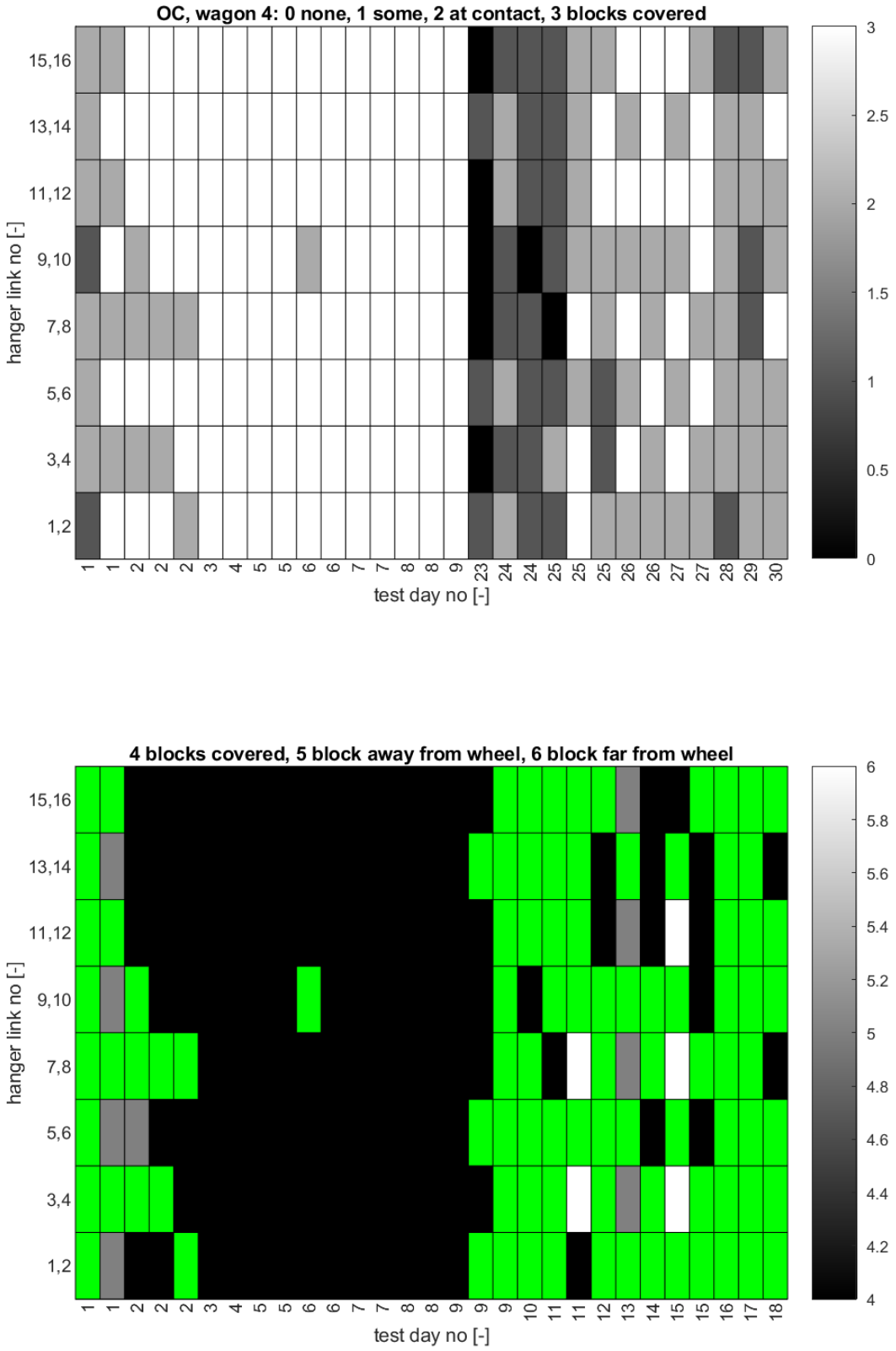

Figure 56 Ice build-up on blocks and holders for tests with organic composite blocks on wagon 4.

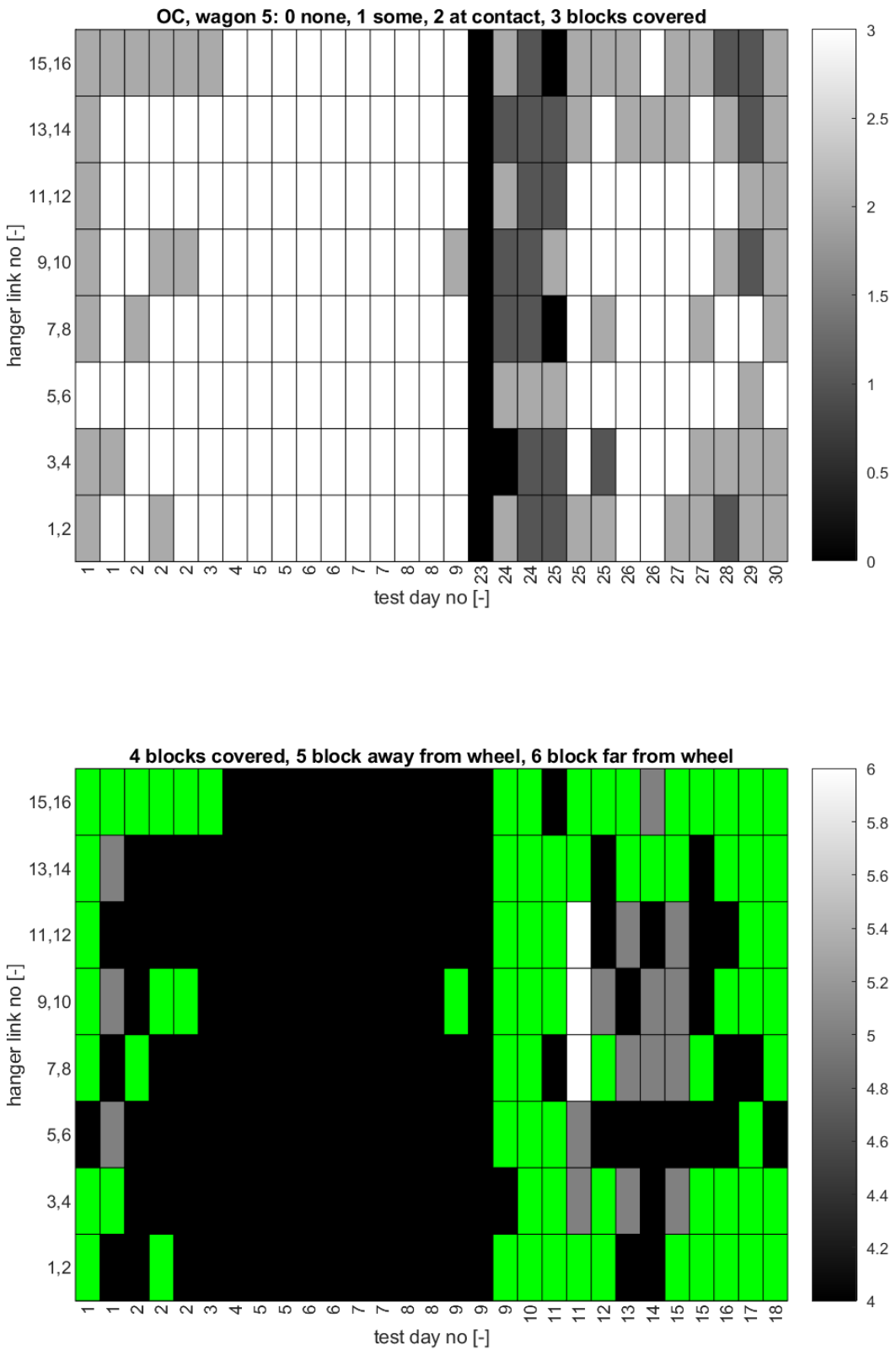

Figure 57 Ice build-up on blocks and holders for tests with organic composite blocks on wagon 5.

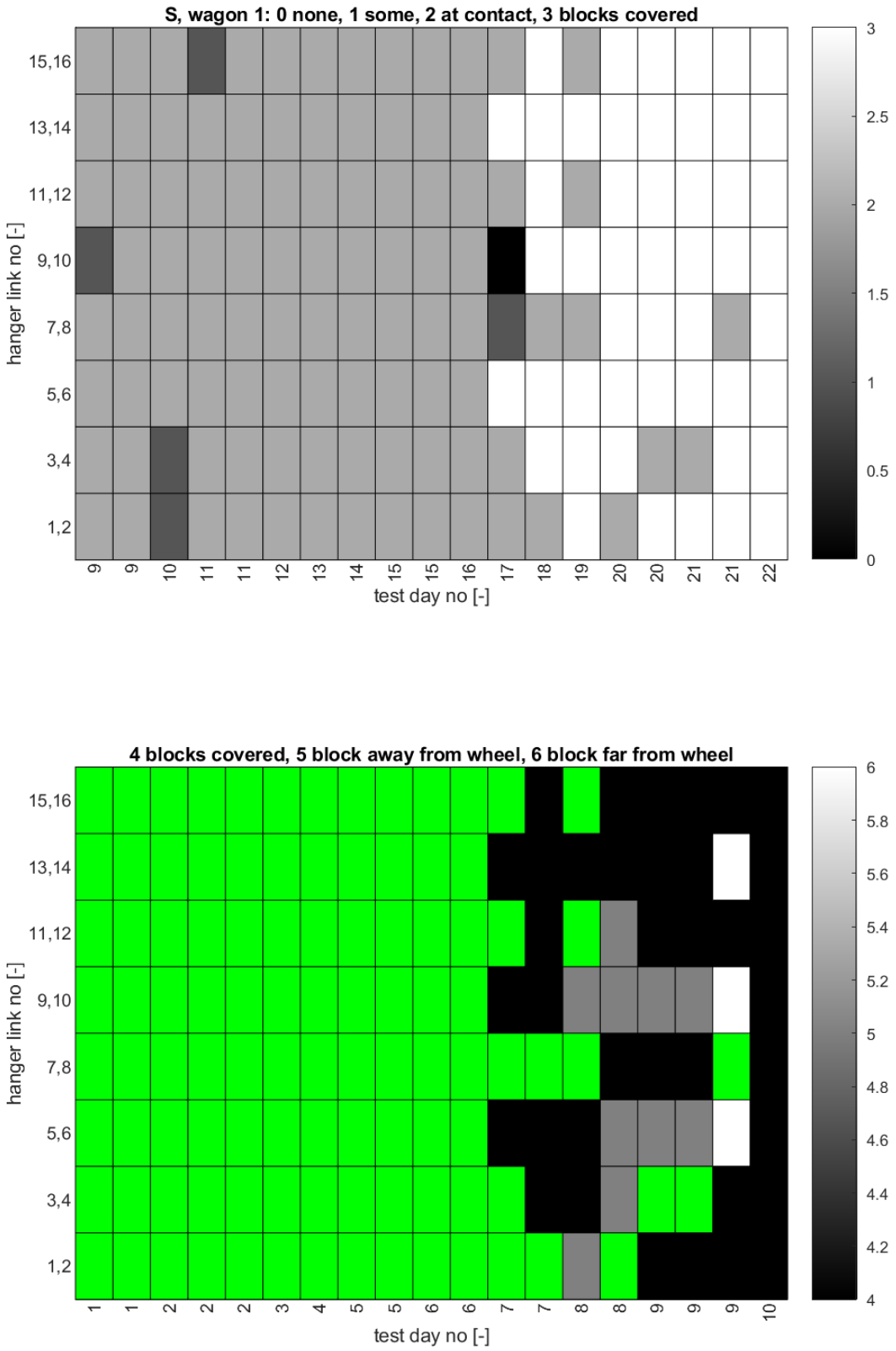

Figure 58 Ice build-up on blocks and holders for tests with sinter blocks on wagon 1.

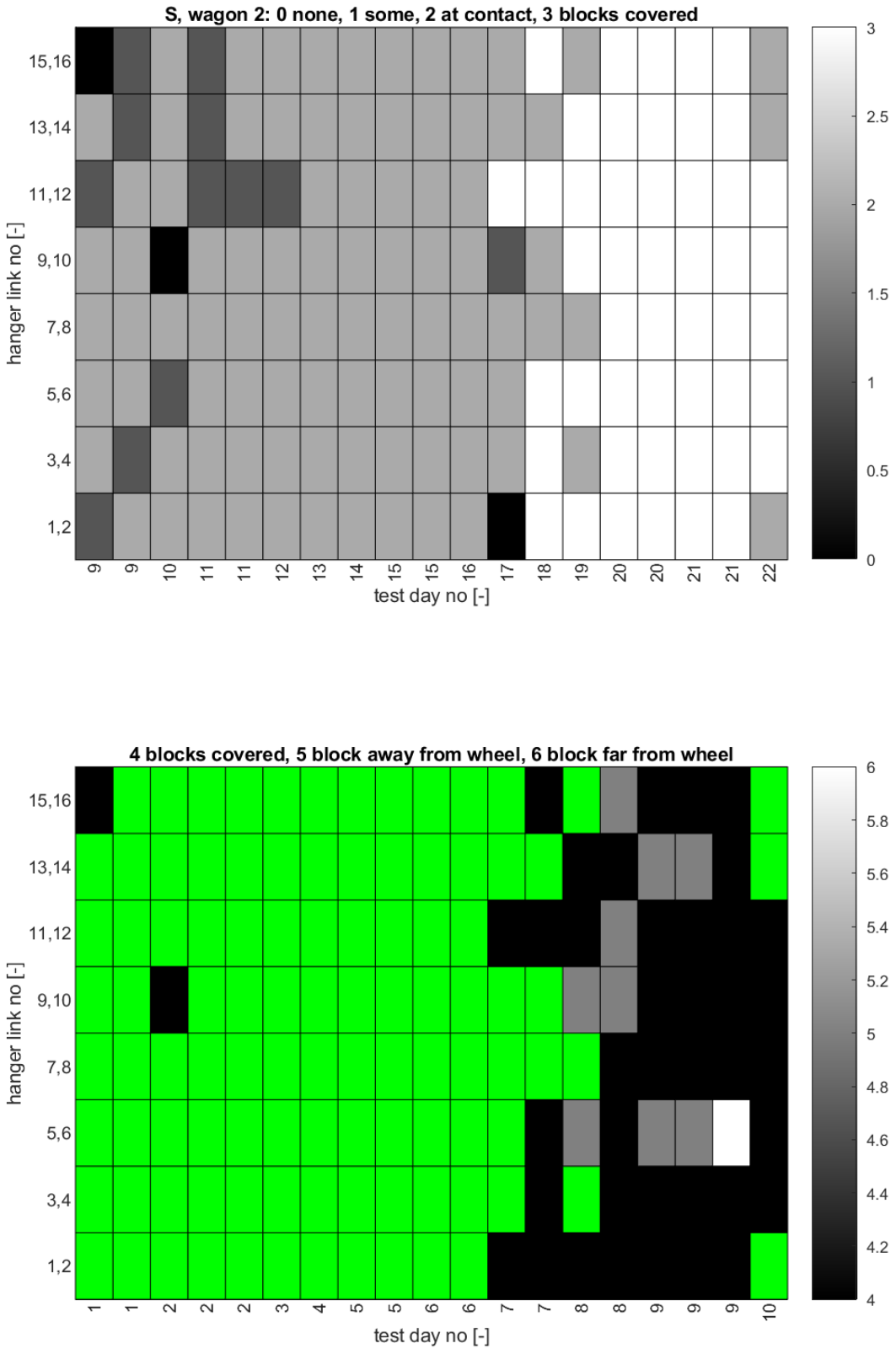

Figure 59 Ice build-up on blocks and holders for tests with sinter blocks on wagon 2.

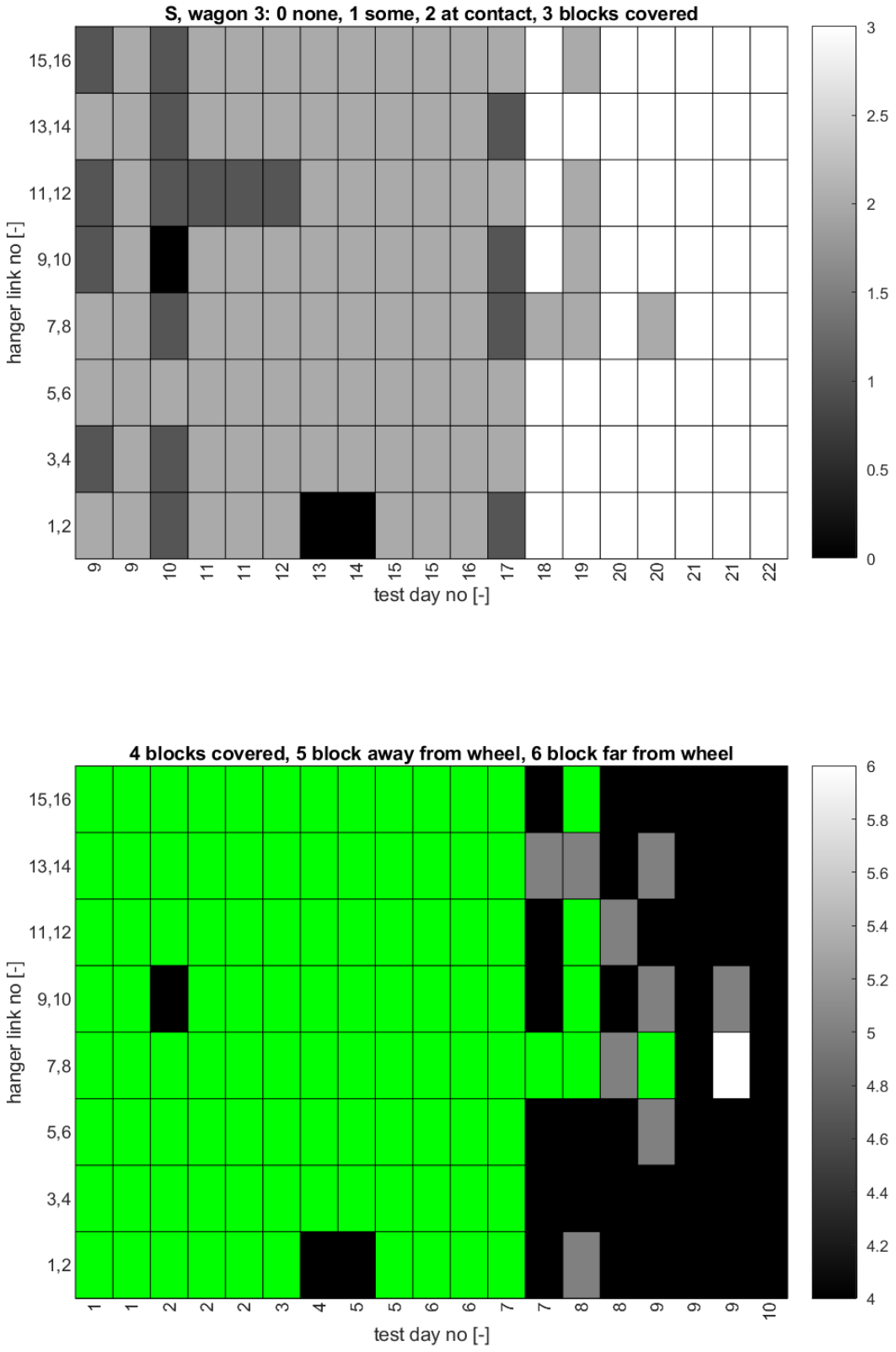

Figure 60 Ice build-up on blocks and holders for tests with sinter blocks on wagon 3.

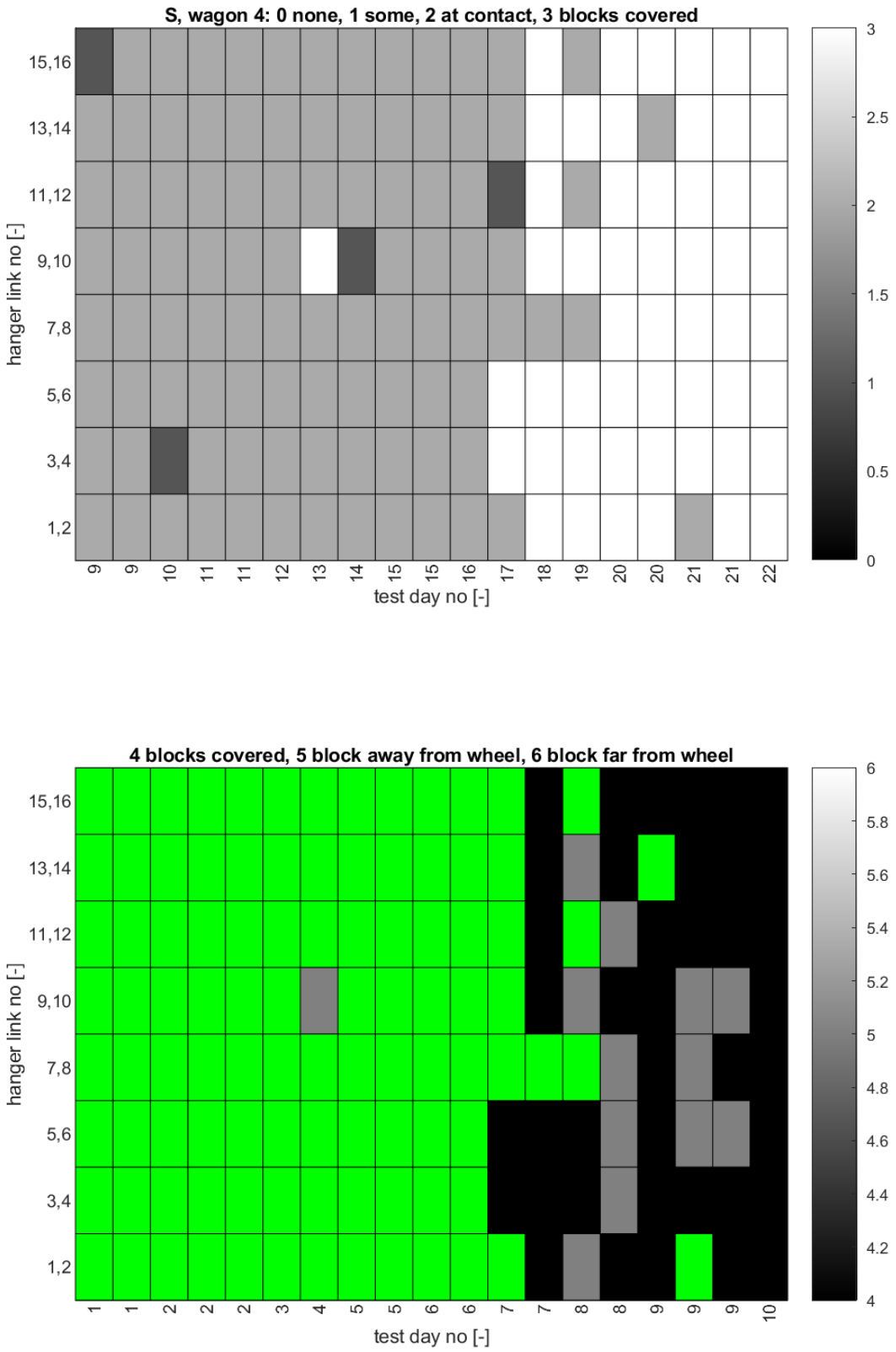

Figure 61 Ice build-up on blocks and holders for tests with sinter blocks on wagon 4.

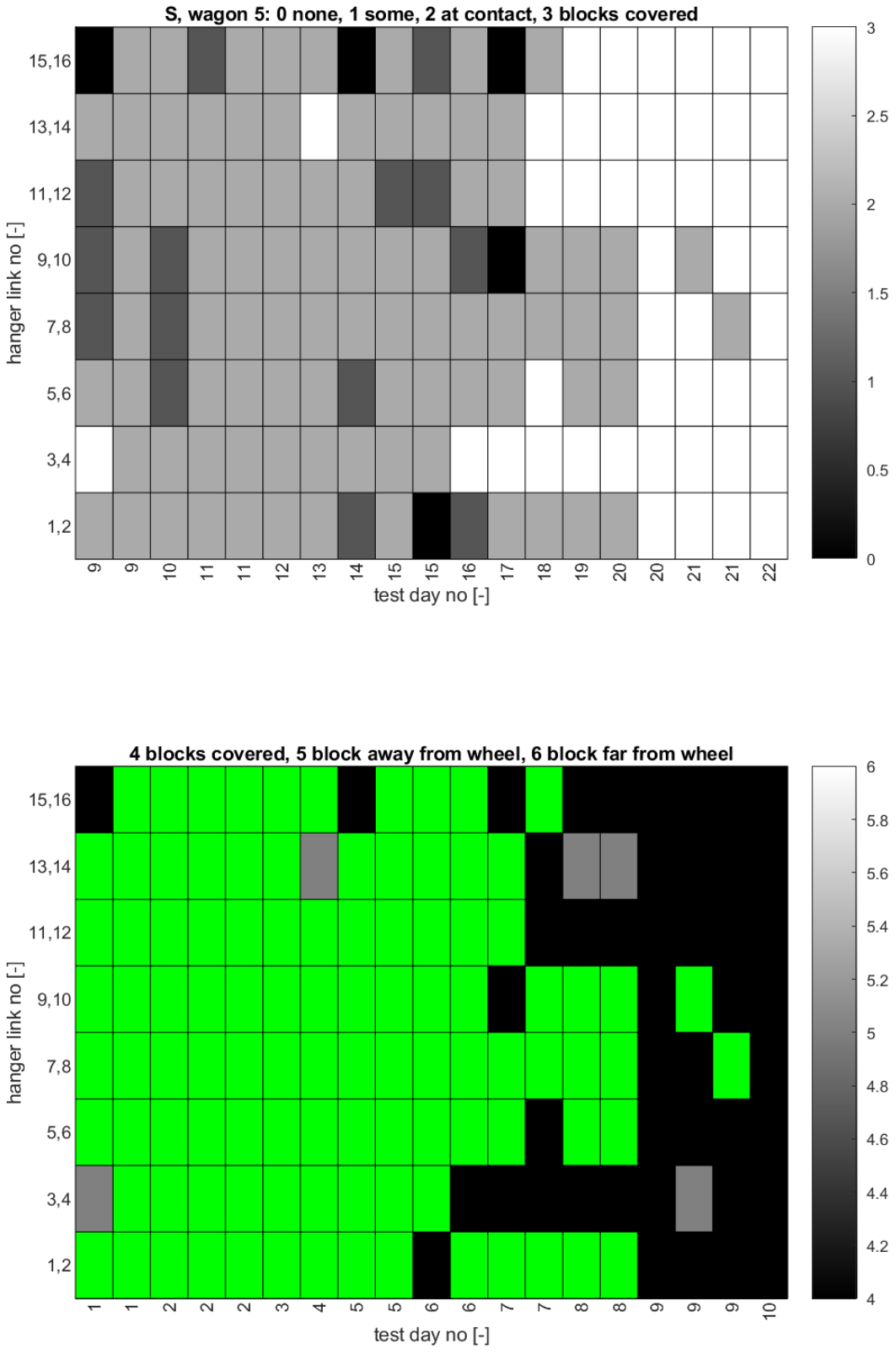

Figure 62 Ice build-up on blocks and holders for tests with sinter blocks on wagon 5.

APPENDIX D ICE BUILD-UP AND MEASURED BLOCK TEMPERATURES

For wagon 3, data are presented for the entire test campaign as function of day of testing for that particular type of blocks. Along with levels of ice, highest block temperatures for the tests performed are presented. Note that temperatures for the first four tests, for which the wagons are loaded, are often higher than the maximum chosen temperature of 50 °C.

Note that thermocouple 1, *i e*, the temperature in the upper block for the sinter tests in the figure below does not measure the block temperature, but instead measures the air temperature (the sensor is not inside the block).

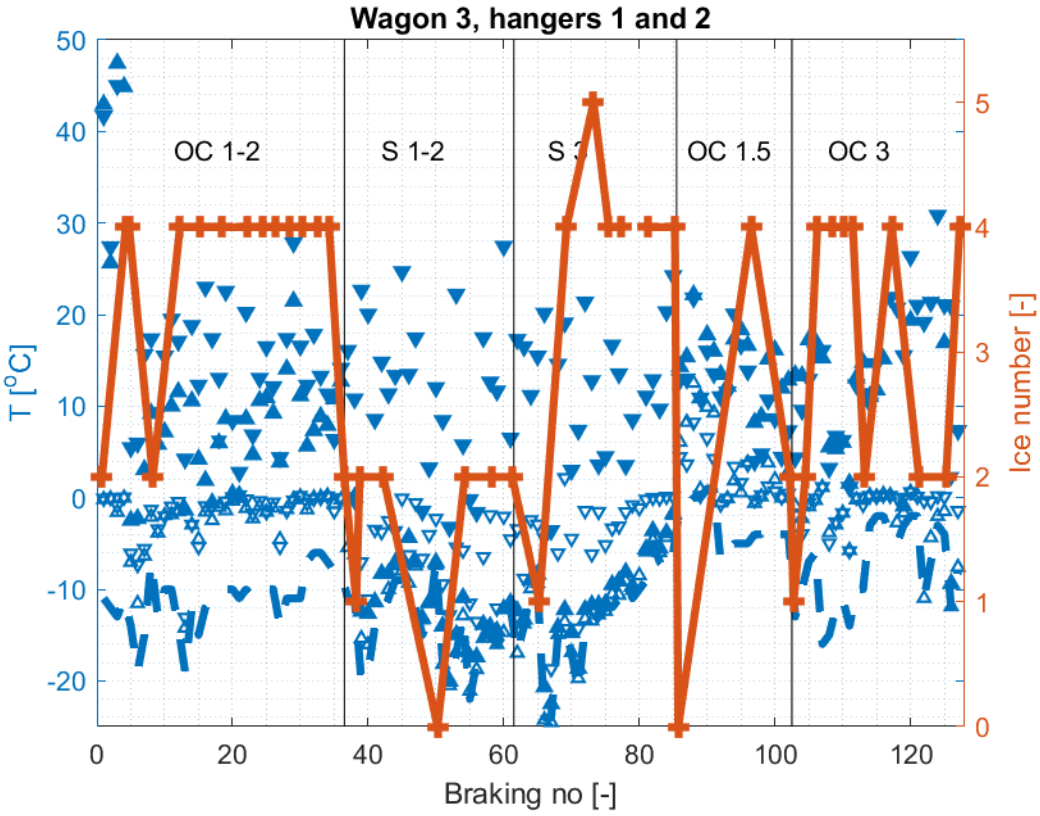

Figure 63 Ice build-up on blocks for holder 1-2 for tests on wagon 3 along with measured block temperatures. Red line is ice number grade, dashed blue line is air temperature, and triangles represent block temperatures. Filled triangles are for maximum temperatures and un-filled ones are initial block temperatures for that brake test. A triangle pointing upwards (▲) is for the upper block and a triangle pointing downwards (▼) is for the lower block. In the inset text at the top: OC indicates organic composite blocks and S indicates sinter. The number indicates driver instruction number employed for that specific range of tests indicated by vertical black lines.

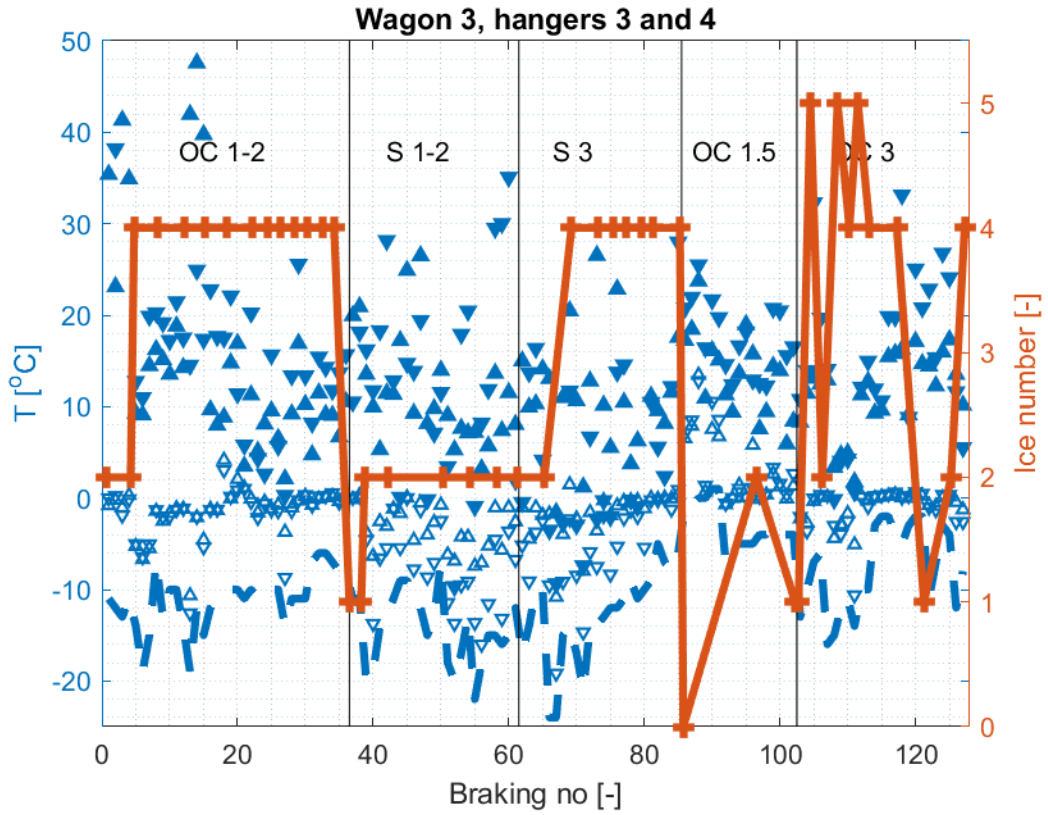

Figure 64 Ice build-up on blocks for holder 3-4 for tests on wagon 3 along with measured block temperatures. Red line is ice number grade, dashed blue line is air temperature, and triangles represent block temperatures. Filled triangles are for maximum temperatures and un-filled ones are initial block temperatures for that brake test. A triangle pointing upwards (▲) is for the upper block and a triangle pointing downwards (▼) is for the lower block. In the inset text at the top: OC indicates organic composite blocks and S indicates sinter. The number indicates driver instruction number employed for that specific range of tests indicated by vertical black lines.

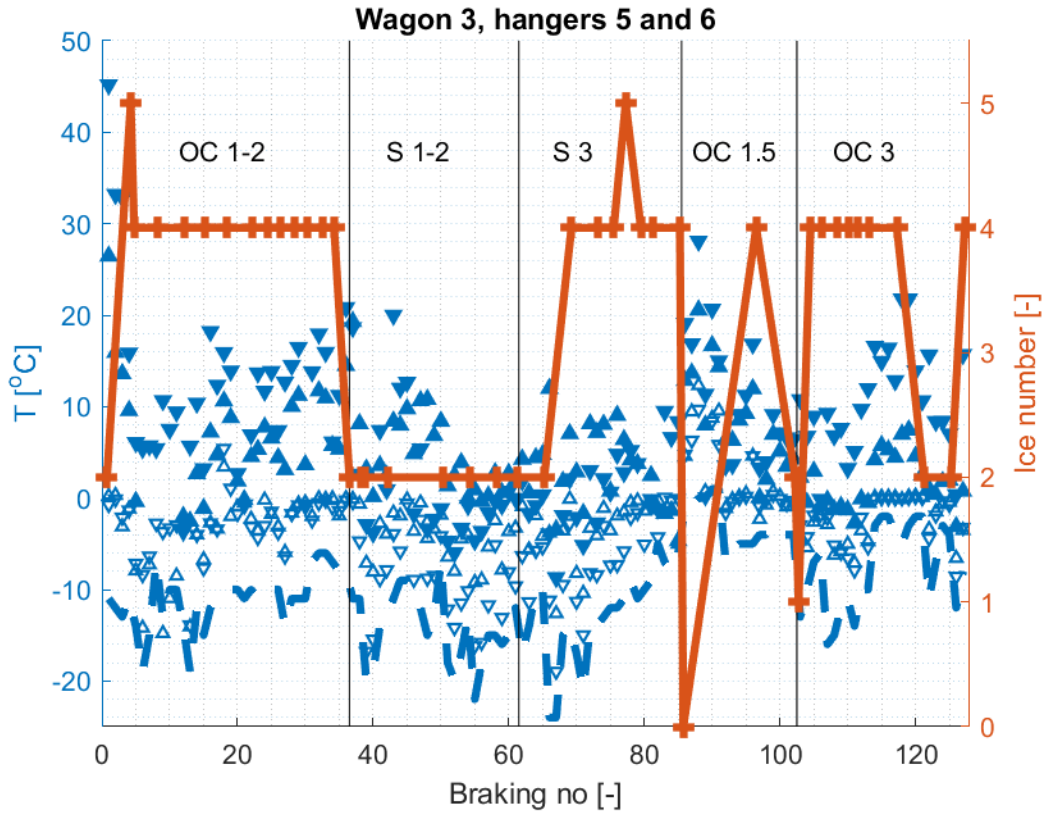

Figure 65 Ice build-up on blocks for holder 5-6 for tests on wagon 3 along with measured block temperatures. Red line is ice number grade, dashed blue line is air temperature, and triangles represent block temperatures. Filled triangles are for maximum temperatures and un-filled ones are initial block temperatures for that brake test. A triangle pointing upwards (▲) is for the upper block and a triangle pointing downwards (▼) is for the lower block. In the inset text at the top: OC indicates organic composite blocks and S indicates sinter. The number indicates driver instruction number employed for that specific range of tests indicated by vertical black lines.

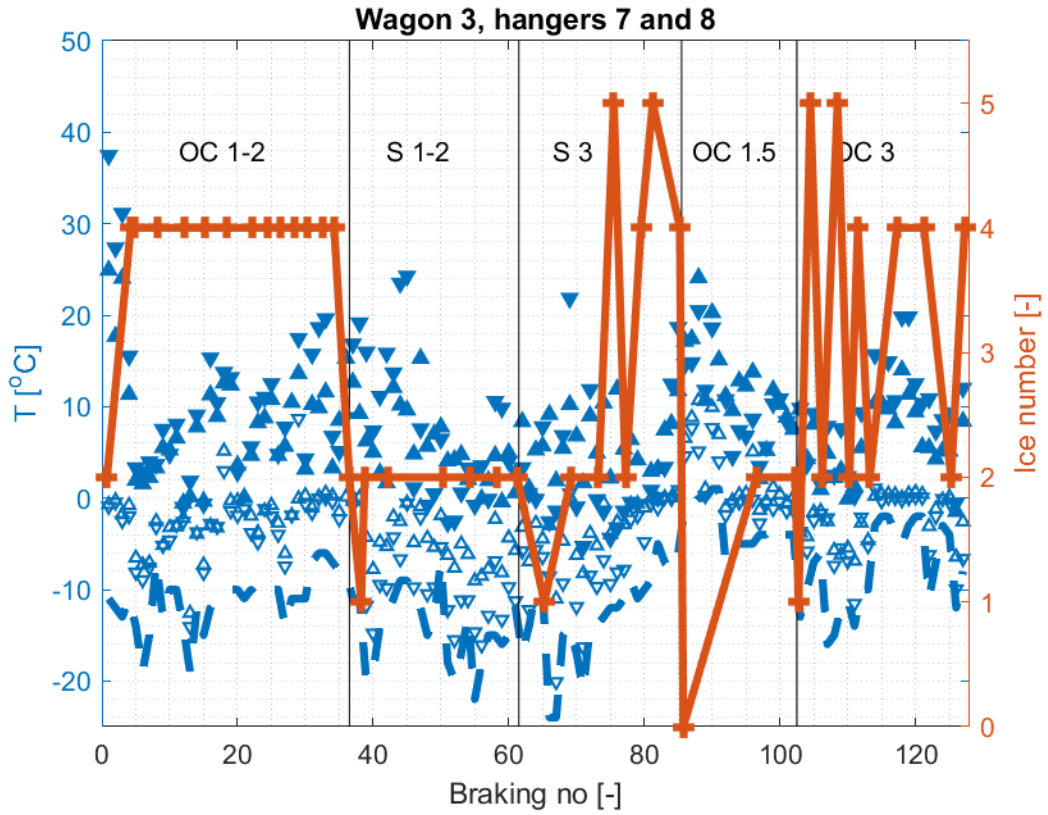

Figure 66 Ice build-up on blocks for holder 7-8 for tests on wagon 3 along with measured block temperatures. Red line is ice number grade, dashed blue line is air temperature, and triangles represent block temperatures. Filled triangles are for maximum temperatures and un-filled ones are initial block temperatures for that brake test. A triangle pointing upwards (▲) is for the upper block and a triangle pointing downwards (▼) is for the lower block. In the inset text at the top: OC indicates organic composite blocks and S indicates sinter. The number indicates driver instruction number employed for that specific range of tests indicated by vertical black lines.

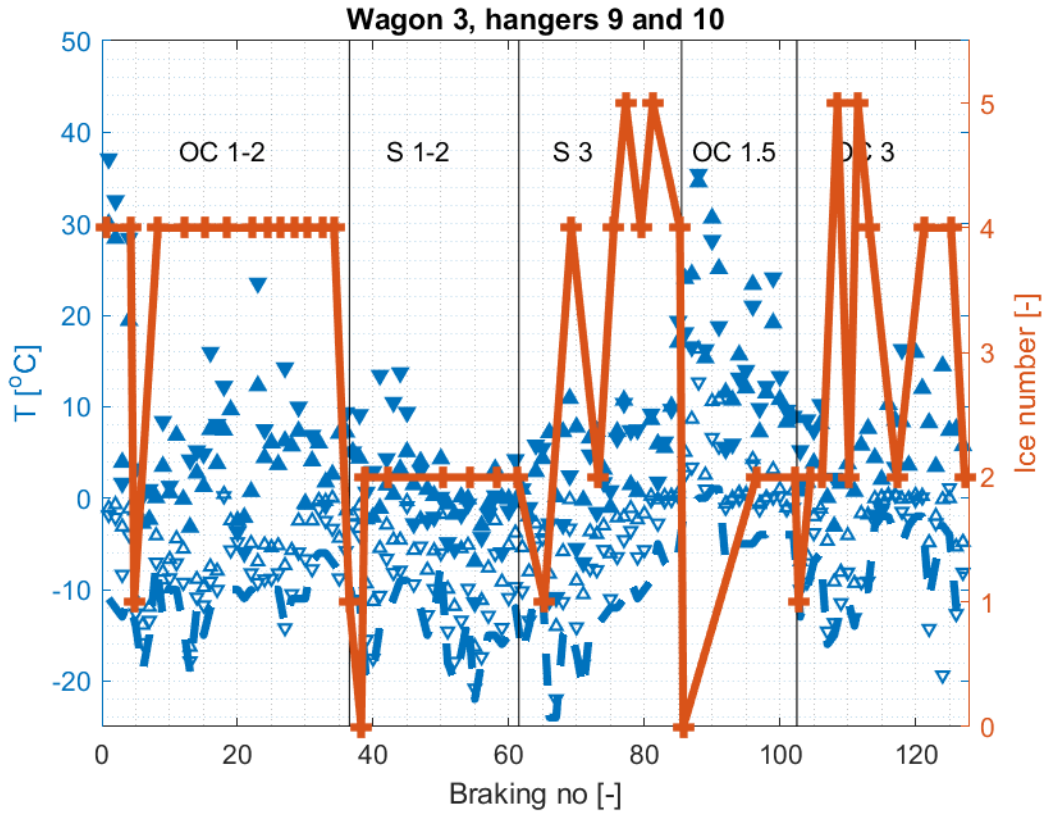

Figure 67 Ice build-up on blocks for holder 9-10 for tests on wagon 3 along with measured block temperatures. Red line is ice number grade, dashed blue line is air temperature, and triangles represent block temperatures. Filled triangles are for maximum temperatures and un-filled ones are initial block temperatures for that brake test. A triangle pointing upwards (▲) is for the upper block and a triangle pointing downwards (▼) is for the lower block. In the inset text at the top: OC indicates organic composite blocks and S indicates sinter. The number indicates driver instruction number employed for that specific range of tests indicated by vertical black lines.

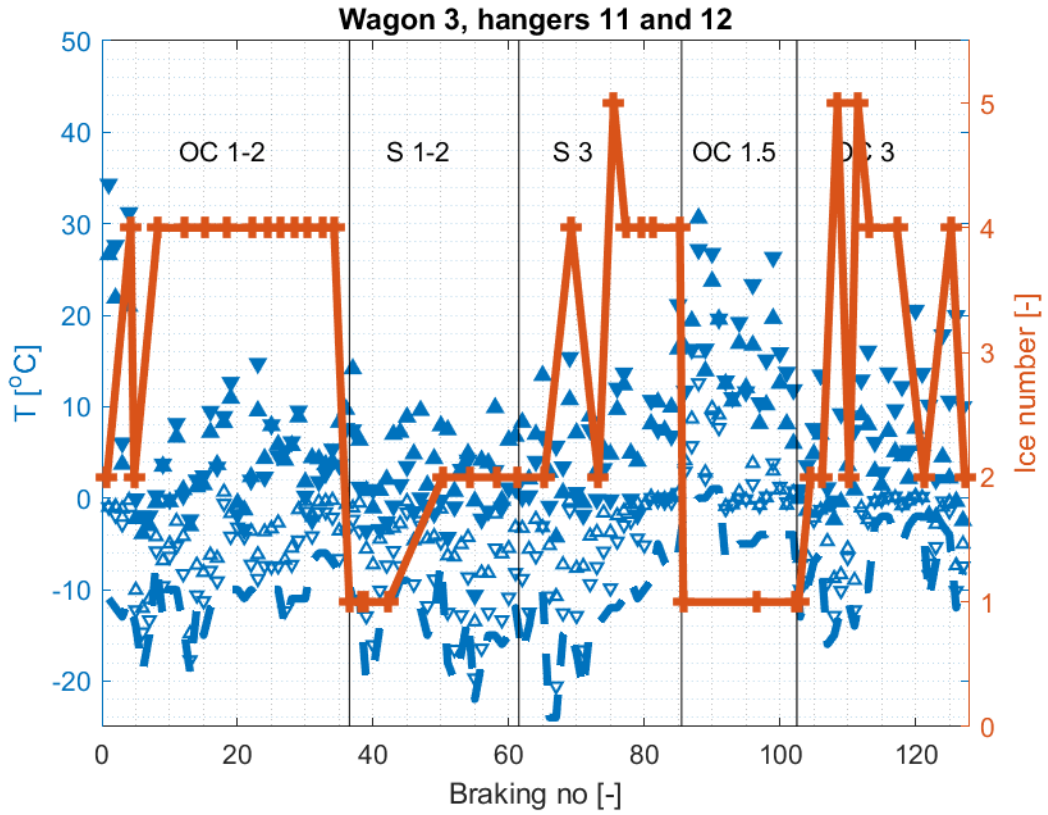

Figure 68 Ice build-up on blocks for holder 11-12 for tests on wagon 3 along with measured block temperatures. Red line is ice number grade, dashed blue line is air temperature, and triangles represent block temperatures. Filled triangles are for maximum temperatures and un-filled ones are initial block temperatures for that brake test. A triangle pointing upwards (▲) is for the upper block and a triangle pointing downwards (▼) is for the lower block. In the inset text at the top: OC indicates organic composite blocks and S indicates sinter. The number indicates driver instruction number employed for that specific range of tests indicated by vertical black lines.

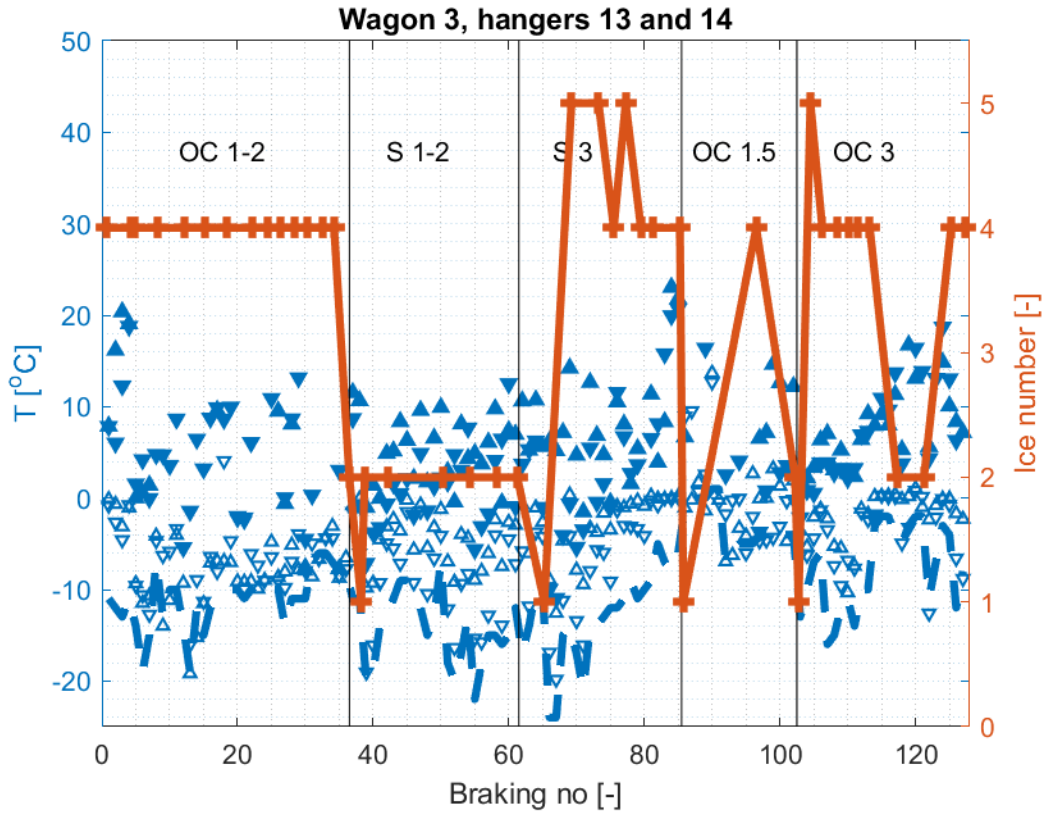

Figure 69 Ice build-up on blocks for holder 13-14 for tests on wagon 3 along with measured block temperatures. Red line is ice number grade, dashed blue line is air temperature, and triangles represent block temperatures. Filled triangles are for maximum temperatures and un-filled ones are initial block temperatures for that brake test. A triangle pointing upwards (▲) is for the upper block and a triangle pointing downwards (▼) is for the lower block. In the inset text at the top: OC indicates organic composite blocks and S indicates sinter. The number indicates driver instruction number employed for that specific range of tests indicated by vertical black lines.

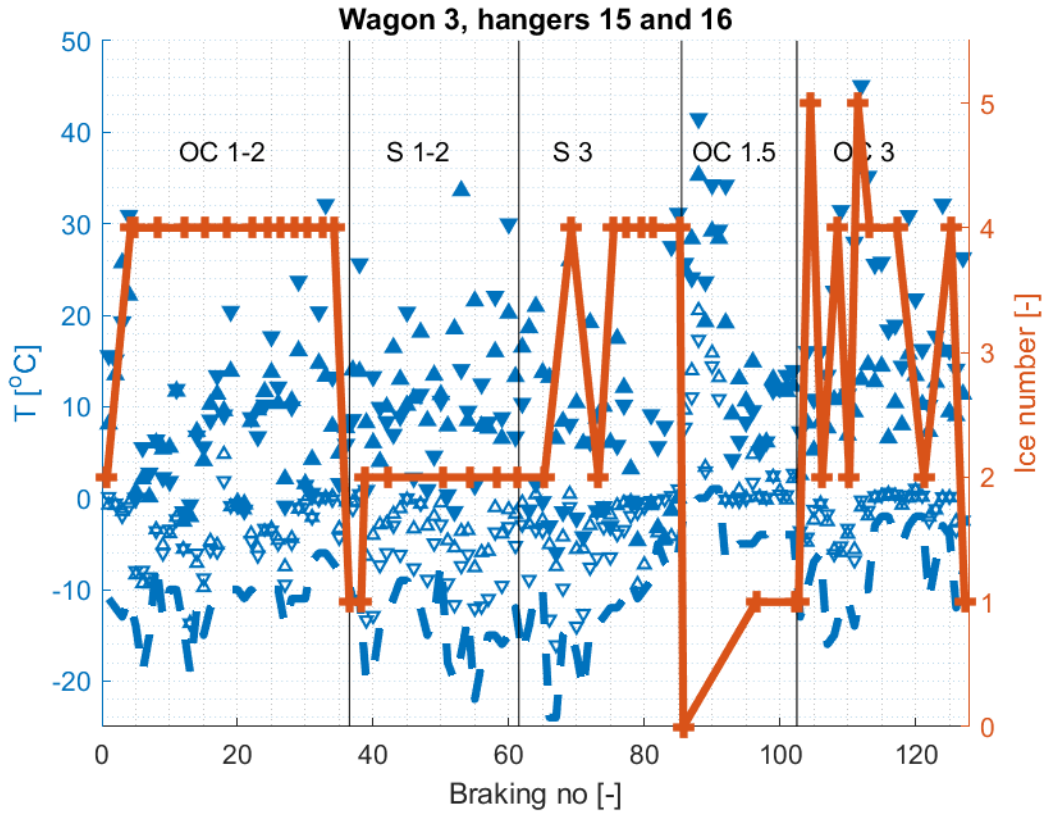

Figure 70 Ice build-up on blocks for holder 15-16 for tests on wagon 3 along with measured block temperatures. Red line is ice number grade, dashed blue line is air temperature, and triangles represent block temperatures. Filled triangles are for maximum temperatures and un-filled ones are initial block temperatures for that brake test. A triangle pointing upwards (▲) is for the upper block and a triangle pointing downwards (▼) is for the lower block. In the inset text at the top: OC indicates organic composite blocks and S indicates sinter. The number indicates driver instruction number employed for that specific range of tests indicated by vertical black lines.

APPENDIX E WAGON BRAKE EFFICIENCY

A study was performed on wagon 6 at the Borlänge workshop on Dec 5, 2020. Results are here only presented for measurement for the inserts of one side of bogie 1, after which the force sensor broke down. Brake block forces were measured[41] by Jan-Ingvar Hermansson of Faiveley Transport Nordic and brake cylinder pressures were measured using the sensors used at the winter testing by Ingemar Brottare of AFRY Testcenter. The wagon rigging system was well lubricated on wagon 6, as on all the other test wagons. The theoretical block force was calculated using the wagon brake calculation, see Appendix F. A photo of the measuring device is given in Figure 71 and the measured data are provided in Table 2, both for brake cylinder pressures corresponding to unloaded wagons (pressure about 1.3 bar) and for loaded wagons (about 3.6 bar). The average calculated efficiency is 0.90 for the one half-bogie of the unloaded wagon and 0.93 for loaded wagon.

Considering the instrumentation of the wagons, the wagon brake efficiency can also be calculated directly from data for the stop braking tests. The block normal forces are then calculated from measured brake triangle forces and hanger link forces, whereas the theoretical block forces are calculated using measured brake cylinder pressures and the information in the wagon brake calculation (Appendix F). The assessment is performed for all brake cycles performed under driver instruction 1 and unloaded wagons. By this method, it is found that the average calculated efficiency is 0.88 for both the instrumented wagons equipped with organic blocks and sinter blocks[42].

Considering the larger set of data for the latter method, the average calculated efficiency is considered to be 88 % for the unloaded wagons.

[41] Measuring instrument ALMEMO 2590 (Ahlborn Mess- und Regelungstechnik GmbH) with block wheel force sensor of Wabtec design.

[42] The calculated average efficiency 0.88 is the same as the average measured for the five Habbins wagons used during the 2019-2020 test campaign, see S. Heinz and C Schmidt, Determining the efficiency of five freight car wagons of Habbiins type, Document 59869-TVP21-192841-PR01, *DB Systemtechnik*, Minden, 2020-02-17.

Figure 71 Photo of data logger and one of the two force transducers that was mounted between blocks and wheel.

Table 2 Results of measurements. Note the variations in brake cylinder pressure that emulate an unloaded or a loaded wagon.

Measurement number	Hanger link number	$p_{cylinder}$[bar]	$\underline{F}_{measured}$ [kN]	$F_{theoretical}$ [kN]	Efficiency [-]
1	1	1,36	11,1	11,8	0,941
2	1	1,36	11,0	11,8	0,937
3	1	3,65	34,0	35,3	0,964
4	1	3,73	34,2	36,1	0,948
5	3	1,37	9,73	11,9	0,820
6	3	1,37	9,63	11,9	0,811
7	3	3,64	30,8	35,2	0,877
8	3	3,73	31,1	36,1	0,863
9	5	1,31	10,3	11,3	0,912
10	5	1,31	10,2	11,3	0,908
11	5	3,62	33,4	35,0	0,954
12	5	3,62	33,1	35,0	0,946
13	7	1,29	10,3	11,1	0,929
14	7	1,29	10,3	11,1	0,929
15	7	3,59	33,5	34,7	0,965
16	7	3,58	32,4	34,6	0,938

APPENDIX F WAGON BRAKE CALCULATION

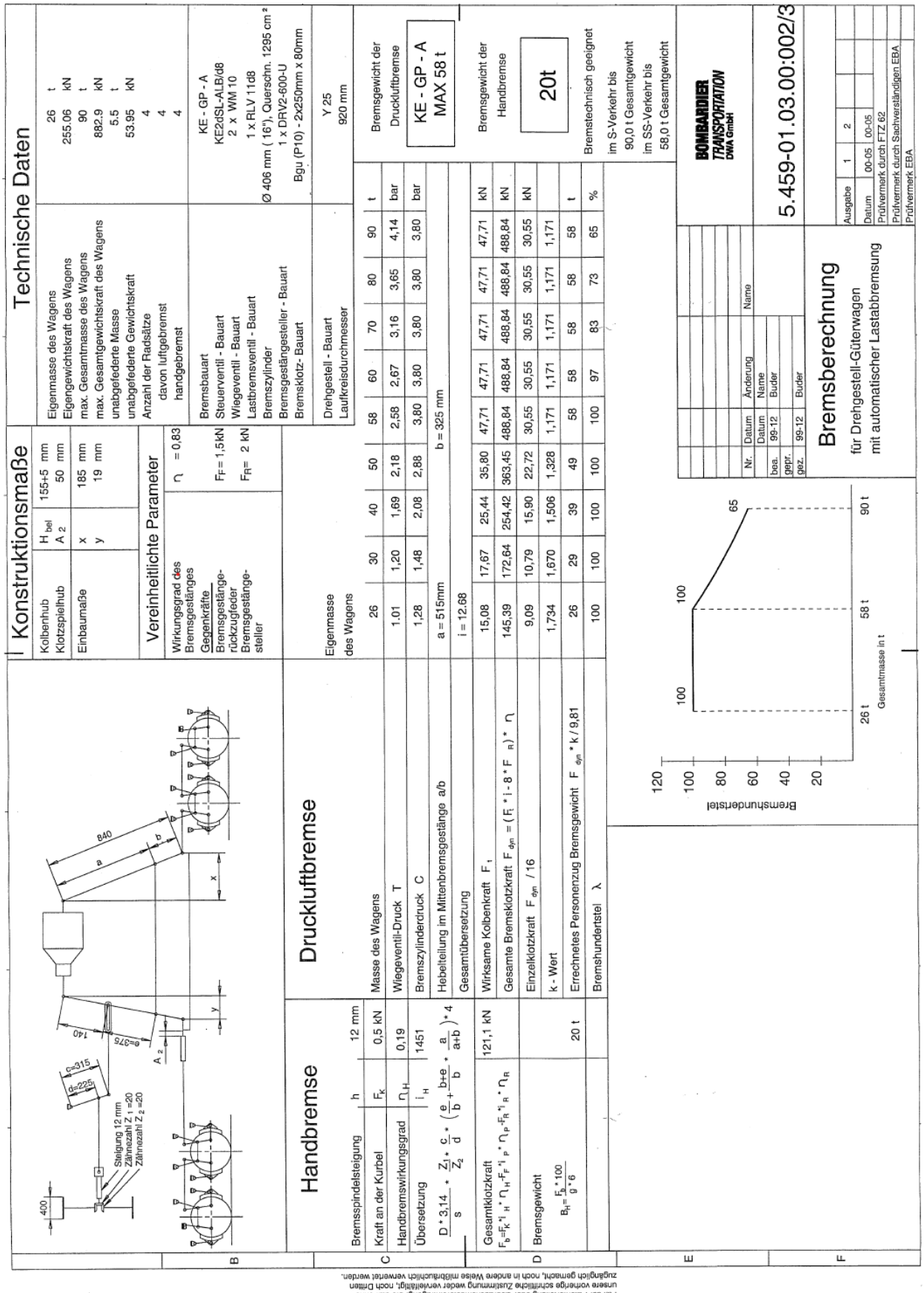

APPENDIX G CLASSIFICATION OF WHIRLING SNOW

The following is adapted from driver instruction provided by Transportstyrelsen, see also photos.
R0 = No whirling snow, see photo R0 below.
UIC2 – UIC3 = Whirling snow with third wagon visible in rear view mirror, see photo R0 below.
UIC4 – UIC5 = Severely whirling snow with first wagon, or parts of first wagon, visible in rear view mirror.